Biodiversity in the extreme world of Pangea

Bethany Janet Allen

Submitted in accordance with the requirements for the degree of

Doctor of Philosophy

The University of Leeds

School of Earth and Environment

July 2021

The candidate confirms that the work submitted is her own except where work which has formed part of jointly authored publications has been included. The contribution of the candidate and other authors to this work has been explicitly indicated below. The candidate confirms that appropriate credit has been given within the thesis where reference has been made to the work of others.

The work in Chapter 2 of the thesis has appeared in the publication:

Allen, B. J., Wignall, P. B., Hill, D. J., Saupe, E. E. & Dunhill, A. M. 2020. The latitudinal diversity gradient of tetrapods across the Permo-Triassic mass extinction and recovery interval. *Proc. R. Soc. B* 287:20201125.

The candidate (BJA) downloaded and reviewed the dataset, contributed additional Paleobiology Database entries, conducted statistical analyses and drafted the manuscript. All authors (BJA and her supervisors) contributed to project direction, data interpretation and editing the manuscript. Here, the introduction has been amalgamated into Chapter 1, the conclusions have been removed, and small editorial changes have been made at the request of the examiners.

Acknowledgements

Abstract

Latitudinal diversity gradients (LDGs) describe the distribution of taxonomic richness by latitude. In the modern, most clades have a unimodal or bimodal LDG with peaks in the low latitudes. However, our knowledge of their causal drivers is limited, and analysis of the fossil record suggests variation in the shape of LDGs through deep time. The middle Permian to Middle Triassic (~270–235 Ma) is associated with extreme global warming, two biotic crises, and the coalescence of landmasses into the supercontinent Pangea, making it an ideal interval for examining the influence of climate and continental configuration on LDGs.

A global database of fossil occurrences was analysed to reconstruct Permian to Triassic LDGs on land and in the oceans, using multiple statistical approaches to address sampling bias. Terrestrial tetrapods had a bimodal LDG, with peaks in diversity at mid palaeolatitudes, throughout the late Permian to Middle Triassic. Brachiopods and bivalves, both clades of marine invertebrates, had unimodal LDGs with low northern latitude peaks in the Early and Middle Triassic. Linear regression was used to compare palaeoenvironmental reconstructions to the invertebrate LDGs, indicating that sea surface temperature was likely the primary LDG driver for both clades, but particularly for brachiopods. A simulation was also constructed to test the viability of methods for calculating spatial variation in origination and extinction from the fossil record. These were then applied to four clades of Permian and Triassic marine invertebrates, revealing general rate homogeneity across latitudes.

Terrestrial and marine LDGs appear to have had relatively consistent but contrasting shapes during the middle Permian to Middle Triassic, perhaps due to differences in the severity of global warming between the two realms. The absence of a relationship between origination, extinction, and diversity within latitude bands also supports the idea that LDG shapes are generally maintained over geological timescales.

Table of Contents

List of Figures

List of Tables

Abbreviations

BC	Boundary-crosser (metric)
CBC	Capitanian biotic crisis
DEM	Digital elevation model
GCM	General circulation (climate) model
GLS	Generalised least squares
IQR	Inter-quartile range
LDG	Latitudinal diversity gradient
LIP	Large igneous province
LSTM	Late Smithian thermal maximum
MAT	Mean annual temperature
MAS	Mean annual salinity
PBDB	Paleobiology Database
PTME	Permo-Triassic mass extinction
SQS	Shareholder quorum subsampling
SST	Sea surface temperature
TT	Three-timer (metric)
WMMT	Warm month mean temperature

Chapter 1 – Introduction

1.1 Latitudinal Diversity Gradients

1.1.1 What are latitudinal diversity gradients?

The latitudinal diversity gradient (LDG), which describes the variation of species richness with latitude, is one of the largest-scale and earliest recognised patterns in ecology (e.g. von Humboldt & Bonpland 1807; Gaston 2000; Willig et al. 2003; Hillebrand 2004; Mannion et al. 2014; Kinlock et al. 2018). Modern species richness is broadly highest in the tropics (Hillebrand 2004; Kinlock et al. 2018) with most groups reaching a unimodal peak in diversity within 30° of the equator (Willig et al. 2003). Terrestrial mammalian diversity peaks in the low latitudes, with over half of species confined to the tropics (Rolland et al. 2014). Plants are also most speciose at low latitudes, with diversity reducing towards the polar regions (Kerkhoff et al. 2014). Modern marine LDGs appear to contrast between different ecologies; most coastal or benthic taxa have a unimodal richness peak at 10–20°N, while pelagic oceanic taxa have a bimodal distribution, with peaks at 10–40°N&S and a dip in diversity near the equator (Tittensor et al. 2010; Powell et al. 2012). Many pelagic clades have higher diversity peaks in the northern hemisphere than in the southern (Chaudhary et al. 2016, 2017, 2021).

Study of the fossil record suggests that the shape of the LDG has changed through time (Crame 2001; Mannion et al. 2014). Analysis of spatial biodiversity patterns in deep time can provide insights which examination of the modern LDG alone cannot, particularly how fluctuation in environmental variables on geological timescales, such as climate, continental drift, and sea level change, affect LDG shape and strength (Powell 2009; Powell et al. 2012; Mannion et al. 2014). It can also provide insight into the influence of macroevolutionary events, such as mass extinctions and radiations, on LDGs (Mannion et al. 2014).

Numerous drivers of LDGs have been proposed (e.g. Gaston 2000; Willig et al. 2003; Currie et al. 2004; Clarke & Gaston 2006; Mittelbach et al. 2007; Schemske et al. 2009; Saupe et al. 2019a). Interaction between highlighted processes, the complexity of feedback cycles, and the covariance of many environmental variables with latitude, complicate efforts to isolate causal mechanisms (Gaston 2000; Willig et al. 2003; Hillebrand 2004; Jablonski 2008; Jablonski et al. 2017; Kinlock et al. 2018). Climate and landmass distribution, however, have been put forward consistently as potential explanatory variables. Here, I discuss previous work on the relationships between these two variables

and LDGs, before exploring the potential that the fossil record holds for providing new perspectives on global biodiversity patterns and their associated causal mechanisms.

1.1.2 The role of climate in driving LDGs

Climate has long been regarded as a primary control on LDGs, particularly temperature, and water availability on land (Brown 1984; Crame 2001; Hawkins et al. 2003; Currie et al. 2004; Field et al. 2009; Naimark & Markov 2011; Fraser et al. 2014; Mannion et al. 2014; Boag et al. 2021; Chaudhary et al. 2021). Sea surface temperature is the only universal predictor of modern spatial species richness patterns in the marine realm (Tittensor et al. 2010).

All organisms have an optimal temperature for cellular and tissue function (Clarke 1993), and internal diffusion and reaction rates are temperature-dependent (Stegen et al. 2012), so metabolic rates are closely linked to temperature (Gillooly et al. 2001). Temperatures which are too cold or too hot can present physiological challenges by reducing the effectiveness of enzymes and altering membrane structures, which under extreme conditions can cumulatively result in death (Willmer et al. 2005). Cold conditions, considered to be approaching 0°C for most organisms, can cause chill injury, and even result in the formation of ice in internal tissues, which is lethal in the absence of freeze tolerance adaptations (Willmer et al. 2005). Most animals have an upper temperature limit of 30–45°C (Willmer et al. 2005), with around 42°C thought to be the upper limit for vertebrates (Pörtner 2002). The production of heat shock proteins can enable survival in high temperatures, but this comes at the cost of other cell functions and energy-demanding behaviours, and as such can only be maintained for short periods of time (Sørensen et al. 2003).

Physiological constraints are translated into spatial patterns as species' distributions are limited by their climatic tolerance (Grinnell 1917; Hutchinson 1957; Brown 1984; Root 1988; Saupe et al. 2014; Antell et al. 2021). Temperature gradients also affect other abiotic variables which can in turn influence richness distributions, particularly in marine environments (Clarke 1993). For example, high temperatures increase organismal oxygen requirements, but lower dissolved oxygen concentrations and increase rates of organic matter decay in the water column, a process which also removes oxygen (Pörtner 2010; Wignall 2015; Boag et al. 2021). This can become sufficiently severe that temperature-dependent anoxia has been proposed as a major kill mechanism during past mass extinction events (Penn et al. 2018). Differences in the temperature solubility of calcite and silica control their

latitudinal availability, and therefore, the metabolic costs of uptake by latitude. Powell & Glazier (2017) hypothesised that this is why modern foraminifera and nannoplankton, which possess calcareous tests, decrease in diversity towards the poles, whereas diatoms and radiolarians, which possess siliceous tests, decrease in diversity towards the equator.

Climatic averages, seasonality, and climate velocity are all likely to be important in determining spatial richness patterns (Clarke 1993; Clarke & Gaston 2006; Powell 2007; Mannion et al. 2014). While short-term environmental fluctuations can be tolerated via phenotypic change or the development of greater plasticity, surviving long-term change *in situ* requires adaptation (Clarke 1993; Valentine et al. 2008; Powell et al. 2015). Instead, species' distributions often shift to track isotherms during climate change (Roy et al. 1995; Valentine et al. 2008; Powell et al. 2015; Reddin et al. 2018), provided that the organisms' dispersal ability facilitates sufficient migration to reach more suitable latitudes, altitudes or bathymetries (Powell 2007; Saupe et al. 2014; Jablonski et al. 2017; Saupe et al. 2019b). Climate change which is too extreme or sudden to allow adaptation or migration can result in extinction, as has been observed at local scales as a consequence of warming temperatures during El Niño events (Clarke 1993).

The 'time and area' hypothesis suggests that modern equatorial species richness has arisen because the tropics have been climatically stable for longer and have simply accrued more species over time (Fine & Ree 2006; Mittelbach et al. 2007; Fine 2015; Svenning et al. 2015; Schluter 2016). The early Eocene was the last greenhouse period to enable tropical species to expand into temperate and polar regions, after which high latitude glaciations perturbed ecosystems, driving extinction and migration into refugia (Schluter 2016). Patterns of biotic recovery subsequent to these glaciation episodes are therefore likely to have been a major determinant of current richness distributions, meaning the modern terrestrial LDG may have been established in the middle Cenozoic, coincident with the onset of Antarctic glaciations (Hillebrand 2004; Mannion et al. 2014; Fine 2015; Svenning et al. 2015; Jablonski et al. 2017; Meseguer & Condamine 2020). Modern coastal animal distributions appear to be more heavily influenced by long-term climate stability than those of pelagic animals, which suggests that dispersal ability may determine the extent to which organisms can "break free" from their historical ranges (Tittensor et al. 2010).

As temperature has a clear effect on the rates of biological processes at a molecular scale, it seems logical that temperature should also play a role in the rate of molecular evolution. This would provide a direct link between high diversity and heightened temperatures in the modern low latitudes. Genetic

divergence within species across latitudinal gradients has been observed (Martin & McKay 2004), but empirical investigations of the relationship between molecular evolution and temperature have been inconclusive, and our understanding of the processes linking molecular evolution and speciation are poor (Mittelbach et al. 2007; Erwin 2009). While tropical plants exhibit higher rates of molecular evolution than those in polar regions, this difference does not produce corresponding differences in speciation rates (Evans & Gaston 2005). Regardless of molecular-level evolution, the 'evolutionary rates hypothesis' proposes that higher temperatures result in higher speciation rates via organismal-scale processes such as shorter generation times and sharper selection pressures (Rohde 1992). Ecological feedback models also suggest that high temperatures are linked to rapid diversification (Stegen et al. 2012).

1.1.3 The role of habitat distribution in driving LDGs

The 'species-area effect' refers to the well-recognised relationship between study area size and the amount of biodiversity found within it (e.g. Schoener, 1976; Rosenzweig 1995; Lomolino 2000; Barnosky et al. 2005). Larger areas are theoretically more species rich because they can support more individuals and incorporate more habitat heterogeneity (Rosenzweig 1995; Barnosky et al. 2005; Valentine et al. 2008). The approximately spherical shape of the Earth has therefore been proposed to contribute to LDGs, as there are large differences in surface area between low and high latitude bands; this is termed the 'mid-domain effect' (Colwell & Lees 2000). Present day equatorial regions have been suggested to simply be more species rich because they contain more ecological niches (Schluter 2016), and are thought to have higher speciation rates as a function of higher standing diversity (Fine & Ree 2006).

The species-area effect is non-linear, and therefore regional richness gradients are generally stronger and steeper than local gradients (Gaston 2000; Hillebrand 2004). Beta diversity, the amount of taxonomic difference observed between distinct communities (and the relationship between alpha [local] diversity and gamma [regional] diversity), is therefore relevant to understanding diversity patterns at large spatial scales (Willig et al. 2003; Dornelas et al. 2014; Fraser et al. 2014; Fraser 2017; Jablonski et al. 2017). The modern tropics appear to have fewer shared taxa between communities, steeper species-area relationships and taxa with smaller geographic ranges, and therefore higher levels of beta diversity (e.g. Rodríguez & Arita 2004; Qian & Ricklefs 2007; Qian et al. 2009; Kraft et al. 2011; Soininen et al. 2018), contributing to greater total biodiversity across the lower latitudes.

When considering the LDG of a specific biome or clade, relevant habitat becomes the important areal constraint. The distribution of shallow continental shelf is a major control on both modern and ancient marine biodiversity patterns (Valentine & Moores 1970; Tittensor et al. 2010; Chaudhary et al. 2016; Zaffos et al. 2017; Close et al. 2020a), and land area distribution during the Mesozoic likely influenced the LDG of dinosaurs (Mannion et al. 2012). The degree of continental aggregation may also influence diversity; for example, supercontinents may present fewer dispersal barriers than fragmented landmasses, enabling high levels of cosmopolitanism, which are often associated with reduced levels of global biodiversity and flatter LDGs (Jablonski 2008; Ezcurra 2010; Button et al. 2017). Continental fragmentation over the Mesozoic is associated with increased diversity in both marine animals and terrestrial vertebrates (Dunhill et al. 2016; Vavrek 2016; Zaffos et al. 2017). The relationship between continental drift and spatial diversity patterns is currently poorly understood, but the fossil record presents ample opportunity to investigate the LDGs associated with different landmass configurations (Erwin 2009; Mannion et al. 2014).

Continental distribution further influences LDGs by interacting with global climate systems via controls on rates of chemical weathering, atmospheric and oceanic circulation and albedo effects (Erwin 2009; Saupe et al. 2020). For example, the existence of the supercontinent Pangea has been proposed as a reason for the prolonged greenhouse conditions of the late Permian and Triassic, as supercontinents may inhibit multiple negative climate feedback loops which prevent runaway greenhouse effects when Earth's landmasses are more fragmented (Wignall 2015). Geography can also facilitate or inhibit the migration of organisms in response to climate change via corridors and dispersal barriers (Saupe et al. 2020).

1.1.4 How do origination, extinction, and migration contribute to LDGs?

Variation in species richness within a given area over time is assumed to result from changes in speciation and/or extinction rates, or migration into or out of the area (Jablonski, 2008; Jablonski et al. 2013; Powell et al. 2015; Jablonski et al. 2017; Powell & Glazier 2017; Meseguer & Condamine 2020). However, the presence of an LDG does not necessarily require contemporary regional differences in rates of diversification. Previously established richness patterns can simply be perpetuated, with 'holdover' taxa contributing more to spatial diversity patterns between adjacent time bins than changes in speciation,

extinction and migration (Mittelbach et al. 2007; Schluter 2016; Powell & Glazier 2017), a concept supported by the fossil record of brachiopods (Powell et al. 2015). It is likely that there have been periods in Earth history when the LDG has changed, followed by periods of relative stability during which the previously established LDG was maintained.

An extensive literature exists discussing whether rates of speciation, extinction and migration are the only control on levels of biodiversity (the "unified neutral theory of biodiversity"), or whether the limited availability of resources means that biodiversity within a given region is capped (e.g. Hubbell 2001; Cornell 2013; Harmon & Harrison 2015; Rabosky & Hurlbert 2015). While the energy input into ecosystems may logically limit the amount of biomass they contain, a direct relationship between biomass, individual abundance and species richness is yet to be proven. One theoretical framework linking these is the 'more-individuals hypothesis', which considers that greater biomass input into an ecosystem produces more individual organisms, which in turn enables more species to maintain a population of sufficient size to buffer against extinction, facilitating higher diversity (Wright 1983; Clarke & Gaston 2006). Variation in speciation rates in ecosystems at carrying capacity would simply translate into differences in turnover rates; an increase in species number would cause the population size of each species to fall, increasing rates of stochastic extinction and maintaining the number of species at a dynamic equilibrium (Allen & Gillooly 2006; Jablonski et al. 2017; Close et al. 2020b).

LDGs may therefore be determined by (a) spatial differences, either present or historic, in rates of diversification, or (b) spatial differences in the ability of ecosystems to accommodate species, i.e. carrying capacities exist and they vary with latitude. These hypotheses are not mutually exclusive, and it is possible that they both play a role in determining spatial richness patterns (Allen & Gillooly 2006; Jablonski et al. 2013; Marshall & Quental 2016; Jablonski et al. 2017). However, they are also both difficult to test empirically (Rosindell et al. 2011; Antell et al. 2020; Close et al. 2020a, b).

Conceptual models based on ecological niche theory promote the idea that the modern tropics have a higher carrying capacity, and that this controls the shape of the modern LDG (Brown 2014). However, empirical evidence for the existence of carrying capacities in real ecosystems, and that they vary by latitude, is often tangential or inconclusive (Currie et al. 2004; Erwin 2009). Biotic interactions appear to be most intense in the modern low latitudes (Schemske et al. 2009), and studies based on anthropogenic introductions to communities indicate that invaders rarely occupy lower latitudes than their natural ranges (Sax 2001; Brown 2014; Schluter 2016), suggesting that carrying

capacities may have been reached in equatorial regions, but not at higher latitudes.

Diversification rates therefore serve as a limiting factor on spatial richness patterns either because community richness is not subject to a species-level carrying capacity, or because that carrying capacity has not been reached (Schluter 2016). However, no consensus has been reached on the extent to which speciation and extinction rates vary, with latitude, through time or between taxa. This is partly due to the fact that these phenomena are difficult to observe and calculate meaningful rates for, both in the modern day and using the fossil record (Jablonski 2008; Kiessling et al. 2010; Mannion et al. 2014; Reddin et al. 2019). The 'out-of-the-tropics' theory attempts to link temperature and diversification rates to LDGs (Jablonski et al. 2006): it suggests that the modern LDG is generated by high rates of origination in the tropics, with a limited number of taxa later migrating poleward (Mittelbach et al. 2007; Powell 2007; Kiessling et al. 2010; Jablonski et al. 2013; Rolland et al. 2014; Jablonski et al. 2017). This theory would also explain the high degree of endemism in tropical ecosystems (Powell et al. 2015). However, some have argued that modern temperate latitudes appear to exhibit the highest speciation and diversification rates in the present day (Weir & Schluter 2007; Schluter 2016; Raja & Kiessling 2021). Examination of the fossil record indicates that median rates of tropical and temperate extinctions in marine animals over the Phanerozoic are not significantly different (Reddin et al. 2019).

1.1.5 Have LDGs been consistent through deep time?

Most of the previous work investigating LDGs using the fossil record provides snapshots of spatial biodiversity patterns in various clades for specific time intervals. For example, acritarchs may have possessed a unimodal southern hemisphere peak in diversity in the Early Cambrian (Zacaï et al. 2021). Peak marine diversity appears to have shifted from the mid to low latitudes between the Middle and Late Ordovician, a possible response to falling global temperatures (Kröger 2018). Terrestrial tetrapods are likely to have been most diverse in the mid palaeolatitudes in the early Permian and Late Triassic (Brocklehurst et al. 2017; Dunne et al. 2021). The late Permian and Middle Triassic LDGs of marine animals may have had a low northern latitude diversity peak, similar to the modern gradient, but the Early Triassic appears to have had a flat LDG (Song et al. 2020). Mesozoic dinosaurs are likely to have been most diverse at temperate palaeolatitudes (Mannion et al. 2012).

Collectively, LDGs reconstructed from the fossil record suggest that climate regime has likely been a major determinant of the shape of the LDG through deep time (Naimark & Markov 2011; Kiessling et al. 2012; Mannion et al. 2014; Meseguer & Condamine 2020). Colder 'icehouse' periods are associated with a steep, unimodal, equatorial peak, while warmer 'greenhouse' periods are associated with shallower, bimodal peaks on either side of the equator (Naimark & Markov 2011; Mannion et al. 2014; Marcot et al. 2016; Meseguer & Condamine 2020). Icehouse intervals may therefore render the tropics a warmer 'refugium', resulting in high diversification at lower latitudes, while the tropics may become too hot during greenhouse intervals, resulting in higher equatorial extinction rates and poleward migration (Sun et al. 2012; Kiessling et al. 2012; Mannion et al. 2014; Reddin et al. 2018). On land, spatiotemporal variation in precipitation may also contribute to this contrast in gradient shape (Hawkins et al. 2003; Fraser et al. 2014; Saupe et al. 2019a).

The latitude of maximum marine diversity has also gradually shifted from the southern hemisphere to the northern through the Phanerozoic (Powell 2009; Naimark & Markov 2011). It is likely that the movement of continental shallow shelf area, due to plate tectonics, is responsible for this trend; however, this needs further investigation (Powell 2009; Mannion et al. 2014; Chaudhary et al. 2016, 2021).

Our understanding of LDGs and their drivers is far from complete, and the hypotheses presented here require more supporting evidence. While modern-day richness gradients fit the trends proposed during icehouse periods in Earth history, the shape of LDGs during greenhouse periods is less well understood (Mannion et al. 2014; Jablonski et al. 2017; Crame 2020). The fossil record presents an opportunity to learn more about LDGs in deep time, but sampling bias acts as a major barrier to accessing this information, and many previous studies have not taken this into account (Mannion et al. 2012; Mannion et al. 2014).

1.2 Sampling Bias

1.2.1 What is sampling bias?

Both modern and fossil taxonomic occurrence data are subject to biases which distort their underlying biological signal (Kidwell & Holland 2002; Willig et al. 2003; Erwin 2009). For example, animals with a relatively small body size, or lacking hard or skeletonised body parts, are less likely to be preserved and discovered (Kidwell & Holland 2002; Cooper et al. 2006; Benton et al. 2011;

Fraser 2017; Shaw et al. 2021). Preservation potential varies between different palaeoenvironments and lithologies (Kidwell & Holland 2002; Shaw et al. 2021). Lagerstätten, which contain a high abundance of fossils or preserve soft-bodied animals, can skew macro-scale diversity analyses (Alroy 2010; Benson & Butler 2011). Difficulties with taxonomic assignments, particularly due to incomplete preservation, are also a source of uncertainty and error (Benton et al. 2011; Mannion et al. 2012; Hendricks et al. 2014).

The inconsistency of the fossil record across space can also have a large impact on perceived biodiversity trends (Barnosky et al. 2005; Benson & Upchurch 2013; Vilhena & Smith, 2013; Close et al. 2020a, b). Available rock and outcrop area varies considerably over geological time, constraining the number of localities in which fossils might be found (Allison & Briggs 1993; Kidwell & Holland 2002; Peters 2005; Smith 2007; Smith & McGowan 2007; Wall et al. 2009; Benton et al. 2011; Mannion et al. 2011; Peters & Heim 2011; Wall et al. 2011; Dunhill et al. 2014a, b; Dunhill et al. 2018a). In the marine realm, this ties in with the 'common-cause hypothesis', which describes how sampling proxies and diversity appear to correlate because both are driven by sea level change (Peters 2005; Benson & Butler 2011; Benton et al. 2011; Hannisdal & Peters 2011; Peters & Heim, 2011; Zaffos et al. 2017). Geographic sampling bias is also strong, particularly due to the underrepresentation of the Global South in large-scale fossil datasets (Allison & Briggs 1993; Clapham et al. 2009; Close et al. 2020a; Dunne et al. 2021).

Online databases such as the Paleobiology Database (http://paleobiodb.org/), the Geobiodiversity Database (http:/geobiodiversity.com/), the Neotoma Paleoecology Database (http://neotomadb.org/), and the Neptune Database (http://nsb.mfn-berlin.de) provide researchers with a source of large volumes of fossil data, increasing the ease, accuracy and reproducibility with which macroevolutionary patterns can be investigated using the fossil record (Kidwell & Holland 2002; Marshall et al. 2018). However, these databases are far from complete; for example, perhaps as few as 3–4% of fossil localities represented in museum collections have been added to the Paleobiology Database (Marshall et al. 2018).

1.2.2 Why does sampling bias matter when examining LDGs in the fossil record?

When reconstructing spatial biodiversity patterns, allowances must be made for the unevenness of the fossil record (Allison & Briggs 1993; Alroy 2010; Benson

& Butler 2011; Benton et al. 2011; Vilhena & Smith 2013; Mannion et al. 2014; Close et al. 2017; Dunne et al. 2021; Jones et al. 2021). Sampling bias is particularly heterogeneous in large-scale analyses of fossil data, as greater variation is captured in many of the individual facets of sampling bias at larger spatial and temporal scales (Benton et al. 2011). Total completeness is an impossible goal, but we can (and should) assess whether the quality of the fossil record is sufficient to answer the questions at hand (Paul 1982; Kidwell & Holland 2002; Benton et al. 2011).

Spatial variation in sampling is of particular concern when reconstructing LDGs (Song et al. 2020; Dunne et al. 2021; Jones et al. 2021). Increasing awareness of spatial sampling bias has raised questions about our ability to identify spatial 'traits' such as geographic distributions and range sizes from the fossil record (e.g. Bernardi et al. 2018; Reddin et al. 2018; Antell et al. 2020; Close et al. 2020a; Jones et al. 2021). Recent work using simulations has indicated that range sizes can be reliably reconstructed from fossil occurrence data (Darroch & Saupe 2018; Darroch et al. 2020), but that the shape of LDGs can only be determined during intervals with relatively high spatial coverage across latitudes (Jones et al. 2021). Some studies with patchy occurrence data have ranged-through their latitude bins when reconstructing LDGs (e.g. Brayard et al. 2006; Powell 2009; Jablonski et al. 2013; Zacaï et al. 2021), but this approach carries many overly-simplistic assumptions and is often not appropriate at large spatial scales or during rapid, extreme evolutionary events such as mass extinctions.

Comparison of LDGs between the modern and deep time is difficult due to discrepancies between their relevant collection methods and sampling biases. For example, while Tittensor et al. (2010) and Powell et al. (2012) both conducted analyses of modern marine LDGs, the latter study included a much higher proportion of taxa with a high preservation potential, such as brachiopods and bryozoans. The taxonomic composition of their dataset was therefore more similar to that seen in fossil datasets, setting a fairer point of comparison for deep time LDGs. Further, while most studies of the modern LDG focus on species, analysis of the fossil record usually necessitates the use of higher taxonomic levels, which cannot be assumed to follow the same spatial trends as species (Willig et al. 2003; Powell 2007; Hendricks et al. 2014; Tomašových et al. 2016).

1.2.3 How is sampling bias taken into account in macroevolutionary analyses?

LDGs in deep time can be estimated reliably if taxonomic and spatial sampling completeness in the clade of interest are relatively high, and consideration is given to partitioning the observed variation in richness likely attributable to sampling biases versus that likely attributable to biological patterns (Fraser 2017; Jones et al. 2021). Where possible, studies should be designed with large spatial scales (Mannion et al. 2014; Fraser 2017) and to incorporate phylogenetic relationships (Kidwell & Holland 2002; Button et al. 2017; Jablonski et al. 2017; Meseguer & Condamine 2020).

Subsampling and extrapolation methods can help alleviate issues of sampling heterogeneity. Simple subsampling (i.e. classical rarefaction) is a traditional approach which draws a uniform number of individuals, or occurrences, from each sample (Alroy 2010). Coverage-based approaches, which determine their subsampled or extrapolated sample size based on the relative frequencies of taxa in the sample, are currently the most effective approach for mitigating the effects of fossil record bias in large-scale biodiversity analyses (Close et al. 2018; Alroy 2020). Examples commonly used on fossil data include shareholder quorum subsampling (SQS; Alroy 2010), the Chao1 extrapolator (Chao & Jost 2012), and the squares extrapolator (Alroy 2018).

Increasingly, simulations are being recognised as a useful tool for addressing macroevolutionary problems (Close et al. 2018; Darroch & Saupe 2018; Dunhill et al. 2018a; Barido-Sottani et al. 2020; Darroch et al. 2020; Saupe et al. 2020). This is particularly true for understanding LDGs, which can be investigated using artificial occurrence data which are free from, or provide insight into, sampling bias (Fraser 2017; Saupe et al. 2019a; Jones et al. 2021). Simulations therefore present an opportunity to develop methods to more accurately reconstruct LDGs in deep time (Barrido-Sottani et al. 2020; Jones et al. 2021).

An interval in deep time for which LDGs are currently poorly understood is the Permian and Triassic. This is an interval renowned for fluctuations in global diversity, including the transition between Sepkoski's (1984) 'Paleozoic' and 'Modern' faunas. The relative spatial completeness of the fossil record at this time (Jones et al. 2021) and onset of strong greenhouse climate conditions (Sun et al. 2012) also make the Permian and Triassic ideal for investigating past LDGs. Song et al. (2020) examined the LDG of marine animals across this interval, but their analyses were conducted at a coarse taxonomic level and with relatively simplistic management of sampling bias, leaving plenty of questions about spatial richness patterns and their formation unanswered.

1.3 The Times of Pangea

The Permian and Triassic stages (~300–200 Ma; Figure 1–1) represent an interesting time in Earth history, characterised by an icehouse-greenhouse transition followed by extensive volcanic activity and extreme global warming (Kiehl & Shields 2005; Sun et al. 2012; Wignall 2015). Continental configuration also contrasted greatly with that seen in the modern day, as the supercontinent Pangea formed in the Cisuralian (early Permian, ~300–273 Ma), and land area was evenly distributed on either side of the equator (Powell 2009; Stampfli et al. 2013). The interval includes Olson's Extinction, associated with global warming and deglaciation (Brocklehurst et al. 2017), followed by the Capitanian biotic crisis and the Permian-Triassic mass extinction, both major extinction events which are coincident with the eruption of large igneous provinces, and likely driven by the associated global warming and oceanic acidification and anoxia (Wignall et al. 2009; Bond & Wignall 2010; Bond et al. 2010; Payne & Clapham 2012; Sun et al. 2012; Penn et al. 2018).
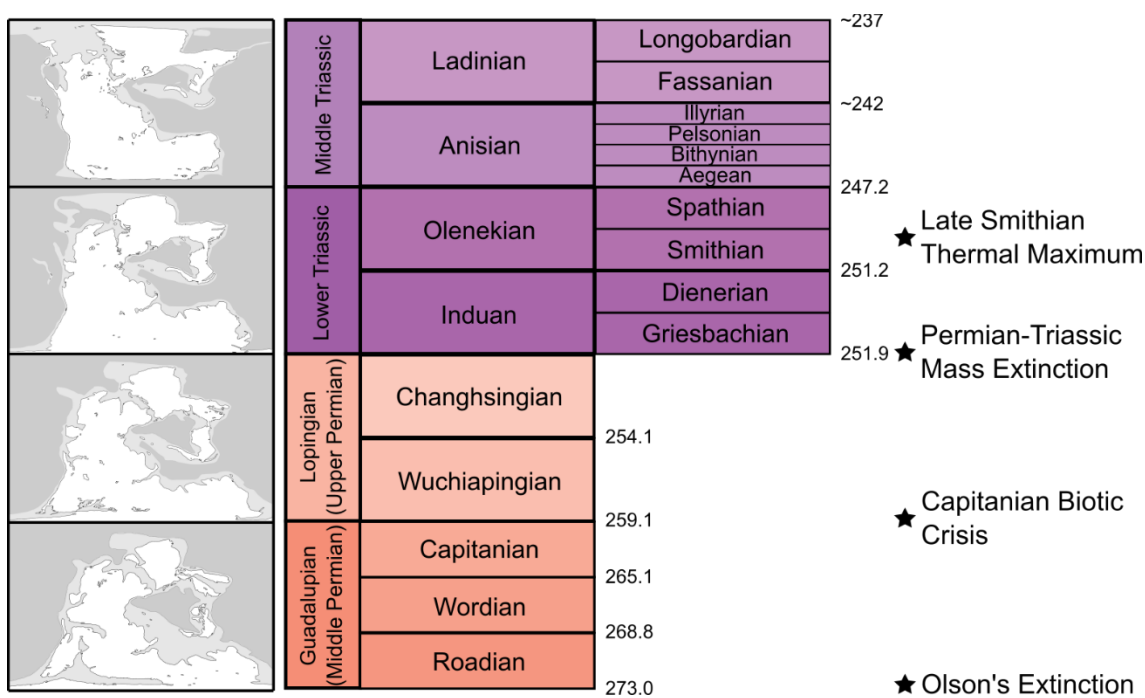
Figure 1–1: The temporal subdivisions of the middle Permian to Middle Triassic. Palaeogeographies are traced from Scotese (2016). The Permian lacks formal substages. Interval colours and dates, presented in millions of years ago (Ma) to one decimal place where available, are taken from the International Chronostratigraphic Chart (version 2021/05; updated from Cohen et al. 2013).

1.3.1 Olson's Extinction

A major faunal turnover has been identified in terrestrial tetrapods at the end of the Cisuralian. Termed Olson's Extinction, the event has been highly controversial, with some considering the turnover to be an artefact of the palaeolatitudinal shift between Cisuralian and Guadalupian (early and middle Permian) terrestrial localities, and not a true extinction event (Benson & Upchurch 2013). A recent re-examination of fossils known from this time by Brocklehurst et al. (2017) provided support that the extinction event is genuine, suggesting that equatorial tetrapod diversity declined while temperate communities experienced a faunal turnover without loss of overall diversity, resulting in a temperate diversity peak during the Cisuralian which strengthened through to the end of the period. This LDG transition coincides with emergence from a glacial period, with climate becoming warmer and drier into the Guadalupian, supporting the icehouse-greenhouse LDG transition described above (e.g. Mannion et al. 2014).

1.3.2 The Capitanian biotic crisis

The Capitanian biotic crisis (CBC, also known as the end-Guadalupian extinction; ~259 Ma) occurred during the eruption of the Emeishan large igneous province, in modern-day southwestern China (Clapham et al. 2009; Wignall et al. 2009; Bond et al. 2010; Wignall 2015; Rampino & Shen 2021). A coincident fall in global sea levels may also have affected marine ecosystems and their preservation potential (Shen & Shi 2004; Clapham et al. 2009; Clapham 2015). Estimates of the taxonomic severity of the CBC have been inconsistent (McGhee et al. 2013; Rampino & Shen 2021), and diversity changes have previously been attributed to back-smearing of the later Permian-Triassic extinction (Foote 2007) or reduced origination in the Capitanian and Wuchiapingian (Clapham et al. 2009). Extinctions associated with the CBC appear to have been highly ecologically selective, resulting in the loss of sponge-microbial reefs, high extinction levels in foraminifera and calcareous algae, and a rapid turnover in ammonoids (Wignall et al. 2009; Bond et al. 2010; McGhee et al. 2013; Clapham 2015; Rampino & Shen 2021).

1.3.3 The Permian-Triassic mass extinction

Large-scale volcanism associated with the Siberian Traps large igneous province resulted in extreme climate change during the late Permian (Parrish

1993; Kiehl & Shields 2005; Preto et al. 2010; Trotter et al. 2015). This drove environmental perturbations that resulted in the most catastrophic mass extinction event of all time at the end of the Permian, around 252 Ma (Payne & Clapham 2012; Wignall 2015). A prolonged interval of extremely high temperatures, which peaked in the Olenekian (late Early Triassic) (Sun et al. 2012), along with ocean anoxia and acidification, have been identified as key extinction mechanisms (Wignall 2015; Penn et al. 2018).

On land, high temperatures and seasonal precipitation in central Pangea resulted in drought (Parrish 1993; Smith & Botha-Brink 2014; Looy et al. 2016; Tabor et al. 2018), while purported ozone depletion, caused by halogen gas release from the Siberian Traps, resulted in high UV-B levels that caused plant sterilisation and extinction (e.g. Beerling et al. 2007; Benca et al. 2018). Tetrapods were profoundly affected by the PTME, with gorgonopsians and pareiasaurs becoming extinct (Wignall 2015). In the immediate aftermath, Early Triassic tetrapod communities were composed almost entirely of "disaster faunas" such as *Lystrosaurus*, a herbivorous burrowing synapsid (Sidor et al. 2013; Smith & Botha-Brink, 2014; Button et al. 2017; Ezcurra & Butler 2018). Early Triassic temperatures at low latitudes are considered to have been beyond the tolerable long-term threshold for both plants and animals, driving extinction and poleward migration (Sun et al. 2012; Bernardi et al. 2018).

Equatorial sea surface temperatures rose from 21°C to 36°C across the Permian-Triassic boundary (Sun et al. 2012). An estimated 83% of marine genera became extinct (McGhee et al. 2013), with losses particularly profound in marine reefs, especially for corals, crinoids, brachiopods, echinoids and bryozoans (Payne & Clapham 2012: Wignall 2015; Martindale et al. 2019). The global functional diversity of marine ecosystems was largely maintained across the PTME, but individual modes of life were occupied by fewer taxa (Foster & Twitchett 2014). Cosmopolitan, generalist "disaster faunas" such as the bivalve *Claraia* dominated benthic marine environments in the earliest Triassic (Chen et al. 2005; Brayard et al. 2006; Song et al. 2011; Kocsis et al. 2018). Reefs did not return to their pre-PTME diversity for ~8 million years (Chen et al. 2005; Martindale et al. 2019), but full structural recovery of marine ecosystems may have taken as long as 50 million years (Song et al. 2018).

1.3.4 Recovery in the Triassic

The maintenance of high temperatures through the Early Triassic delayed recovery from the PTME (Song et al. 2011; Petsios et al. 2019), with tropical seawater temperatures peaking at 38°C during the late Smithian Thermal

Maximum (LSTM; Sun et al. 2012). The climate of the Middle Triassic has received less attention, but is thought to have been characterised by continued terrestrial aridity in lower latitudes, with cyclical temperature fluctuations overprinting a general trend of steady cooling after the final eruptions of the Siberian Traps in the Olenekian (Preto et al. 2010; Trotter et al. 2015).

The Early Triassic saw a "reef eclipse", with most known reefs being microbialites inhabited by microscopic metazoans, generally in the low palaeolatitudes (Martindale et al. 2019). Platform margin reefs did not return until the late Anisian (late Middle Triassic), approximately coincident with the beginning of the rifting of Pangea, which may have provided a more varied seafloor bathymetry, aiding the recovery (Martindale et al. 2019). Brachiopods were severely affected by the mass extinction, with pre- and post-PTME brachiopod faunas almost entirely taxonomically distinct (Powell et al. 2015), and the clade has maintained a low diversity and shallow LDG since the extinction event (Powell 2009).

Pelagic animals such as ammonoids and conodonts appear to have recovered relatively quickly after the PTME (Stanley 1988; Brayard et al. 2006; Song et al. 2011, 2018). The ammonoids that survived the event exhibited low disparity, and may represent a monophyletic group (Brayard et al. 2006; Wignall 2015). Brayard et al. (2006) found that recovery in the Early Triassic corresponded with a gradual strengthening of the ammonoid LDG to form a unimodal equatorial peak in the Smithian. The clade experienced further extinction associated with the LSTM, but their recovery in the Spathian was stronger, resulting in a likely bimodal LDG with a dip at the equator, more endemic clades and greater boreal occupancy (Brayard et al. 2006). The first marine reptile fossils are known from the Olenekian, but the group was highly diverse by the Anisian, including basal sauropterygians and ichthyosaurs (Benson & Butler 2011).

On land, plant communities remained simple during the Early Triassic (Wignall 2015), and there is evidence for some taxa migrating poleward as a result of the high temperatures (Kerp et al. 2006). A coincident 'coal gap' indicates the loss of peat swamps at this time (Kerp et al. 2006; Preto et al. 2010; Sun et al. 2012). Temnospondyl amphibians and their cynodont predators were common in the Early Triassic (Wignall 2015), after which archosauromorphs diversified to become the dominant terrestrial animals; although abundant in the Late Triassic, phylogenetic analysis indicates that they radiated in the Olenekian, but their fossil record is poor at this time (Ezcurra & Butler 2018). Both tetrapods and macroflora had developed distinct latitudinal communities by the Late Triassic (Ezcurra 2010; Whiteside et al. 2011).

1.4 Summary

It is clear that understanding LDGs and their drivers is not straightforward. Evidence is accruing which implicates climate and habitat distribution in dictating LDGs throughout Earth history (Erwin 2009; Tittensor et al. 2010; Naimark & Markov 2011; Mannion et al. 2012, 2014), but their relative importance, and the role of other factors, is poorly understood. There is still much to be learned by examining LDGs in the fossil record, particularly during greenhouse intervals, about which we know much less than icehouse intervals (Mannion et al. 2014; Jablonski et al. 2017). The Permian and Triassic periods present an opportunity to investigate the relationship between continental distribution, climate and LDGs during a time of mass extinction, a confounding variable which has been given limited consideration thus far (Mannion et al. 2014). Here I present three chapters of my own research in which I investigate Permian and Triassic LDGs on land and in the oceans, and the role of variation in origination and extinction rates in producing these trends.

Chapter 2 – The latitudinal diversity gradient of tetrapods across the Permian-Triassic mass extinction and recovery interval

2.1 Introduction

Two previous studies have offered perspectives on the distribution of tetrapods across the Permian-Triassic boundary. Sun et al. (2012) used oxygen isotopes in conodont apatite to examine sea surface temperature (SST) change across the late Permian and Early Triassic, recovering remarkably high SSTs throughout the interval but particularly during the late Smithian Thermal Maximum (LSTM; ~248 Ma), when equatorial SSTs may have approached 40°C. Their qualitative analysis of tetrapod occurrences revealed an equatorial 'tetrapod gap' in the Early Triassic, hypothesised to have occurred due to the extreme warm temperatures that may have approached or exceeded the thermal tolerances of vertebrates (around 42°C; Pörtner 2002). Bernardi et al. (2018) also examined the distribution of individual tetrapod skeletal and footprint occurrences through the extinction and recovery interval, finding evidence for a poleward shift in tetrapod abundance in the northern hemisphere, but only in the Induan (earliest Triassic). This biogeographic pattern is congruent with a study of tetrapods immediately prior to the PTME, which found higher tetrapod diversity at temperate than equatorial latitudes during the middle and late Permian (Brocklehurst et al. 2017). These latter two studies both employed methods which attempted to ameliorate the effects of sampling bias.

Here, I explore further the terrestrial and marine Permian-Triassic fossil tetrapod record by comparing species-level tetrapod biodiversity across latitudinal bins. I apply coverage-based interpolation and squares extrapolation to reconstruct LDGs from the late Permian (before the PTME), Early Triassic (in the aftermath of the PTME) and Middle Triassic (during recovery). These LDGs are then assessed in light of the hypothesis that higher diversity will be found in the cooler refugia of the mid to high latitudes during extreme greenhouse conditions, such as during the late Permian to Middle Triassic.

2.2 Methods

I conducted an in-depth literature review to maximise the completeness and robustness of my late Permian to Late Triassic dataset for tetrapods. All tetrapod fossils from the Wuchiapingian (early late Permian) through Carnian (early Late Triassic) were downloaded from the Paleobiology Database (PBDB)

(see Supplementary Information). Genus names from this download were used to conduct a systematic literature search in Google Scholar, and any new taxa and occurrences were added to the PBDB. Once completed, the same criteria were used to download the enlarged dataset (in October 2018). I manually reviewed each 'collection', representing fossils from a particular locality and considered to be of a similar age, to increase temporal resolution. A literature search for formation names was conducted, with publications that listed the ages of specific beds or members further refining the geological date of collections, where possible (see Supplementary Information). I streamlined the mode of preservation and taxon habitat categories, reduced to either 'body' or 'trace', and 'marine' or 'terrestrial', respectively. Finally, the modern latitude and longitude of fossil localities were rotated to their palaeo-position at the time of deposition by filtering occurrences on a stage-by-stage basis, then using the PALEOMAP Global Plate Model (version 2; Scotese 2016), implemented in GPlates (version 2.1.0; Müller et al. 2018). The final dataset constituted 3,563 unique tetrapod occurrences assigned to stage level, with my search efforts contributing 490 of these occurrences (13.8%).

All subsequent data manipulation and plotting was carried out in R (version 3.5.1; R Core Team 2018) using the 'tidyverse' suite of packages (Wickham et al. 2019). Since abundance data in the PBDB are relatively incomplete and inconsistently applied, the presence of a species within any given collection was treated as a single occurrence. The final dataset was filtered to include only records representing species unique to the spatiotemporal bin of interest, comprising those identified to species level, and those identified to a clade not already represented within occurrences identified to a more precise taxonomic level. Using this approach, fossil occurrences dated to a single geological stage were used to produce raw sampled-in-bin tetrapod richness curves.

To compare tetrapod richness patterns across space between the late Permian, Early Triassic, and Middle Triassic, stage-level occurrences were binned using 20° latitudinal bands, from 90°S to 90°N (the central bin includes the equator, from 10°N to 10°S), on the basis of their palaeo-coordinates. Terrestrial and marine body fossils were analysed separately, with 'marine tetrapods' referring to species whose morphology indicates life in marine habitats. This informal group is polyphyletic and includes basal ichthyosaurs, sauropterygians, tanystropheids and thalattosaurs. At present, their oldest known fossils are dated to the Olenekian (late Early Triassic).

I applied two analytical approaches to account for spatiotemporal sampling biases in occurrence data: coverage-based interpolation (Chao & Jost 2012; Hsieh et al. 2016) and squares (Alroy 2018). Both were applied to collections

within latitudinal bins for the late Permian, Early Triassic, and Middle Triassic time intervals (analyses were repeated for individual stages, see Figure S2–2). Only body fossils were used for these analyses, due to the biological non-equivalence of trace fossil and body fossil species; one animal can produce multiple trace fossils, and traces are not easily allied to individual body fossil species.

Richness estimates were generated using coverage-based interpolation following the approach of Dunne et al. (2018) using the R package iNEXT (Hsieh et al. 2016). This approach conducts coverage-based rarefaction using the equations of Chao & Jost (2012) (analogous to shareholder quorum subsampling (SQS); Alroy 2010; Close et al. 2018) and extrapolation based on the Chao1 estimator. Extrapolated estimates were discarded if more than three times the observed sample size, as this suggests a high species-to-occurrence count ratio that indicates the bin under consideration is likely to be undersampled (Hsieh et al. 2016). Bins containing fewer than three species (see Table S2–1) were incompatible with subsampling and therefore excluded from analyses. Coverage-based rarefaction curves are also provided (Figure S2–3) to illustrate the relationship between coverage and coverage-standardised diversity estimates in each bin (Close et al. 2018; Dunne et al. 2018).

In addition to coverage-based interpolation, richness estimates were generated using the squares method (Alroy 2018). Squares is an extrapolater based on the proportion of singletons in a given sample, and is considered more robust to biases arising from small sample sizes and uneven richness distributions than other interpolation methods (Alroy 2018; 2020). Squares richness estimates were produced using the equation stated by Alroy (2018).

Finally, I tested whether variation in sampling intensity between time bins influenced richness estimates, particularly given the expected reduction in Early Triassic tetrapod occurrences following the PTME. I subsampled to the same number of collections in each time interval (late Permian, Early Triassic and Middle Triassic) using a bootstrap routine. For each time bin, I randomly sampled 250 collections for terrestrial tetrapods and 30 collections for marine tetrapods. Collections were allocated to their corresponding latitudinal bin and species richness was quantified across collections within each bin. This process was repeated 100 times. Diversity curves were produced using the mean species diversity in each latitude bin across the 100 replicates, allowing for comparison of LDGs among time bins given an artificially-fixed sampling intensity.

2.3 Results

2.3.1 Sampling

Raw richness, squares and interpolation estimates produced similar diversity-through-time curves (Figure S2–1). The number of collections with terrestrial tetrapod body fossils was relatively consistent through time (late Permian, 291; Early Triassic, 307; Middle Triassic, 354), while the number of collections containing marine tetrapods increased from the Early to Middle Triassic (Early Triassic, 32; Middle Triassic, 207). Curves of raw species richness by latitude bin produced by bootstrapping to the same number of collections for each time interval were near-identical to those using the full dataset (Figure S2–4).

2.3.2 Terrestrial distribution

Terrestrial tetrapod occurrences were broadly distributed but clustered throughout the studied interval (Figure 2–1a). Both squares and interpolation analyses of terrestrial tetrapods by latitude (Figure 2–1c) show a consistent bimodal richness distribution throughout the late Permian to Middle Triassic, with a persistent dip in diversity in the low southern latitudes. In the northern hemisphere, diversity peaked at 40°N in the late Permian. By the Early Triassic, the peak in species diversity had shifted to the 20°N bin (Figure 2–1b), with stage-level analyses indicating this occurred in the Olenekian (Figure S2–2b). In the Middle Triassic, the northern hemisphere peak returned to 40°N. The gradient in the southern hemisphere remained relatively unchanged throughout the late Permian to Middle Triassic, characterised by a consistent 60°S diversity peak.

2.3.3 Marine distribution

Marine tetrapod occurrences were generally restricted to the northern hemisphere during the Early and Middle Triassic, despite having a relatively broad longitudinal distribution (Figure 2–1a). Early Triassic marine tetrapods were most diverse in the 20°N bin, with the only other occurrences found in the 40°N bin (Figure 2–1d). The 20°N peak in biodiversity persisted into the Middle Triassic, but with new occupation of the equatorial and 20°S bins. The stage-level analyses generally show comparable trends to those seen in the epoch-

level time bins, but often with fewer bins occupied, producing patchier and less constrained gradients (Figure S2–2).
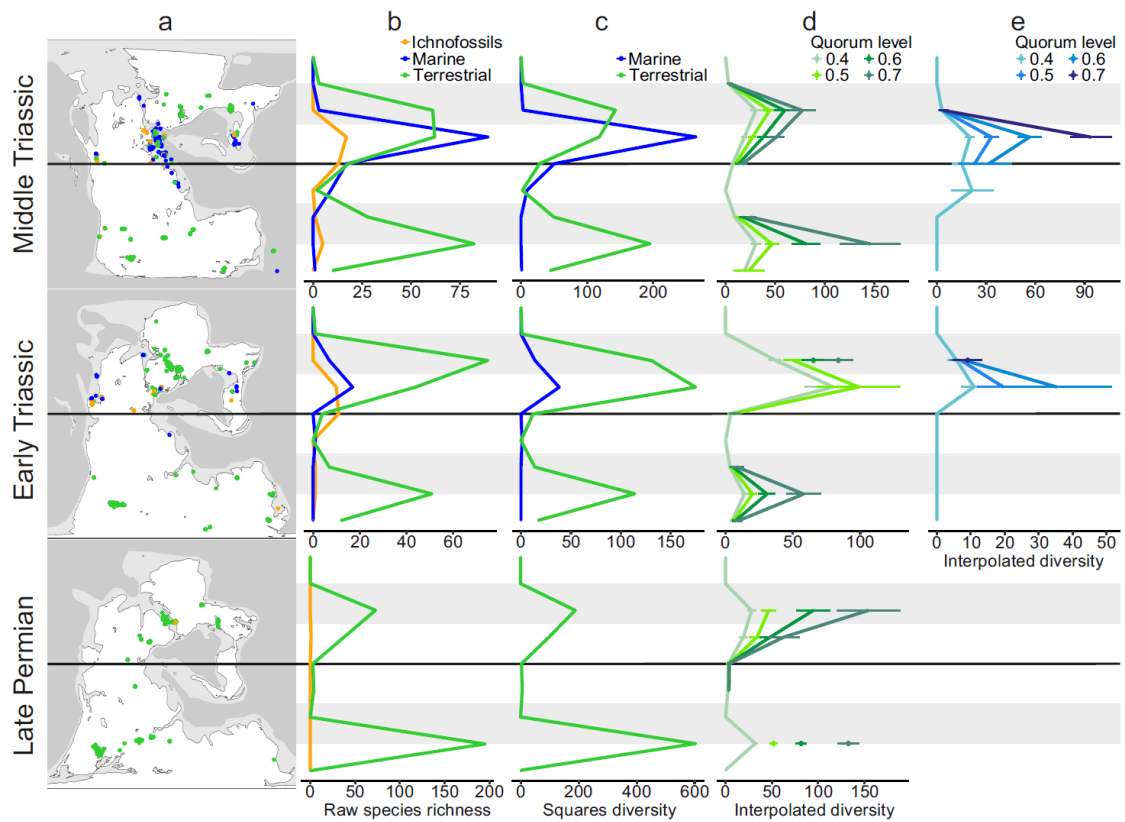
Figure 2–1: Tetrapod diversity by latitude in the late Permian, Early Triassic and Middle Triassic. The grey bars indicate 30–60°N and S.

a. Palaeo-rotated occurrence locations plotted over maps from Scotese (2016); maps represent the Lopingian, Induan-Olenekian, and Ladinian.

b. Raw occurrences within 20° latitude bins (e.g. central bin is 10°N–10°S).

c. Squares diversity by latitudinal bin for terrestrial (green) and marine (blue) tetrapods.

d. Interpolated diversity by latitudinal bin for terrestrial tetrapods. Bins with < 3 species have been plotted as '0', while missing points indicate an estimated diversity of more than three times the observed value. Error bars indicate 95% confidence intervals.

e. Interpolated diversity by latitudinal bin for marine tetrapods. Bins with < 3 species have been plotted as '0', while missing points indicate an estimated diversity of more than three times the observed value. Error bars indicate 95% confidence intervals. The oldest marine tetrapod fossils are Olenekian (late Early Triassic; 251–247Ma) in age.

2.3.4 Comparison with modern LDGs

The Early Triassic terrestrial LDG produced by interpolation was compared to LDGs of modern birds, mammals and amphibians (Figure 2–2; modern data derived from http://biodiversitymapping.org, as used by Saupe et al. 2019a). The modern curves have unimodal distributions that peak at low latitudes (maximum diversity at 9.5°S for birds and amphibians, 2.5°N for mammals), whereas the Early Triassic terrestrial curve peaks at higher latitudes, with a clear bimodal distribution (maximum diversity at 32.5°N and 62.5°S).
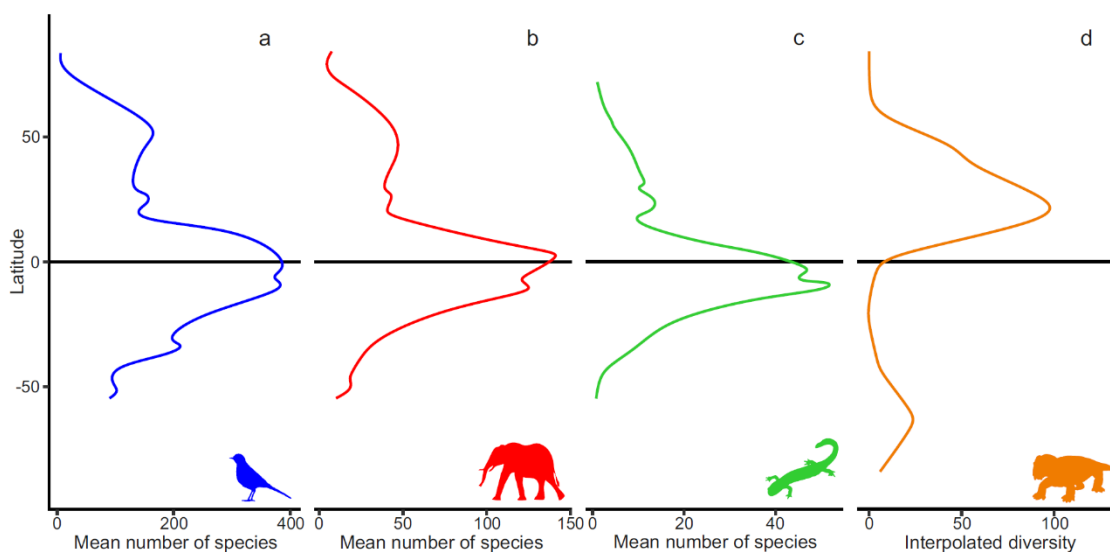
Figure 2–2: Smoothed latitudinal gradients for species of modern birds (a), mammals (b), and amphibians (c), compared with Early Triassic terrestrial tetrapods (as an example) based on interpolation analyses (d). Modern gradients derive from data obtained from http://biodiversitymapping.org.

2.4 Discussion

In contrast to gradients for modern terrestrial tetrapods (Hillebrand 2004; Kinlock et al. 2018), the Permian-Triassic terrestrial tetrapod gradient was likely bimodal with reduced diversity at low latitudes (10°N–30°S) (Figure 2–1). The general shape of the terrestrial tetrapod richness gradient, particularly its bimodality, remained relatively constant throughout the late Permian to Middle Triassic, and may reflect the prevailing climate regime (greenhouse versus icehouse) (Naimark & Markov 2011; Mannion et al. 2014; Saupe et al. 2019b; Meseguer & Condamine 2020). Interestingly, the shape of the gradient did not

seem affected by the PTME or even higher temperatures of the Early Triassic (equatorial SSTs increased from ~24°C in the latest Permian to ~40°C during the LSTM; Sun et al. 2012). Marine tetrapods, by contrast, maintained a diversity peak at low latitudes in the northern hemisphere from the Early to Middle Triassic (Figure 2–1). The bimodal terrestrial LDG obtained here is comparable to the distribution of raw Early Triassic tetrapod occurrences from Sun et al. (2012) and Bernardi et al. (2018), and suggests continuity of LDG shape from the middle Permian (Brocklehurst et al. 2017) and into the Late Triassic (Dunne et al. 2021). The shape of the gradient is also broadly comparable to the gradient of Mesozoic dinosaurs, which Mannion et al. (2012) attributed to the distribution of land area during the break-up of Pangea. This congruence suggests terrestrial LDGs may have been bimodal for much of the Permian to mid Cenozoic, with modern LDGs only developing as global climate gradually cooled through the late Paleogene and early Neogene (Fraser et al. 2014; Mannion et al. 2014; Marcot et al. 2016; Meseguer & Condamine 2020).

Although latitude is a reasonable proxy for temperature in the modern, this relationship does not hold for the Triassic (Preto et al. 2010). The latitudinal temperature gradient today largely reflects the operation of Hadley cells, but these cells may have collapsed in the late Permian to give way to a more zonally asymmetric atmospheric system, with strong seasonal variation in temperature and precipitation (Parrish 1993; Preto et al. 2010; Tabor et al. 2018). Although the Tethyan coastal regions experienced supermoonsoons, considerably less precipitation reached the continental interior, resulting in high aridity, particularly in the southern low to mid latitudes (Parrish 1993; Wignall 2015). Climate model reconstructions for the latest Permian suggest large areas of central Pangea were desert, with seasonal average temperatures up to 45°C in the arid subtropics at 20–25°N and S (Roscher et al. 2011). Late Permian palaeoenvironmental evidence from localities in South Africa indicates considerable drought even at relatively high latitudes (~65°S; Smith & Botha-Brink, 2014). As a result, much of the supercontinent interior may have been uninhabitable in the late Permian, which could explain the bimodal, asymmetric tetrapod LDG reconstructed here. However, in contrast to Permian climates, Triassic climates have not been well studied (Preto et al. 2010; Trotter et al. 2015), and the development of high-resolution climate models for the Triassic is essential for determining the key drivers of tetrapod extinction and migration during this interval.

The bimodal richness distributions found here are cautiously interpreted as biologically meaningful, particularly given the agreement between the different sampling methodologies employed. In addition, collections from southern low

latitude regions are consistently of low alpha diversity throughout the entire late Permian to Middle Triassic, in comparison with some very high levels of alpha diversity in mid-latitude collections during the same intervals (Table S2–2). However, the spatial and temporal resolution of the analyses, and our certainty in the observed distributions representing biological patterns, would benefit from better geographic spread and higher density of samples (Benson & Upchurch 2013; Vilhena & Smith 2013; Close et al. 2017). New discoveries from the southern low to mid latitudes could particularly help to distinguish between low biodiversity and poor sampling, but fossiliferous outcrops of this age and palaeolatitude are uncommon, particularly from terrestrial environments (Figure S2–5; Preto et al. 2010; Benson & Upchurch 2013; Tabor et al. 2018). Although extensive shallow and marginal marine deposits, such as those in Oman, are rich in invertebrate fossils (e.g. Krystyn et al. 2003), vertebrate fossils are known only from a handful of localities, such as Gour Laoud in Algeria (*Jesairosaurus lehmani, Odenwaldia* sp., indeterminate amphibians; palaeolatitude 9°S; Jalil 1999) and Mariakani in Kenya (*Kenyasaurus mariakaniensis*; palaeolatitude 42°S; Harris & Carroll 1977). Unfortunately, the age of fossils from these localities is poorly constrained and were therefore not included in our analyses.

Although broad stasis in bimodal richness gradients was observed over the ~23 million year interval considered here (late Permian–Middle Triassic), smaller-scale variability can be detected among time bins. Both squares and interpolation analyses suggest a shift in peak diversity in the northern hemisphere towards the equator in the Early Triassic, before returning to mid-latitudes in the Middle Triassic. This shift is also supported by the relatively high number of trace fossil occurrences in the equatorial and 20°N bins during the Early Triassic (Figure 2–1b). An Early Triassic equatorward shift in diversity in the northern hemisphere seems surprising given that global temperatures were increasing at the time. Instead, this shift may reflect differential sampling bias. Most of the interpolation rarefaction curves are exponential in shape, but the Early Triassic 20°N bin has a more asymptotic curve (Figure S2–3), indicating sampling completeness may be substantially higher in this bin relative to the others, inflating diversity estimates (Close et al. 2018). This peak in diversity corresponds to the high density of tetrapod fossils known from the Olenekian of Eastern Europe (Shishkin & Novikov 2017).

Chapter 3 – Investigating drivers of the latitudinal diversity gradients of brachiopods and bivalves during the Permian and Triassic

The palaeoclimate modelling included in this chapter was conducted by the Bristol Research Initiative for the Dynamic Global Environment (BRIDGE) Group, led by Paul Valdes, in the School of Geographical Sciences at the University of Bristol. The climate outputs from these models were kindly processed and provided for use within this research by Alex Farnsworth.

3.1 Introduction

Although spatial aspects of recovery from the Permian-Triassic mass extinction (PTME) have been widely reported on (e.g. Chen et al. 2005; Payne & Clapham 2012; Sun et al. 2012; Song et al. 2018; Martindale et al. 2019), only three studies have previously examined latitudinal diversity gradients (LDGs) in the marine realm at this time. Powell (2009) reconstructed the LDG of brachiopods across the Phanerozoic, and found a shallow, unimodal richness gradient both before and after the PTME. This result was reiterated by Powell et al. (2015), who examined the relationship between LDG shape and latitudinal variation in evolutionary rates.

Brayard et al. (2006) found that ammonoids had a flat LDG during the Griesbachian, immediately after the PTME, but developed a unimodal equatorial peak in diversity during the subsequent Dienerian and Smithian substages. Following taxonomic turnover associated with the late Smithian Thermal Maximum (LSTM), a bimodal distribution in richness was recovered in the Spathian, more similar to that of pelagic taxa in the modern day (Chaudhary et al. 2016, 2021). However, this study disregarded occurrences discovered outside of the richest basin faunas, and failed to account for sampling bias beyond a simplistic range-through approach.

Song et al. (2020) investigated the LDG of 20 major marine animal clades together in a single diversity curve, from the late Permian to Late Triassic. They found that the late Permian, Middle Triassic and Late Triassic had unimodal LDGs with peaks in the low northern latitudes. However, the Early Triassic LDG, during PTME recovery, was much flatter, fitting the hypothesis that greenhouse climate conditions in deep time were associated with shallow or bimodal LDGs (e.g. Mannion et al. 2014). The collapse of tropical reef ecosystems associated with the PTME may also have contributed to a fall in diversity at low latitudes

(e.g. Martindale et al. 2019). Song et al. (2020) mentioned temperature, shallow shelf area, contrasting rates of biotic recovery, and sampling bias as possible drivers of the spatial diversity patterns observed during this interval. However, the coarse taxonomic resolution used by Song et al. (2020) may have masked more complex dynamics in the LDGs of the constituent clades. Furthermore, the higher latitudes (45–90°N and S) were grouped together into a single latitudinal band, limiting the ability of this study to comment on spatial richness patterns at mid to high latitudes.

Here, I investigate the spatial biodiversity patterns of brachiopods and bivalves, two benthic marine invertebrate clades with relatively rich fossil records, during the Permian and Triassic. I apply coverage-based interpolation and an equal area subsampling regime to reconstruct LDGs for each geological stage from the Roadian (early middle Permian) to the Ladinian (late Middle Triassic). Linear regression is then used to test the fit of estimates of palaeoclimate and shallow shelf area against the LDGs, to determine whether these environmental factors drove the spatial diversity trends of benthic marine invertebrates in the Permian and Triassic.

3.2 Methods

3.2.1 Fossil dataset

Similar to Chapter 2, I conducted an in-depth literature review to improve the completeness and robustness of my fossil dataset. I downloaded a list of brachiopod and bivalve genera with occurrences dated from the Roadian (early middle Permian) to the Ladinian (late Middle Triassic) from the Paleobiology Database (PBDB). This list was used to conduct a systematic literature search in Google Scholar, and any missing taxa and occurrences were added to the PBDB. A recent comprehensive review of Triassic bivalve genera (Ros-Franch et al. 2014) was used to find additional occurrences and to update taxonomy. A list of formation names containing 10 or more brachiopod and/or bivalve occurrences from the same time interval was then downloaded. These formation names were used in a literature search to identify the most refined, recently reported geological date for each formation, which was then used to update the ages attributed to the relevant collections directly in the PBDB.

The enlarged dataset was downloaded from the PBDB (in February 2021), including all occurrences of Brachiopoda or Bivalvia dated between the Roadian and Ladinian (see Supplementary Information). Fossils from non-marine palaeoenvironments, those dated more coarsely than to a single stage, and

those with uncertainty expressed in their generic identification, were excluded from the dataset. To determine the palaeo-coordinates of the fossils at their time of deposition, occurrences were filtered on a stage-by-stage basis and rotated from their modern latitudes and longitudes using the PALEOMAP Global Plate Model (version 3; Scotese 2018), implemented in GPlates (version 2.1.0; Müller et al. 2018).

3.2.2 LDGs

Subsequent data manipulation and plotting was conducted in R (version 4.0.4; R Core Team, 2021) using the packages 'iNEXT' (Hsieh et al. 2016), 'maptools' (Bivand & Lewin-Koh 2020), 'raster' (Hijmans 2020), 'rgdal' (Bivand et al. 2021), 'rgeos' (Bivand & Rundel 2020), and 'sp' (Bivand et al. 2013), alongside the 'tidyverse' suite of packages (Wickham et al. 2019).

As abundance data are lacking for many PBDB collections, the presence of a taxon within a collection was considered a single occurrence. However, PBDB collections vary considerably in their spatio-temporal extents. To increase the equivalency of occurrences, collections dated to the same substage and modern latitude and longitude to the nearest 0.01°, which mostly constituted different beds within the same geological section, were considered to be a single locality and were 'pooled' into one occurrence. Due to uncertainty around the taxonomic identification of brachiopods and bivalves at species level, richness was calculated at generic level. The final dataset constituted 22,979 unique genus-level brachiopod and bivalve occurrences, 1,333 (5.8%) of which I added to the PBDB during this project.

To examine brachiopod and bivalve richness across space, fossil occurrences were allocated to 20° latitudinal bands using their palaeo-coordinates, from 90°N to 90°S, with the central band straddling the equator (10°N to 10°S). Raw generic diversity counts by latitude for both clades were then calculated for each stage from the Roadian to the Ladinian. As described in Chapter 2 (and using the same protocol), coverage-based interpolation as applied using the R package iNEXT (Chao & Jost 2012; Hsieh et al. 2016) was also used to estimate richness within latitudinal bands for each stage, to a quorum level of 0.5. Estimates extrapolated to more than three times their measured sample size were removed due to the unreliability associated with overextrapolation (Hsieh et al. 2016).

Additional richness estimates were calculated that account for differences in the geographic area sampled between latitudinal bands. An equal area grid was

produced by splitting a sphere with Earth's radius into 1° latitudinal bands, each of which was then subdivided longitudinally to create cells as close as possible to 10 km^2 in area. All fossil occurrences were then allocated to grid cells based on their palaeo-coordinates. To estimate richness, five grid cells were selected from each 20° latitudinal band, with the occurrences present within those cells used as a subsample from which generic richness was calculated. Latitudinal bands containing less than five occupied grid cells for a given clade were excluded from the analysis. This subsampling routine was conducted 100 times for each stage to produce mean richness counts across replicates. To further account for sampling bias, this regime was also repeated with the additional application of the squares extrapolater (Alroy 2018) to generic diversity, as described in Chapter 2.

3.2.3 Environmental data

Palaeoclimate model simulations were used to estimate the climatic conditions experienced by the brachiopods and bivalves during life. The simulations were produced using the HadCM3L general circulation model (GCM), specifically HadCM3LB-M2.1 (Valdes et al. 2017). HadCM3L is a fully coupled atmosphere-ocean GCM incorporating the Gent & McWilliams (1990) oceanic mixing scheme and the MOSES 2.1 land surface scheme, including the fully interactive vegetation model TRIFFID (top-down representation of interactive foliage and flora including dynamics; Cox 2001). The model operates across 19 vertical atmospheric levels and 20 oceanic depth levels, each at a spatial resolution of 2.5° latitude by 3.75° longitude. Boundary conditions in the model were defined using the PALEOMAP Paleo-Digital Elevation Models (DEMs) (Scotese & Wright 2018), interpolated from 1° latitude-longitude cells to the coarser resolution required by the GCM. HadCM3L has been shown to accurately reconstruct climate patterns in deep time at a range of spatial scales (Farnsworth et al. 2019a) and has previously been used in multiple palaeontological studies (Fenton et al. 2016; Chiarenza et al. 2019; Saupe et al. 2019b; Antell et al. 2021; Dunne et al. 2021).

Separate simulations were run for each geological stage from the Roadian to the Ladinian, using the palaeo-DEM and reduced solar constant (Gough 1981) relevant to the stage, following the standardised methodology of Lunt et al. (2016). Atmospheric CO_2 concentrations for each stage were based on the estimates of Foster et al. (2017), but it should be noted that CO_2 levels during the Permian and Triassic are contentious and likely to have changed considerably, including a proposed sixfold increase at the Permian-Triassic

boundary (Wu et al. 2021). Each simulation was run for approximately 1,400 years, at which point atmospheric and upper ocean systems had reached equilibrium states and the deep ocean was close to equilibrating (Farnsworth et al. 2019b).

Eight climatic variables were estimated from the model outputs: mean annual temperature at the sea surface (MAT), mean annual temperature at 100m below sea level, warm month mean temperature (WMMT), cold month mean temperature, mean annual salinity at the sea surface (MAS), mean annual salinity at 100m below sea level, maximum monthly mean salinity, and minimum monthly mean salinity. Metrics of seasonal temperature and salinity variation were also calculated as the difference between warm and cold monthly mean temperatures, and maximum and minimum monthly salinity. These climatic variables were extracted for each collection, or locality, in the marine invertebrate dataset, from the GCM grid cell containing their palaeo-coordinates. Due to an imprecise fit between the collections and palaeo-DEMs, some localities were on land according to the palaeogeographies; for these, climatic information was extracted from the closest ocean grid cell within a 4 x 4 cell radius. Climatic data were available for a total of 5,353 brachiopod and/or bivalve-bearing collections (65.3% of all collections in the dataset). Mean values for each variable by latitude were calculated by subdividing fossil collections into their respective clades and averaging across collections found within each 20° palaeolatitudinal band.

Estimates of the amount of continental shallow shelf area within each latitudinal band for each stage were also produced using the PALEOMAP Paleo-DEMs (Scotese & Wright 2018). All 1° latitude-longitude cells with elevations between 350 metres above and below sea level were identified for each stage model, then were allocated to the same 20° latitudinal bands as those used for the fossil occurrences. This altitude and bathymetry was chosen to account for considerable uncertainty in the placement of coastlines in the palaeogeographies, especially considering the amount of coastline change possible over the duration of a geological stage (on average, ~10 million years). The equal area grid was then applied over these data to estimate the number of 10 km^2 cells containing continental shallow shelf for each latitudinal band.

3.2.4 Linear regression

I implemented generalised least squares (GLS) models to test for relationships between diversity, sampling, climate, and shallow shelf area by latitude for brachiopods and bivalves. Model fit was assessed using the Akaike Information

Criterion for small sample sizes (AICc; Hurvich & Tsai 1989). Models were composed of different combinations of MAT, MAS, MAT at 100m depth, MAS at 100m depth, WMMT, temperature seasonality, salinity seasonality, shallow shelf area, collection counts and number of occupied equal area grid cells, for each stage-palaeolatitude band spatio-temporal bin, with their fit assessed against each of the four diversity curves (raw, interpolated, equal area, equal area + extrapolation) for brachiopods and bivalves separately.

Prior to model fitting, transformations were applied to some of the variables to increase the normality of their residuals: the salinity and seasonality values were rank-ordered, and both sampling proxies (collection counts and number of occupied equal area grid cells) and all four types of diversity estimate were log10-transformed. High levels of collinearity (> 0.8 Pearson's r) were present between the temperature variables, the salinity variables, and the two sampling proxies, so models were not tested which contained more than one of each variable category. Sampling proxies accounted for by the methods implemented to create each diversity curve were not included: models fitted to the interpolated curves did not include the number of collections, models fitted to the equal area curves did not include the number of equal area cells occupied, and models fitted to the equal area curves with the squares extrapolator applied did not include either sampling proxy. The influence of temporal autocorrelation (the tendency of diversity in a given spatio-temporal bin to be dependent upon the diversity in the same palaeolatitude bin in the previous stage) was also investigated by comparing the fit of models with and without the addition of a first-order autoregressive model (AR-1). Model fitting was conducted in R using the packages nlme (Pinheiro et al. 2021) and MuMIn (Barton 2020).

3.3 Results

3.3.1 Sampling

The spatial spread of fossil occurrences was sufficient to occupy all 20° latitudinal bands for most stages during the middle Permian to Middle Triassic (Figure 3–1). Occurrence counts were generally highest at the equator for both clades throughout the interval. The Wuchiapingian appeared to deviate from this trend, with brachiopod occurrences being particularly abundant in the mid southern latitudes during this stage, while bivalves were most abundant in the low northern latitudes. Brachiopod occurrence numbers were heavily reduced by the PTME (3,149 in the Changhsingian, 275 in the Induan), but bivalves became more abundant (733 in the Changhsingian, 1,334 in the Induan). The
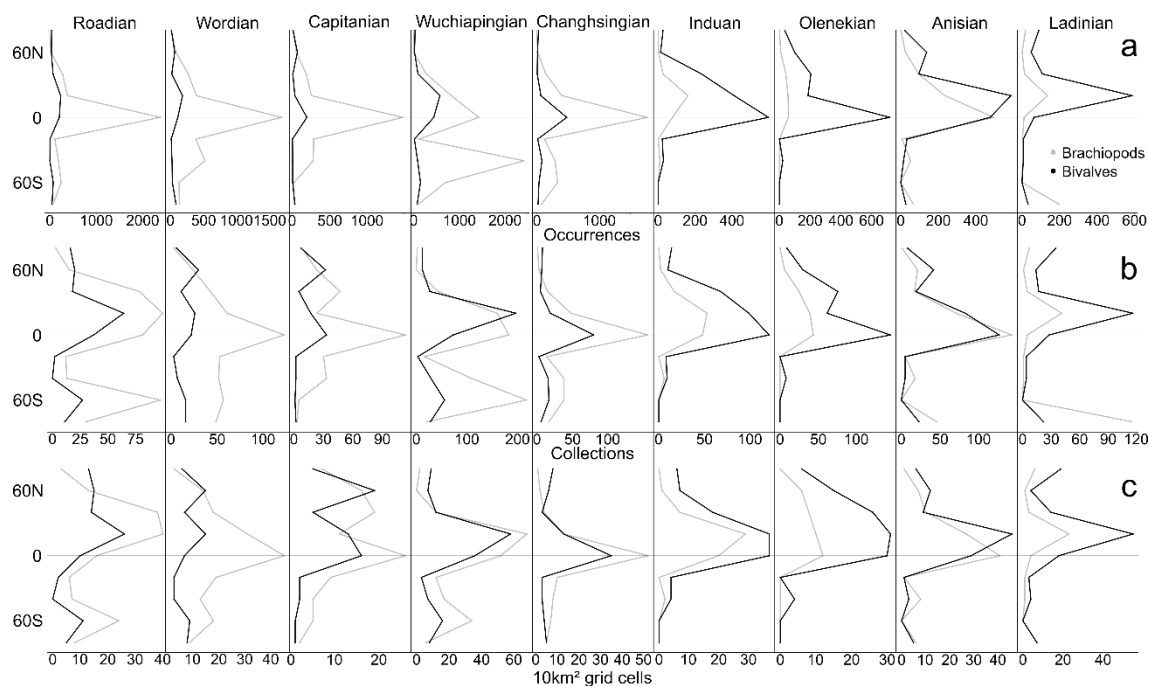
Figure 3–1: Bivalve (black) and brachiopod (grey) sampling proxies from the Roadian (early middle Permian) to the Ladinian (late Middle Triassic) in 20° latitudinal bands. Sampling metrics are a. number of occurrences; b. number of collections containing brachiopods and/or bivalves (analogous to localities); c. occupied 10 km² equal area grid cells.

spatial distribution of these occurrences did not change substantially across the Permian-Triassic boundary for either clade.

Counts of collections (localities) and occupied 10 km² grid cells were similarly distributed by latitude throughout the interval for both brachiopods and bivalves (Figure 3–1). Both counts indicate a stronger northern hemisphere representation in the dataset, particularly in the Triassic. The highest levels of sampling were from the equatorial (10°N–10°S) or low northern hemisphere (10–30°N) latitudinal bands for most stages.

3.3.2 Brachiopod and bivalve richness by latitude

Throughout the studied interval, the four diversity metrics produced brachiopod and bivalve richness curves that were broadly comparable in shape (Figure 3–2). Brachiopods had a consistently unimodal richness distribution, with highest diversity levels at the equator during the middle and late Permian, but with the diversity peak shifting into the northern low latitudes in the Early and Middle Triassic. Bivalves appear to have had a relatively even richness distribution by latitude in the middle Permian, but an equatorial peak in diversity developed in

the Changhsingian. This peak continued through the Early Triassic, before moving into the low northern latitudes in the Middle Triassic.
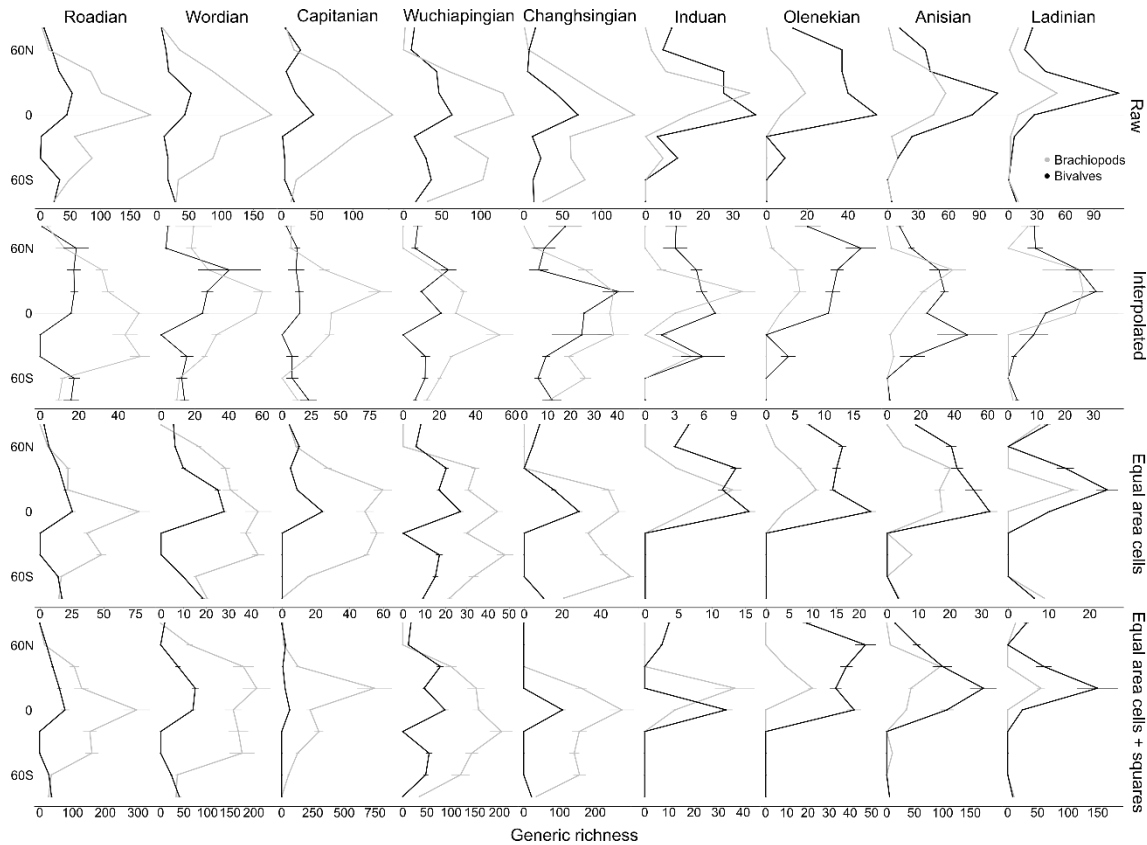
Figure 3–2: Bivalve (black) and brachiopod (grey) generic richness from the Roadian (early middle Permian) to the Ladinian (late Middle Triassic) in 20° latitudinal bands. Rows show (from top to bottom):

1. Raw generic diversity.

2. Estimated diversity using interpolation in iNEXT (Hsieh et al. 2016), to a quorum level of 0.5. Bins containing < 3 genera are plotted as '0', while missing values indicate an estimated diversity of more than three times the measured sample size. Error bars indicate 95% confidence intervals.

3. Mean diversity across 100 bootstraps of 5x equal area grid cells within each latitudinal band. Error bars indicate standard error across bootstraps.

4. Mean diversity across 100 bootstraps of 5x equal area grid cells within each latitudinal band, extrapolated using the Squares method (Alroy 2018). Error bars indicate standard error across bootstraps.

3.3.3 Drivers of marine invertebrate diversity

The addition of the AR-1 autoregressive model improved the fit of the brachiopod GLS models for all four diversity curves, by approximately 5 AICc points. However, for bivalves, the AR-1 model only improved the fit of models applied to the equal area diversity curves, and was not included in models for the other three diversity metrics.

Sampling was an important driver of raw spatial richness patterns, with the number of fossil-bearing collections being a component of nine of the ten best-fitting models between the two clades (Table 3-1). However, there was also evidence that palaeotemperature played a role in controlling these trends, as MAT was included in the best-fitting model for brachiopods, and the second-best-fitting model for bivalves, showing a positive relationship with diversity for both (Table 3-2). WMMT (alongside number of collections) also appeared in the top five best-fitting models for both clades.

For both brachiopods and bivalves, the best-fitting model for the interpolated diversity curves was the null model, while the second-best-fitting model only included the number of equal area grid cells occupied (Table 3-3). The palaeoenvironmental parameters were therefore a poor fit to these diversity curves.

The best-fitting model for the brachiopod equal area diversity curve was MAT alone (Table 3-5), and all of the five best-fitting models for this clade include a palaeotemperature parameter, all showing greater diversity at higher temperatures (Table 3-6). In contrast, the number of fossil collections alone was the best-fitting model for the bivalve equal area curve, and this proxy was included in all of the five best-fitting models (except the fourth, which was the null model). WMMT was included in the second-best-fitting model for bivalves, but the AIC weighting of this model is considerably lower than that of the number of collections in isolation (0.05 compared to 0.85; Table 3-5).

The best-fitting model for the equal area and squares-extrapolated diversity curves for both clades was MAT, with WMMT being the second-best-fitting model (Table 3-7), again positively related to diversity (Table 3-8). The null model was the third-best-fitting for brachiopods, with an AIC weighting relatively close to the top two models (0.36 for MAT, 0.28 for WMMT and 0.25 for the null), but the top five best models for bivalves only included palaeotemperature and salinity parameters.

Collectively, these results suggest that palaeotemperature was most likely to have been an important driver of marine invertebrate spatial diversity patterns in the Permian and Triassic, particularly for brachiopods. The relationship between

MAT and brachiopod and bivalve diversity across latitudes is summarised in Figure 3–4.
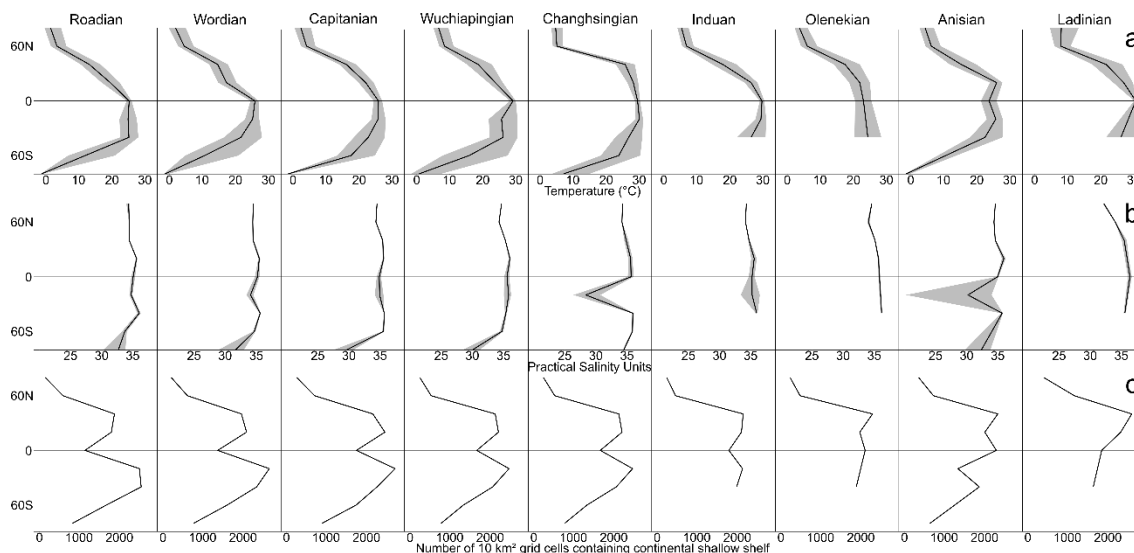
Figure 3–3: Ocean surface temperature, salinity and shallow shelf area from the Roadian (early middle Permian) to the Ladinian (late Middle Triassic), within 20° latitudinal bands.

a. Mean palaeotemperature of brachiopod- or bivalve-containing localities (collections) obtained from HadCM3L palaeoclimate models. Figure shows mean annual temperature (black) and seasonality (grey; upper value is warm month mean temperature, lower value is cold month mean temperature).

b. Mean palaeosalinity of brachiopod- or bivalve-containing localities (collections) obtained from HadCM3L palaeoclimate models. Figure shows mean annual salinity (black) and seasonality (grey; upper value is maximum monthly mean salinity, lower value is minimum monthly mean salinity).

c. Number of 10 km² grid cells containing continental shallow shelf (between 350m and -350m elevation) in the PALEOMAP Paleo-Digital Elevation Models (Scotese & Wright 2018).

Table 3-1: Top five model fits to raw richness, in order of AICc.

Brachiopods

Regression model	Pseudo-R^2	Log like.	AICc	AICc weight
MAT + collections + AR1	0.7737132	-16.69678	44.44619	0.4177702
MAT at 100m + collections + AR1	0.7706989	-17.20106	45.45475	0.2523089
Collections + AR1	0.7174718	-19.36492	47.41949	0.0944698
WMMT + collections + AR1	0.7612224	-18.40369	47.86001	0.0757942
MAT + EA cells + AR1	0.7595321	-18.43576	47.92415	0.0734016

Bivalves

Regression model	Pseudo-R^2	Log like.	AICc	AICc weight
Collections	0.5987188	-4.459565	15.28277	0.9659562
MAT + collections	0.6151807	-7.964083	24.54355	0.0094190
WMMT + collections	0.6132328	-8.147056	24.90950	0.0078440
MAT at 100m + collections	0.6109925	-8.223730	25.06284	0.0072651
Seasonal salinity + collections	0.6111363	-9.014911	26.64521	0.0032933

Table 3-2: Summary of explanatory variables in top five models for raw richness, in line with Table 3-1.

Brachiopods

	Intercept			Variable 1			Variable 2		
Model	Estimate	SE	p	Estimate	SE	p	Estimate	SE	p
MAT + collections	0.2184	0.1621	0.1829	0.0260	0.0066	0.0003	0.5561	0.0730	<0.0001
MAT at 100m + collections	0.3151	0.146	0.0353	0.0237	0.0064	0.0004	0.5637	0.0737	<0.0001
Collections	0.6242	0.1388	<0.0001	0.5627	0.0807	<0.0001			
WMMT + collections	0.2209	0.1704	0.1999	0.0221	0.0067	0.0016	0.5455	0.0759	<0.0001
MAT + EA cells	0.3496	0.1520	0.0249	0.0249	0.0066	0.0004	0.6666	0.0927	<0.0001

Bivalves

	Intercept			Variable 1			Variable 2		
Model	Estimate	SE	p	Estimate	SE	p	Estimate	SE	p
Collections	0.5563	0.0774	<0.0001	0.5870	0.0583	<0.0001			
MAT + collections	0.4955	0.0843	<0.0001	0.0049	0.0029	0.0951	0.5715	0.0582	<0.0001
WMMT + collections	0.4818	0.0898	<0.0001	0.0045	0.0029	0.1175	0.5752	0.0581	<0.0001
MAT at 100m + collections	0.5075	0.0837	<0.0001	0.0047	0.0032	0.1506	0.5753	0.0583	<0.0001
Seasonal salinity + collections	0.4915	0.0886	<0.0001	0.0021	0.0014	0.1482	0.5785	0.0581	<0.0001

Table 3-3: Top five model fits to SQS richness, in order of AICc.

Brachiopods

Regression model	Pseudo-R^2	Log likelihood	AICc	AICc weight
Null + AR1	0.2745799	-30.88141	68.20727	0.2461714
EA cells + AR1	0.3252272	-29.99863	68.75198	0.1874805
MAT + AR1	0.3831977	-30.16219	69.07909	0.1591929
MAT at 100m + AR1	0.3754844	-30.56172	69.87816	0.1067603
WMMT + AR1	0.3725423	-30.68574	70.12619	0.0943081

Bivalves

Regression model	Pseudo-R^2	Log likelihood	AICc	AICc weight
Null	4.44x10^{-16}	-27.68588	59.55926	0.7006050
EA cells	0.03353515	-27.88374	62.14844	0.1919728
MAT	0.06951791	-29.86734	66.11563	0.0264105
MAT at 100m	0.06349311	-29.96942	66.31978	0.0238476
WMMT	0.06349311	-30.18469	66.75033	0.0192288

Table 3-4: Summary of explanatory variables in top five models for SQS richness, in line with Table 3-3.

Brachiopods

	Intercept			Variable 1			Variable 2		
Model	**Estimate**	**SE**	**p**	**Estimate**	**SE**	**p**	**Estimate**	**SE**	**p**
Null	1.0907	0.1065	<0.0001						
EA cells	0.7854	0.1689	<0.0001	0.3157	0.1446	0.0333			
MAT	0.6712	0.1646	0.0001	0.0265	0.0084	0.0027			
MAT at 100m	0.7720	0.1423	<0.0001	0.0247	0.0082	0.0040			
WMMT	0.6172	0.1865	0.0016	0.0246	0.0083	0.0045			

Bivalves

	Intercept			Variable 1			Variable 2		
Model	**Estimate**	**SE**	**p**	**Estimate**	**SE**	**p**	**Estimate**	**SE**	**p**
Null	1.0320	0.0436	<0.0001						
EA cells	0.8787	0.1108	<0.0001	0.1601	0.1066	0.138			
MAT	0.8859	0.0787	<0.0001	0.0092	0.0042	0.0311			
MAT at 100m	0.9038	0.0744	<0.0001	0.0098	0.0047	0.0397			
WMMT	0.9034	0.0744	<0.0001	0.0098	0.0047	0.0397			

Table 3-5: Top five model fits to 5x equal area cell richness, in order of AICc.

Brachiopods

Regression model	Pseudo-R^2	Log likelihood	AICc	AICc weight
MAT + AR1	0.4929598	-11.48460	31.83877	0.2976375
WMMT + AR1	0.4868186	-11.79210	32.45376	0.2188489
MAT + collections + AR1	0.5321204	-11.00143	33.33619	0.1407753
MAT at 100m + AR1	0.4758821	-12.34611	33.56179	0.1257587
WMMT + collections + AR1	0.5182699	-11.74017	34.81366	0.0672508

Bivalves

Regression model	Pseudo-R^2	Log likelihood	AICc	AICc weight
Collections + AR1	0.4726870	9.597286895	-10.343510	0.8492152
WMMT + collections + AR1	0.5350754	7.887668281	-4.470989	0.0450626
MAT + collections + AR1	0.5323751	7.720053780	-4.135760	0.0381085
Null + AR1	0.3194688	5.056315629	-3.612631	0.0293377
MAT at 100m + collections + AR1	0.5110272	6.734248747	-2.164150	0.0142198

Table 3-6: Summary of explanatory variables in top five models for 5x equal area cell richness, in line with Table 3-5.

Brachiopods

	Intercept			Variable 1			Variable 2		
Model	**Estimate**	**SE**	**p**	**Estimate**	**SE**	**p**	**Estimate**	**SE**	**p**
MAT	0.8001	0.1227	<0.0001	0.0265	0.0063	0.0001			
WMMT	0.7182	0.1416	<0.0001	0.0260	0.0063	0.0001			
MAT + collections	0.5420	0.1756	0.0034	0.0251	0.0061	0.0001	0.1862	0.0935	0.0521
MAT at 100m	0.9078	0.1060	<0.0001	0.0245	0.0062	0.0002			
WMMT + collections	0.5052	0.1832	0.0082	0.0239	0.0061	0.0003	0.1686	0.0965	0.0871

Bivalves

	Intercept			Variable 1			Variable 2		
Model	**Estimate**	**SE**	**p**	**Estimate**	**SE**	**p**	**Estimate**	**SE**	**p**
Collections	0.6391	0.1155	<0.0001	0.3168	0.0760	0.0001			
WMMT + collections	0.5712	0.1062	<0.0001	0.0095	0.0037	0.0124	0.2496	0.0805	0.0032
MAT + collections	0.6005	0.106	<0.0001	0.0093	0.0807	0.0140	0.2537	0.0807	0.0028
Null	1.0932	0.0614	<0.0001						
MAT at 100m + collections	0.6033	0.1092	<0.0001	0.0079	0.0040	0.0532	0.2797	0.0799	0.0010

Table 3-7: Top five model fits to 5x equal area cell richness plus squares extrapolation, in order of AICc.

Brachiopods

Regression model	Pseudo-R^2	Log likelihood	AICc	AICc weight
MAT + AR1	0.4200882	-25.99314	60.96188	0.3575119
WMMT + AR1	0.4130567	-26.22688	61.42936	0.2829951
Null + AR1	0.2572363	-27.54324	61.65790	0.2524368
MAT at 100m + AR1	0.3824793	-27.35875	63.69311	0.0912459
Shelf area + AR1	0.3951240	-31.11948	71.21456	0.0021230

Bivalves

Regression model	Pseudo-R^2	Log likelihood	AICc	AICc weight
MAT	0.4310126	-12.90818	32.38778	0.6124529
WMMT	0.4096023	-13.69603	33.96348	0.2785566
MAT at 100m	0.3775372	-14.78220	36.13582	0.0940150
MAT + salinity at 100m	0.4386528	-17.05424	43.08408	0.0029134
Salinity at 100m	0.2910112	-18.39825	43.36793	0.0025279

Table 3-8: Summary of explanatory variables in top five models for 5x equal area cell richness plus squares extrapolation, in line with Table 3-7.

Brachiopods

	Intercept			Variable 1			Variable 2		
Model	Estimate	SE	p	Estimate	SE	p	Estimate	SE	p
MAT	1.1695	0.1820	<0.0001	0.0335	0.0091	0.0006			
WMMT	1.0625	0.2138	<0.0001	0.0329	0.0092	0.0009			
Null	1.7191	0.1295	<0.0001						
MAT at 100m	1.3175	0.1655	<0.0001	0.0303	0.0095	0.0027			
Shelf area	1.0205	0.2411	0.0001	0.0004	0.0001	0.0020			

Bivalves

	Intercept			Variable 1			Variable 2		
Model	Estimate	SE	p	Estimate	SE	p	Estimate	SE	p
MAT	1.1851	0.0739	<0.0001	0.0243	0.0042	<0.0001			
WMMT	1.1085	0.0885	<0.0001	0.0243	0.0044	<0.0001			
MAT at 100m	1.2394	0.0723	<0.0001	0.0252	0.0049	<0.0001			
MAT + salinity at 100m	1.2102	0.0812	<0.0001	0.0361	0.0090	0.0016	-0.0036	0.0047	0.4484
Salinity at 100m	1.2090	0.0902	<0.0001	0.0104	0.0025	0.0001			
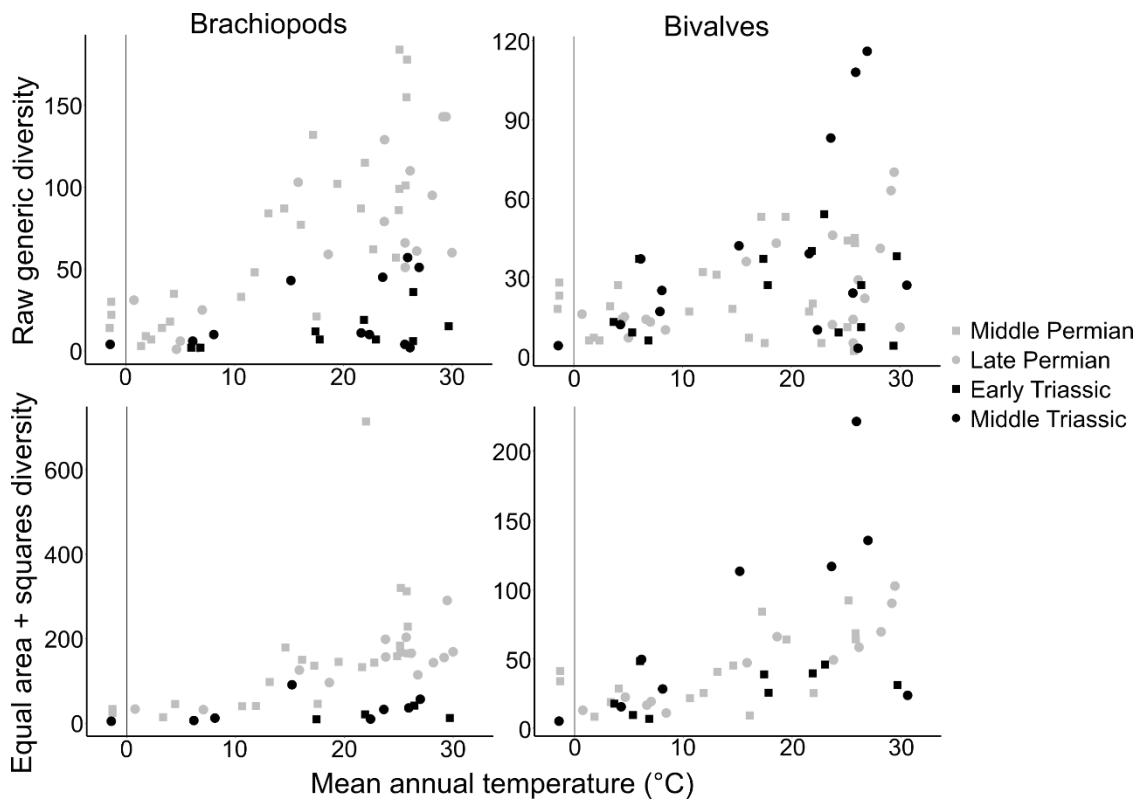
Figure 3–4: Mean annual sea surface temperatures, calculated across palaeoclimate model estimates corresponding to brachiopod or bivalve localities, for each spatio-temporal bin (palaeolatitudinal band – stage) included in the linear models, plotted against raw generic diversity (top) and generic diversity estimated using equal area subsampling and squares extrapolation (bottom).

3.4 Discussion

For both brachiopods and bivalves, the four different diversity metrics produced broadly congruent spatial biodiversity patterns (Figure 3–2), indicating that the LDG shapes reconstructed are relatively robust to sampling bias. Brachiopods had a consistently unimodal LDG throughout the middle Permian to Middle Triassic, with the diversity peak shifting from equatorial to low northern latitudes (10–30°N) across the Permian-Triassic boundary. Bivalves had a relatively flat LDG in the Permian, but a single equatorial diversity peak developed in the Changhsingian, moving into the northern low latitudes (10–30°N) in the Early and Middle Triassic. These results suggest that there was little latitudinal variation in extinction rates for these clades during the PTME, across which the bivalve LDG did not change, and the brachiopod LDG shifted only slightly, perhaps due to preferential extinction at equatorial latitudes (Song et al. 2020; see Chapter 4).

The unimodal brachiopod and bivalve LDGs reconstructed during the Triassic contrast with the coincident flat LDG for all marine animals recovered by Song et al. (2020) for the Early Triassic, but fit with their low northern latitude peak in diversity in the Middle Triassic. The Triassic brachiopod LDG produced here matches that reconstructed by Powell (2009) and Powell et al. (2015), who showed that the clade maintained a northern low to mid-latitude diversity peak throughout the Mesozoic and Cenozoic to the present day, possessing a similar peak in the southern hemisphere since the Cretaceous (Powell et al. 2015). Bivalves presently have a strong LDG, peaking in diversity at 10–20°N (Roy et al. 2000; Powell et al. 2012; Jablonski et al. 2013), meaning their Middle Triassic LDG was likely to have been very similar to their modern richness distribution (Figure 3–2). There is no evidence of a marine invertebrate fossil gap in the Early Triassic equatorial or low southern latitudes, which has been observed in the terrestrial tetrapod fossil record (Sun et al. 2012; Bernardi et al. 2018; see Chapter 2).

The consistency of the shape of the brachiopod LDG throughout the middle Permian to Middle Triassic, while apparent observationally (Figure 3–2), is also supported by the fact that GLS model fit was improved by accounting for temporal autocorrelation for all four diversity metrics, which was not the case for bivalves (Table 3-1, Table 3-3, Table 3-5, Table 3-7). Brachiopod LDGs have previously been described as heavily conserved throughout the Phanerozoic, with 'holdover' taxa contributing strongly to maintaining the shape of spatial diversity patterns over geological timescales (Powell et al. 2015).

The GLS analyses indicated that sampling acted as a strong control on the spatial diversity patterns observed, particularly for bivalves, for which raw and equal area diversity curves were best explained using only the number of fossil-bearing collections (Table 3-1, Table 3-5). This is not surprising, as the heavy influence of sampling bias on LDG shapes reconstructed using the fossil record has been widely reported on (e.g. Allison & Briggs 1993; Vilhena & Smith 2013; Mannion et al. 2014; Jones et al. 2021). The fact that bivalve spatial diversity patterns appear to be more strongly controlled by sampling than those of brachiopods is interesting; it may be due to a contrast in the completeness of the fossil records between these two groups, suggesting that the bivalve fossil record is patchier and less complete (Foote & Sepkoski 1999; Foote et al. 2015).

In contrast, the GLS results indicated that for brachiopod LDGs, while sampling still played a role, palaeotemperature was the strongest control, with MAT featuring in many of the best-fitting models, including for the raw data (Table 3-1). The brachiopod diversity curve produced using equal area subsampling

and squares extrapolation was best explained using only MAT (Table 3-7). The importance of temperature in determining LDGs has been highlighted previously, particularly for the marine realm (e.g. Currie et al. 2004; Tittensor et al. 2010; Mannion et al. 2014; Chaudhary et al. 2016, 2021), with SSTs alone predicting 53-99% of modern marine biogeographic distributions (Belanger et al. 2012).

The interpolated diversity curves were best fitted by null models for both clades, with the second-best models being the number of occupied equal area cells. This result was also obtained by a study employing a highly similar methodology to examine the drivers of the Late Triassic tetrapod LDG (Dunne et al. 2021). The failure of the palaeoenvironmental data to fit these curves may reflect the fact that the reconstructed LDGs are not driven by these variables; however, this was not the case for the other three diversity metrics. Alternatively, it may indicate that this interpolation approach fails to adequately account for differences in the areal coverage of localities between samples (Alroy 2010), and that this should be accounted for additionally when estimating differences in diversity between samples (e.g. Close et al. 2020a).

Examination of the relationship between MAT and diversity within stage-palaeolatitude bins suggests that the highest diversity levels were found in the range of 22-28°C for both brachiopods and bivalves, with the highest WMMT from any GCM cell containing fossils being 31.7°C (Figure 3–3, Figure 3–4). This is considerably cooler than the ~40°C equatorial sea surface temperatures estimated for the Early Triassic by Sun et al. (2012) based on $\delta^{18}O_{apatite}$ records. The apparent discrepancy is likely due to a failure of the GCM to reproduce such extreme temperatures, although a lack of brachiopod and bivalve fossils from the hottest regions, either due to a true absence or a failure to preserve, may also be a contributory factor.

The 22–28°C maximum diversity range seen here is slightly higher than the 15–25°C recovered for Cretaceous to modern molluscs by Boag et al. (2021). They suggested that this relationship is controlled by temperature-dependent aerobic limits on diversity, with temperatures above and below this range resulting in reduced aerobic capacity or water oxygenation levels respectively, each of which restrict biodiversity. In further support of this relationship, modern marine diversity has declined or plateaued over the last 60 years at latitudes where SSTs exceed 20°C (Chaudhary et al. 2021). Low levels of diversity are found in some spatio-temporal bins across the whole temperature range, which may be due to variation in sampling completeness artificially limiting diversity in some bins, or indicate that other variables are providing additional controls on diversity levels.

Based on the evidence presented here, palaeotemperature is the most likely candidate for an environmental driver of brachiopod and bivalve spatial diversity patterns in the Permian and Triassic. MAT was the best-fitting temperature variable, particularly for the brachiopod LDGs, suggesting that average annual surface temperatures were more important than seasonality in determining levels of diversity. However, the temperature variables were highly correlated with each other, and the estimates produced by the palaeoclimate models carry a considerable degree of uncertainty. Palaeogeographic reconstructions and palaeoclimate models are likely to improve in their accuracy and resolution in future, which may provide further insight into the most important facets of temperature for driving marine LDGs.

In contrast to previous analyses examining both fossil (Powell 2009; Naimark & Markov 2011) and modern marine LDGs (Tittensor et al. 2010; Chaudhary et al. 2016, 2021), shallow shelf area does not appear to have been an important driver of brachiopod and bivalve LDGs. However, there was a relatively poor fit between the palaeogeographies and the palaeo-localities of the fossils, with 34.7% of collections placed too far from an ocean to enable association with reconstructed climate values. A wide, and perhaps unrealistic, range of altitudes and bathymetries (350m above and below sea level) was chosen as the limits for calculating shallow shelf area, in part due to this poor fit. This wide definition of "shallow shelf", and uncertainty in the palaeogeographies, may have affected the accuracy of the estimates of shallow shelf area produced here, and therefore the lack of relationship found.

Chapter 4 – Estimating spatial variation in Permian and Triassic marine invertebrate origination and extinction

4.1 Introduction

Origination and extinction are two of the most fundamental processes in evolution, structuring taxonomic diversity across space and time (Allen & Gillooly 2006; Jablonski 2008). Understanding spatial variation in origination and extinction can help to unravel the mechanisms underlying macroevolutionary patterns, such as latitudinal diversity gradients (Mittelbach et al. 2007; Mannion et al. 2014; Powell et al. 2015; Saupe et al. 2019a; Meseguer & Condamine 2020), and provide deeper insight into the sequence of events behind biotic crises and radiations (Jablonski 2008; Saupe et al. 2014; Kocsis et al. 2018; Reddin et al. 2019). Although methods have been developed for estimating global origination and extinction rates from the fossil record, no framework exists for applying these methods to restricted spatial regions. Raw evolutionary rates have been calculated previously within latitude bands (e.g. Powell et al. 2015; Song et al. 2020), but this approach does not take into account variation in the sampling completeness of the fossil record (Benson & Upchurch 2013; Vilhena & Smith 2013; Mannion et al. 2014; Fraser 2017; Close et al. 2020a; Jones et al. 2021; Shaw et al. 2021), and the relationship between these estimates and the true, biological values is uncertain. Other studies have attempted to circumvent the issue by categorising taxa based on the latitude at which they are most abundant (e.g. Clapham et al. 2009; Reddin et al. 2019), but such an approach can involve compromises when taxon ranges cross latitude bins. Some studies have also examined regional extinction within latitudinal bands (e.g. Dunhill et al. 2018b), but this can conflate extirpation with true extinction.

Extinction and origination rates varied substantially during the Permian and Triassic, an interval including the Capitanian biotic crisis (CBC) and the Permian-Triassic mass extinction (PTME), both major extinction events coincident with the eruption of large igneous provinces and likely driven by the associated global warming and oceanic acidification and anoxia (Wignall et al. 2009; Bond et al. 2010; Payne & Clapham 2012; Sun et al. 2012; Penn et al. 2018). In light of the relative stability of the environmental niches of marine invertebrates over geological timescales (Saupe et al. 2014), previous discussion of the kill mechanisms associated with the PTME offers two hypotheses concerning the spatial distribution of extinctions:

(a) Increasing temperatures in lower latitudes rendered these regions inhospitable for most animals, driving high extinction rates at the equator and poleward migration (Sun et al. 2012; Bernardi et al. 2018; Song et al. 2020; see Chapter 2)

(b) Increasing temperatures (and anoxia) in the polar regions left cool-adapted organisms with no temperature-suitable habitat, leading to high extinction rates at high latitudes (Penn et al. 2018)

These hypotheses are not mutually exclusive and can be tested independently. Evidence supporting the first hypothesis has been reported previously for marine environments during other intervals of global warming in Earth history, including the Triassic-Jurassic mass extinction (Kiessling & Aberhan 2007; Dunhill et al. 2018b; Reddin et al. 2019).

To investigate whether spatial differences in origination and extinction can be estimated reliably using fossil data, I tested the ability of three different rate metrics to reconstruct spatial patterns of origination and extinction variation using simulations. The metrics were then applied to empirical datasets, of Permian and Triassic marine invertebrate occurrences, to examine the evidence for contrasting origination and extinction rates among clades and between high and low latitudes.

4.2 Methods

All analyses were conducted in R (R Core Team 2021) using the tidyverse (Wickham et al. 2019) and pspearman (Savicky 2014) packages.

4.2.1 Simulation

To test the efficacy of rate estimation methods (see 4.2.2), I constructed a simulation to produce fossil occurrence data using the protocol of Barido-Sottani et al. (2020). This approach allowed "true" origination and extinction to be measured as a benchmark for method comparison, which cannot be achieved using empirical fossil data. Simulated datasets were designed to fit the standard format of fossil occurrences available in the Paleobiology Database (PBDB), i.e. a list of occurrences, each representing the presence of a particular species within a "collection" or locality, agglomerated across a specified geographic area. Simulation input parameters were initially based on values calculated from Permian-Triassic marine invertebrate occurrences in the PBDB (see 4.2.3), then

subsequently amended to increase the range of values included within the simulation outputs.

Initial starting conditions (t_0) consisted of a "world" split into six spatial bins, each containing 1,000 species' occurrences (here considered akin to 30° latitudinal bands, but they could equally represent any six spatial subdivisions, such as bioregions, marine basins, or continents; see Figure 4–1a). The size of the global species pool was drawn at random, containing between 100 and 800 species, and each spatial bin was generated independently by drawing species' identities at random from the global species pool.

The simulated occurrences were then subjected to three iterations of "origination" and "extinction" to produce a four-slice time series (t_0, t_1, t_2, t_3). To produce each subsequent time slice, a random proportion of occurrences from a given spatial bin, between 0% and 20%, were selected to survive, with the others going extinct. Origination was simulated by adding a random number of occurrences to the spatial bin, between 0 and 300, with their identities selected from a pool consisting of species present in any of the six spatial bins in the previous time slice, plus a random number of between 0 and 400 new species. These processes were carried out independently for each spatial bin, operating at the level of a local population. This procedure allowed migration of species between spatial bins across the different time slices: for example, a particular species could suffer local extinction(s) in t_1 but be selected as the identity for local origination(s) in t_2, a process which would not be counted as a "true" extinction or origination, regardless of the spatial bins within which these phenomena took place (Figure 4–1b).

Once each bin had been populated with occurrences, I replicated the sampling filters known to exist in the fossil record by subsampling each spatial bin in every time slice once. Subsampling was achieved by drawing a random proportion of the occurrences contained within it. The described simulation protocol was repeated across 10,000 iterations to incorporate variation in origination, extinction, and sampling completeness (Figure 4–2). I also ran simulations of 5,000 iterations using different combinations of low, medium and high origination and extinction levels, to investigate the impact of turnover rate on the accuracy of estimates (Figures S4–2 to S4–7).
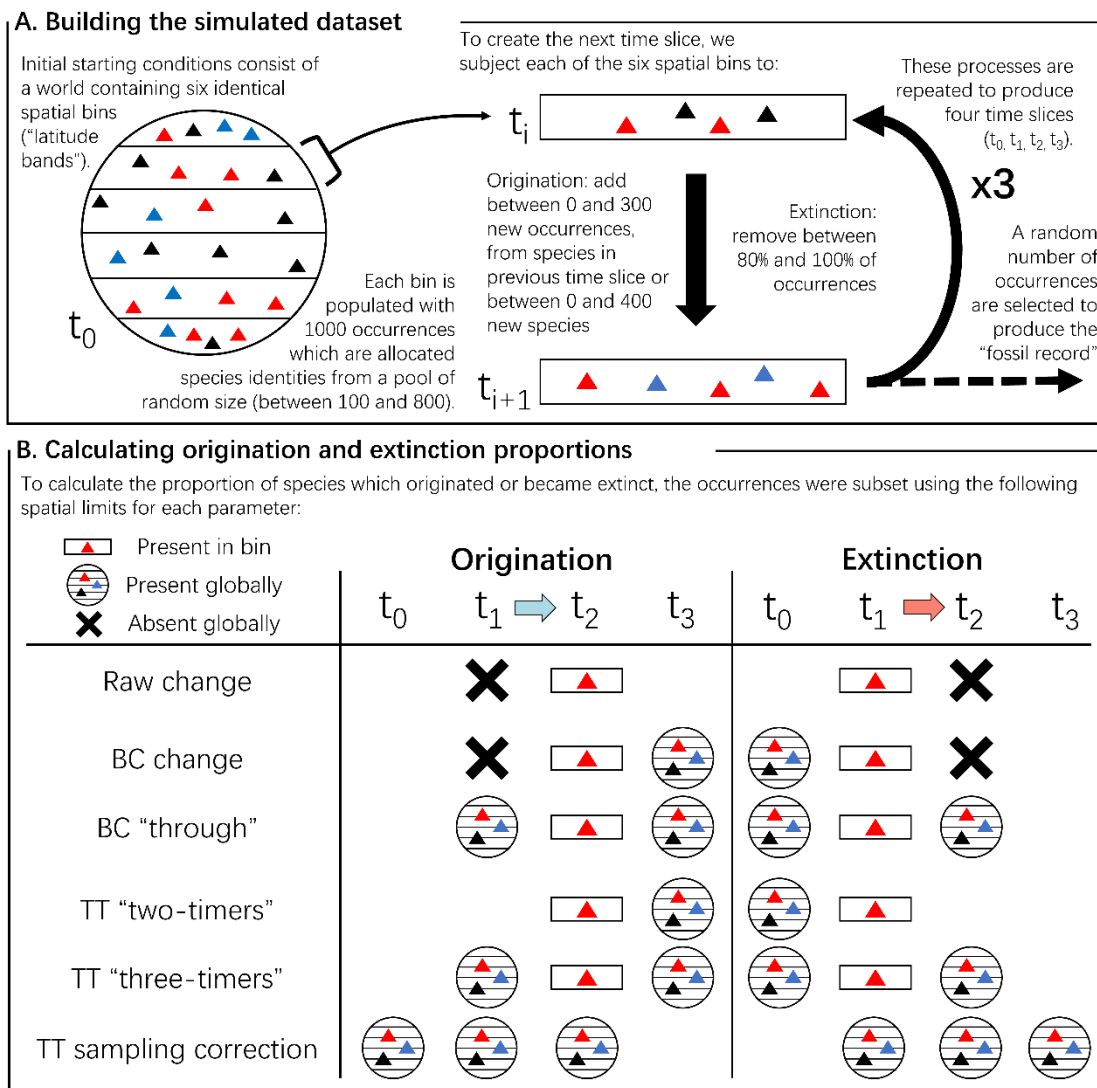
Figure 4–1: Schematic explaining construction of the simulated dataset and implementation of the different methods of estimating origination and extinction proportions in a specific spatial bin. "BC" refers to the "boundary-crosser" method (Foote 1999) and "TT" refers to the "three-timer" method (Alroy 2008).

The simulation is purposefully simplistic and may have produced occurrence data that lack some nuances present in empirical fossil datasets. For example, the six latitude bins were initially allocated equal numbers of occurrences, which does not reflect the difference in habitat area available across true latitude bands. The ability of species to migrate between any two latitudinal bands is also unrealistic, but the ways in which species' ranges alter on geological timescales is poorly understood, and the approach used here therefore avoids applying potentially false assumptions to this facet of the simulation.
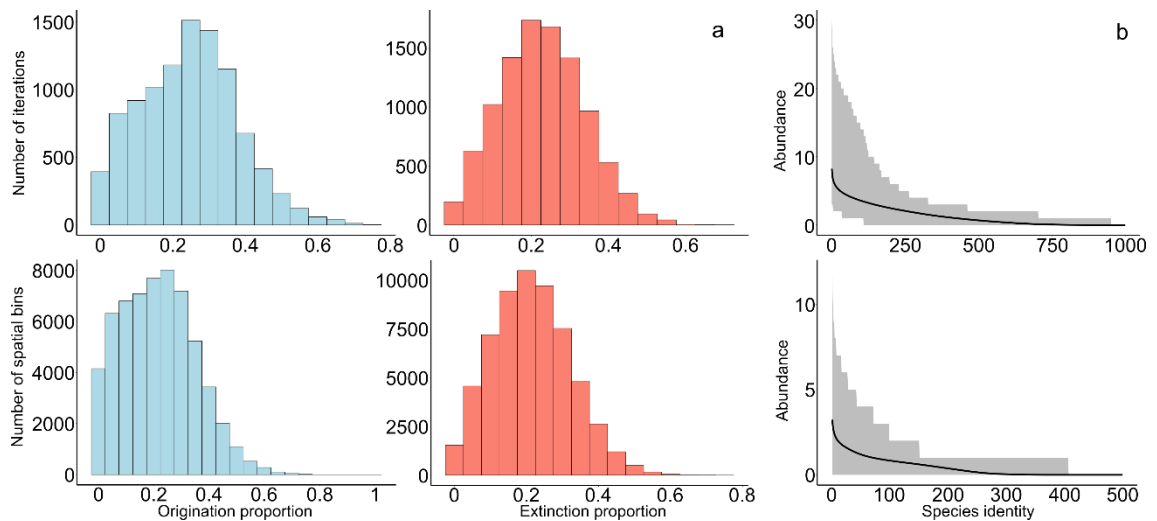
Figure 4–2: a. Distribution of "true" origination and extinction proportions generated within the simulated dataset, globally (top; 10,000 iterations) and for individual spatial bins (bottom; 6 x 10,000 = 60,000 bins).

b. Species abundance distributions for t_1 and t_2 (the time bins for which origination and extinction were calculated), globally (top; 2 x 10,000 = 20,000 spatio-temporal bins) and for individual spatial bins (bottom; 2 x 6 x 10,000 = 120,000 spatio-temporal bins). The black line is the mean abundance of the species found at the given identity rank, with the grey error bars showing the maximum and minimum abundance at that rank.

4.2.2 Comparison between metrics

Origination and extinction were calculated as proportions, indicating the fraction of species within the focal time slice, using three different metrics (Figure 4–1b).

(a) Raw values were calculated as the proportion of taxa in a given spatial bin that were not represented in the previous (origination) or subsequent (extinction) time interval. Raw values calculated using the complete (unsampled) datasets were deemed the "true" values to which all other estimates were compared.

(b) The "boundary-crosser" (BC) method is based on cohort analysis (Raup 1978) and evaluates the proportion of taxa which do not cross the "bottom" (originations) or "top" (extinctions) of a given time interval. While the method was developed by Foote (1999), the proportions calculated here are based on the equations of Alroy (1996), which exclude singletons (species known only from a single time slice).

(c) The "three-timer" (TT) method, described by Alroy (2008), is also based on cohort analysis, but incorporates an estimate of sampling probability.

The method uses the proportion of "part-timers", taxa which are present in the first and third slices of a time series but not the second, relative to "three-timers", which are present in all three time slices, to adjust the calculated proportions of origination and extinction.

The three-timer approach has been further developed, including the "gap-filler" (Alroy 2014) and "second-for-third" (Alroy 2015) modifications. While the additional complexity of these methods makes them well suited to interrogating changes in global biodiversity through time, uncertainty in evolutionary rates within restricted spatial regions is likely to be greater, particularly due to the smaller sample sizes involved, and influenced by other factors, and therefore I do not test them here.

The implementation of raw, BC and TT methods to assess origination and extinction for a single spatial bin is demonstrated in Figure 4–1b. Only the focal time slice (t_1 for extinction, t_2 for origination) was filtered to the relevant spatial bin, and all comparisons were made with global datasets in the other time slices. This meant that species that migrated between spatial bins, experiencing local but not global origination and extinction, were taken into account accordingly in estimates.

The performance of the three metrics was assessed using two different approaches. Numerical difference, i.e. subtraction, was used to evaluate the absolute accuracy of estimates for individual spatial bins. The ability to recreate the gradient of origination and extinction proportions across the six spatial bins in a single iteration was also assessed, using multiple approaches:

- Evaluation of whether the maximum and minimum values were attributed to the same spatial bins
- Calculation of Pearson correlation coefficient and Spearman's Rank correlation coefficient between the estimated and "true" values
- Examination of the number of spatial bins with overestimated values, rather than underestimated or identical values, to indicate the consistency of the direction (or sign) of numerical difference within individual iterations or "worlds"

4.2.3 Application of the metrics to fossil data

Having investigated the efficacy of the evolutionary rate estimation methods, I applied them to the Permian and Triassic marine invertebrate fossil record. Occurrences identified to genus or species level from four major invertebrate clades (Ammonoidea, Bivalvia, Brachiopoda, Gastropoda) were downloaded

from the Paleobiology Database (PBDB) in March 2021. The occurrences date from the Artinskian (middle early Permian) to the Norian (middle Late Triassic), enabling origination and extinction proportions to be estimated for the Roadian (early middle Permian) to the Ladinian (late Middle Triassic). Identifications expressing uncertainty in genus allocation were excluded, as well as any collections from non-marine environments or dated less precisely than to a single stage. This cleaned dataset included a total of 90,209 occurrences (see Supplementary Information).

Occurrences were allocated to 30° latitudinal bands, approximately representing tropical (0–30°), temperate (30–60°), and polar (60–90°) regions in each hemisphere. Raw, BC, and TT proportions of origination and extinction were then calculated for each latitudinal bin containing more than five genera in every stage, as described in Figure 4–1b. To increase the completeness of the available fossil record, origination and extinction were evaluated at the genus level (Figure 4–7), but estimates were also calculated for species (Figure S4–8).

4.3 Results

4.3.1 Metric performance: individual spatial bins

To test the accuracy of the three rate estimation methods, I calculated the numerical difference between estimated proportions of origination and extinction and their corresponding true value for individual spatial bins (n = 6 spatial bins x 10,000 iterations = 60,000 bins). Randomly sampling the simulated occurrences, to emulate the patchy nature of the fossil record, reduced both the precision and accuracy of origination and extinction estimates (Figure 4–3a). Following sampling, raw and BC metrics performed similarly, tending to slightly overestimate both origination and extinction (Figure 4–3a, Table S1). TT estimates were more accurate in that the median difference from the true value was closer to zero with a narrower inter-quartile range (IQR) than the raw or BC metrics. For all metrics, extinction estimates were marginally more accurate than origination estimates (Figure 4–3). These trends were also seen when applying the metrics to the global datasets (n = 10,000 iterations), but with slightly smaller ranges and IQRs (Figure S4–1).

Dividing estimates into groups based on the sampling completeness of the relevant spatial bin (Figure 4–3b) revealed that, for all three metrics, the ranges and IQRs of difference between estimated and true values reduced as sampling completeness increased. However, while TT estimates approached the true value with increasing sampling, raw and BC estimates did not, instead tending

towards overestimation of ~0.1–0.2. Additional analyses examining the effect of low versus high origination and extinction levels on estimate accuracy indicated that the range of differences increased in response to faster turnover (Figure S4–4).
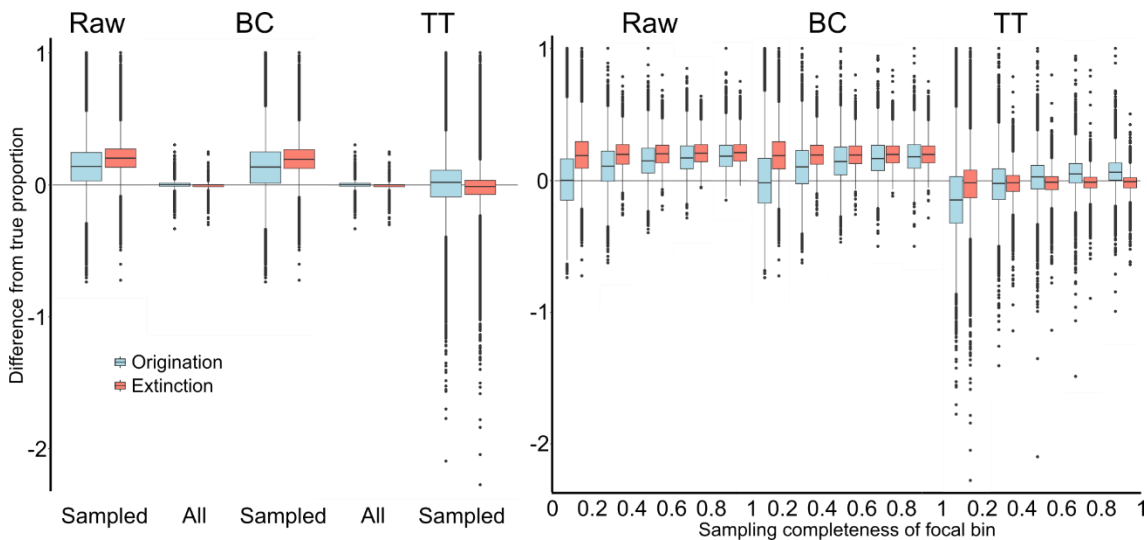
Figure 4–3: a. Difference between "true" and estimated proportions of origination and extinction across all spatial bins (n = 60,000) produced in simulation.

b. Difference between "true" and estimated proportions of origination and extinction following sampling in individual spatial bins, subdivided depending on the proportion of occurrences sampled in the focal bin (width = 20% of occurrences).

4.3.2 Metric performance: gradient within an iteration

The accuracy of rate estimation methods was also assessed by considering the gradient of origination and extinction proportions across spatial bins in a single iteration (n = 10,000 iterations). I compared true and estimated proportions of origination and extinction to test (a) whether maximum and minimum values were attributed to the same spatial bins, (b) whether true and estimated values were correlated with one another, and (c) whether estimated values were consistently overestimated (or underestimated) within each iteration. As all TT

values were offset using a global sampling correction, the gradients of BC and TT estimates for any given iteration were identical.

After sampling, spatial bins with the highest and lowest proportions of origination and extinction were correctly identified only in a third of the iterations, regardless of the metric used (Figure 4–4). Raw estimates were slightly more successful than BC and TT estimates. Across metrics, the spatial bin with the highest origination was more likely to be identified correctly than the bin with the lowest origination proportion. For extinction, maximum and minimum bins were equally likely to be identified correctly. Additional analyses examining low *versus* high origination and extinction levels showed that faster turnover resulted in a slight reduction in the ability to correctly identify maximum and minimum spatial bins (Figure S4–5).
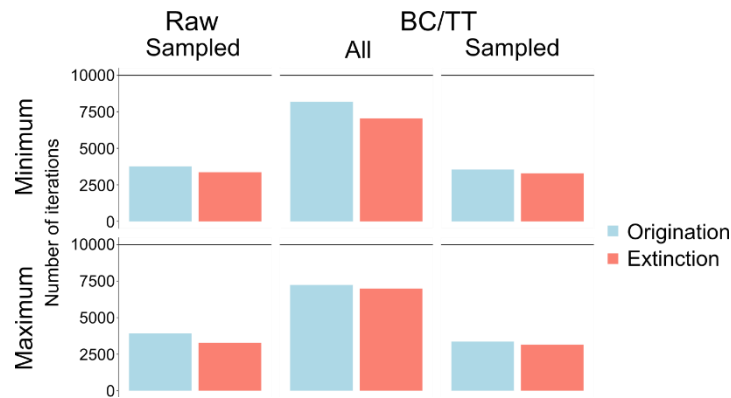
Figure 4–4: Number of iterations for which the identity of the bin with minimum and maximum proportion is preserved following sampling. Boundary-crosser and three-timer methods produced identical results.
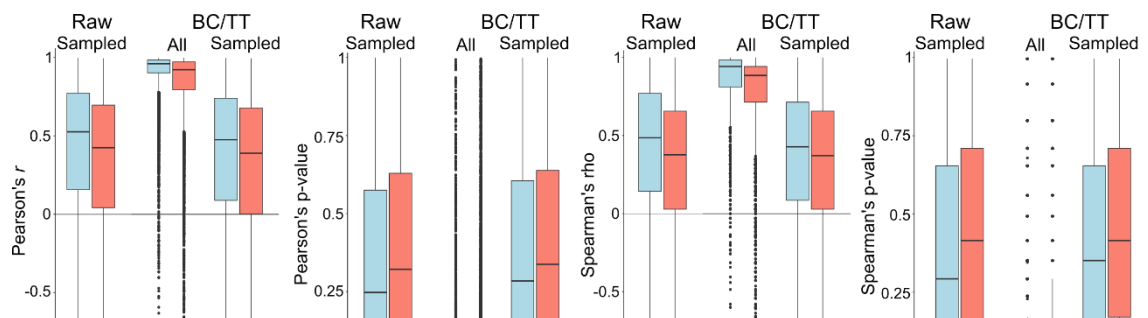
Figure 4–5: Distribution of correlation coefficients and p-values across iterations, when comparing "true" proportions of extinction and origination to those produced post-sampling and estimation. Tests examined both linear correlation using Pearson's *r* (left) and rank correlation using Spearman's ρ (right). Boundary-crosser and three-timer methods produced identical results.

Correlation between the post-sampling estimates and true values was comparable when considered linearly (Pearson's *r*) relative to when considered ranked (Spearman's ρ) (Figure 4–5). In most iterations, the correlation between post-sampling estimates and true origination and extinction values was positive and of intermediate strength (~0.3–0.7), but with corresponding p-values indicating a non-significant relationship (median value across iterations, p~0.3). These results were echoed in the simulation runs with varying origination and extinction levels (Figure S4–6).

The number of spatial bins with overestimated origination and extinction proportions in each iteration (Figure 4–6) fit closely with the skew of median differences for spatial bins in isolation (Figure 4–3a). Following sampling, raw and BC estimates generally overestimated proportions in five, or all six, of the spatial bins. In contrast, TT estimates were more likely to overestimate proportions in two to four of the spatial bins, suggesting a relatively even distribution of differences above and below the true values within a single iteration.
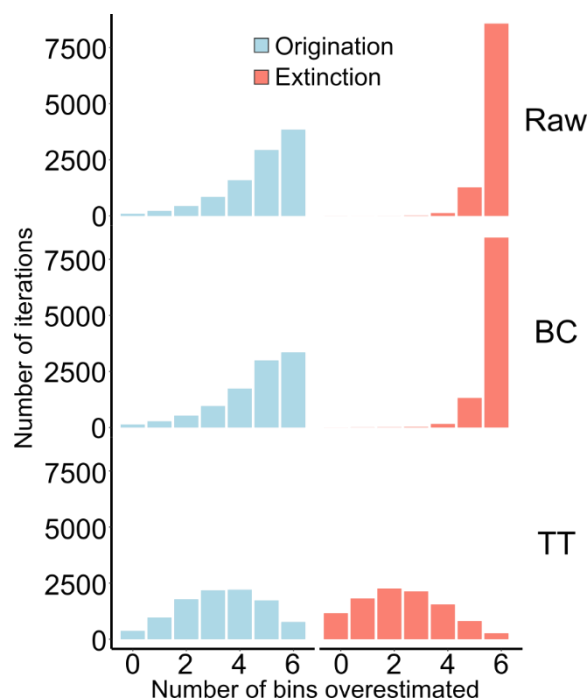
Figure 4–6: Distribution of number of spatial bins for which proportions of origination and extinction are overestimated compared to their "true" value within a given iteration; for example, a value of six would mean that all bins in the iteration were overestimated, whereas a value of zero would mean that all bins in the iteration were underestimated.

4.3.3 Spatial variation in origination and extinction during the Permian and Triassic

Permian and Triassic marine invertebrate fossil occurrences were used to calculate raw, BC and TT estimates for generic origination and extinction proportions within 30° latitudinal bands. The marine invertebrate fossil record for the Permian and Triassic varies considerably in its sampling completeness, across space, through time and among clades. As a result, origination and extinction metrics could not be calculated for some of the spatio-temporal (latitude-stage) bins, particularly using the BC and TT metrics, which have a higher sample size threshold. However, spatial coverage was still sufficient to indicate broad-scale patterns in origination and extinction (Figure 4–7). Species-level analyses produced similar trends but with generally higher levels of origination and extinction (Figure S4–8).

Both origination and extinction appear to have been uniformly low, mostly below 50% of genera, across latitudes for marine invertebrates in the Permian. There is little evidence of heightened extinction in the Capitanian, although ammonoids underwent considerable diversification in the Wuchiapingian, particularly in the low latitudes (around 80% of genera).

The effect of the Permian-Triassic mass extinction (PTME) is clearly visible, with high extinction globally in the Changhsingian. Ammonoids experienced highest extinction levels at low latitudes (around 90%), and reduced extinction in the southern mid-latitudes (around 40%). Brachiopods and bivalves appear to have exhibited the opposite gradient, with slightly lower extinction proportions at low latitudes (around 90% at high latitudes versus 70% at low latitudes for brachiopods, and 65% versus 40% for bivalves).

The brachiopod, bivalve and gastropod records are sparse during the Early Triassic, particularly in the southern hemisphere, hindering the production of reliable estimates. Origination appears not to have been unusually high in the Induan, in the aftermath of the mass extinction, except perhaps for the ammonoids. While extinction was generally reduced and spatially uniform in the Induan, brachiopods experienced a high proportion of extinction in the low northern latitudes. Ammonoids exhibited both high origination and extinction globally in the Olenekian (both around 85%), indicating rapid turnover in the clade, whereas bivalves experienced reduced extinction rates (around 20%). In the Middle Triassic, origination and extinction gradients became more spatially uniform and stable for all four clades, although ammonoids appear to have undergone turnover in the high northern latitudes during the Ladinian.
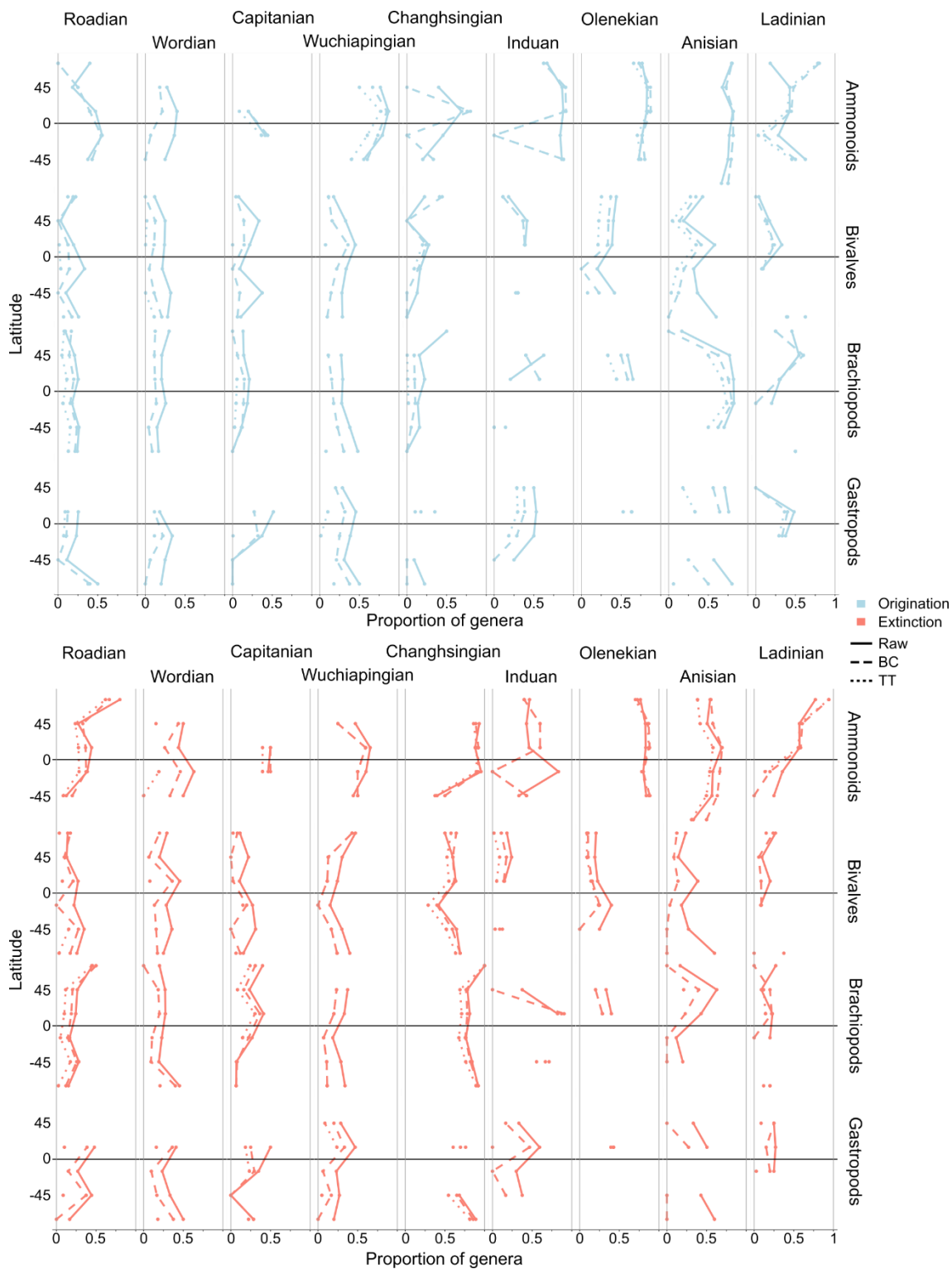
Figure 4–7: Generic origination and extinction by latitude of four different marine clades in each stage of the middle Permian to Middle Triassic. Occurrences were split into six 30° latitude bins. Estimates were calculated for each spatio-temporal bin containing five or more genera. Missing points indicate insufficient occurrences to calculate a proportion.

4.4 Discussion

These results show that raw, boundary-crosser (BC) and three-timer (TT) origination and extinction metrics can be applied to spatial subsamples of fossil datasets and produce estimates with only slightly less accuracy than when used globally (Figure 4–3, Figure S4–1). The increased uncertainty is likely due to the necessary reduction in sample size (number of occurrences) resulting from creating spatial subdivisions within a global dataset. As expected, sampling bias presents a significant barrier to the accurate estimation of origination and extinction rates. However, the results highlight some clear recommendations for increasing the accuracy of estimates produced using the approach outlined here.

Three-timer estimates were generally more accurate than those calculated using raw or BC methods (Figure 4–3). However, using the TT method requires occurrences to be present in a given latitude bin across multiple time slices (Figure 4–1b), which may not always be available. BC estimates produced the same gradient of origination and extinction in latitude bins within a given iteration, so can be used as a reasonable compromise when comparing estimates within a time slice. Surprisingly, raw estimates were slightly more successful at identifying spatial bins with the highest and lowest levels of origination and extinction (Figure 4–4). Calculating all three metrics when possible to allow comparison may be the best approach.

The most accurate estimates were produced using the TT method on spatial bins with a high sampling completeness (Figure 4–3b), and variation in sampling completeness between spatial bins appears to hinder efforts to identify the bins that experienced highest and lowest origination and extinction (Figure 4–4, Figure S4–5). These evolutionary rate metrics should therefore be applied to the largest dataset possible. Using higher taxonomic levels may increase the number of usable occurrences, but the patterns observed should not be assumed to be analogous to trends at lower taxonomic levels (Hendricks et al. 2014).

Estimates produced for low levels of origination and extinction were slightly more accurate than those for high levels (Figure S4–4). This was expected for BC and TT estimates; these methods exclude singletons, so when turnover rates are increased, a larger proportion of species are represented as singletons in the fossil record, and the effective sample size is reduced. However, the difference in accuracy observed in the simulated data is relatively small, and therefore the uncertainty around high origination and extinction

estimates should not be considered significantly greater than that around smaller estimates.

The analyses of Permian–Triassic ammonoids, brachiopods, bivalves and gastropods provide little evidence for high extinction in these clades during the Capitanian biotic crisis (CBC) (Figure 4–7). Brachiopods experienced slightly higher extinction in the low and high northern latitudes (around 40% of genera), which supports the results of Clapham (2015), who identified a generic turnover in Capitanian–Wuchiapingian faunas from Iran and South China. Extinction in the clade was higher at the species level, particularly in the northern hemisphere (around 75%; Figure S4–8), but somewhat lower than the 87% reported by Shen & Shi (1996) for South China. Globally, low origination and extinction levels (both around 20%) indicate that bivalves also appear to have been largely unaffected by the CBC, in agreement with Bond et al. (2010). By contrast, ammonoids and gastropods experienced moderate extinction levels at low latitudes (around 50%) during the CBC. My results support a generic turnover of ammonoids during the Capitanian (Villier & Corn 2004; Rampino & Shen 2021), but their fossil record is highly spatially restricted at this time, so it is unclear whether this turnover took place globally or only in the southern low latitudes. I found high ammonoid origination levels across low-mid latitudes in the Wuchiapingian, in agreement with Clapham et al. (2009) and McGhee et al. (2013). Collectively, the results presented here support the hypothesis that the CBC was highly selective (McGhee et al. 2013), with some marine clades undergoing turnover, particularly at low latitudes (ammonoids and gastropods), while others were seemingly unaffected (bivalves and brachiopods).

High extinction levels during the Changhsingian, associated with the Permian-Triassic mass extinction (PTME), are seen globally in all four marine invertebrate clades (around 90% for brachiopods, 85% for ammonoids, 75% for gastropods and 65% for bivalves; Figure 4–7). For bivalves, gastropods and brachiopods, the highest extinction levels were at the mid-high latitudes. These results support those of Reddin et al. (2019), who reported that benthic marine invertebrates experienced higher extinction rates further from the equator during the PTME. Slightly reduced extinction levels at low latitudes in these clades may be an artefact caused by the occurrence of "mixed faunas". These are communities of benthic invertebrates, particularly well-known from sections in South China, which survived the Changhsingian only to become extinct in the earliest Induan (Song et al. 2013). The presence of a low-latitude Induan extinction peak for brachiopods marks the loss of these "mixed faunas". In contrast, ammonoids experienced the highest Changhsingian extinction levels at low latitudes. The late Permian ammonoid fossil record is relatively spatially

restricted in comparison with the Early Triassic record, which may contribute to this result (Dai & Song 2020); the low extinction level in the southern mid latitudes corresponds to a handful of localities in northern India, and may therefore reflect incomplete sampling.

Bivalves, gastropods, and ammonoids had highest origination levels at the low latitudes during the Induan. The discrepancy between raw and BC rates seen in some ammonoid and brachiopod bins for the stage is likely due to "disaster faunas" contributing a high number of temporal singletons. Ammonoids underwent rapid turnover across all latitudes in the Olenekian; this matches an observed increase in their endemism during the stage, as well as the influence of a possible extinction event around the Smithian-Spathian boundary (~251Ma) (Brayard et al. 2006; Song et al. 2011; Wignall 2015; Dai & Song 2020). For all four clades, origination and extinction levels reduced and became more globally homogenous in the Anisian and Ladinian, corresponding to the amelioration of global temperatures and the re-establishment of diverse benthic communities (Sun et al. 2012; Martindale et al. 2019).

In general, both origination and extinction were relatively consistent across latitudes for all four clades during the middle Permian to Middle Triassic (Figure 4–7). Some variation can be seen, through time and between latitude bands, but it is difficult to discern that which represents true, biological patterns rather than simply being artefacts of sampling bias. Regardless, the taxonomic identity of a genus appears to be a more important factor in determining extinction vulnerability than the palaeolatitudes it occupied, indicating a stronger phylogenetic signal in selectivity than for latitude.

If interpreted as biological, the Changhsingian latitudinal gradients of extinction seen in the benthic clades (bivalves, brachiopods, gastropods) align with the hypothesis that extinction during the PTME was most severe at high latitudes due to the loss of suitable habitat for cool-adapted taxa, as advocated for by Penn et al. (2018). However, the extinction gradient of ammonoids, the only pelagic clade examined here, better fits the hypothesis that extremely high equatorial temperatures resulted in tropical extinction and poleward migration, a mechanism proposed by Sun et al. (2012) and supported by Song et al. (2020). My results therefore suggest a contrast in the spatial distribution of PTME responses on the basis of palaeoecology. Variation in the rate of post-PTME recovery has previously been identified between these two ecologies, with ammonoids and conodonts recovering more rapidly than benthic reef dwellers (Brayard et al. 2006; Song et al. 2011; Song et al. 2018; Martindale et al. 2019), a trend also observed after the Triassic-Jurassic mass extinction (Dunhill et al. 2018b). Penn et al. (2018) hypothesised that these two contrasting extinction

gradients may reflect differences in primary kill mechanism, with extinctions at higher latitudes linked to oxygen depletion, and extinctions at low latitudes linked to temperatures beyond thermal tolerance levels. Oceanic oxygen depletion tends to be more severe in bottom waters (e.g. Liao et al. 2010), leaving benthic animals more vulnerable to anoxia than pelagic animals. In addition, the elevated extinction levels experienced by ammonoids during the late Smithian Thermal Maximum (LSTM) may support the presence of a high sensitivity to extremes of temperature within the clade (Brayard et al. 2006; Dai & Song 2020). Investigating spatial variation in origination and extinction in other pelagic clades, such as conodonts and fishes, and directly testing the timing and direction of migration in marine invertebrates, would develop this argument further.

Chapter 5 – Discussion

5.1 Comparing terrestrial and marine LDGs in the Permian and Triassic

The results presented in Chapters 2 and 3 indicate that during the middle Permian to Middle Triassic, latitudinal diversity gradients (LDGs) may have had contrasting shapes between the marine and terrestrial realms. Terrestrial tetrapods had a bimodal richness distribution, with diversity peaks in the mid latitudes, throughout the interval (Figure 2–1; also Brocklehurst et al. 2017). However, brachiopods had a consistently unimodal LDG, with an equatorial peak during the Permian which shifted into the low northern latitudes in the Triassic, while bivalves had a flat LDG from the Roadian to Wuchiapingian, developing a low latitude diversity peak from the Changhsingian onwards (Figure 3–2). Marine reptiles, the oldest fossils of which are known from the Early Triassic, were generally restricted to the northern hemisphere, and were most diverse in the low northern latitudes in the Middle Triassic (Figure 2–1), similar to the marine invertebrates. While the terrestrial tetrapod LDG fits the shallow, bimodal shape expected during greenhouse periods (Naimark & Markov 2011; Mannion et al. 2014; Meseguer & Condamine 2020), the marine gradients appear not to.

Chapters 2 and 3 both reiterate the importance of considering sampling bias when reconstructing LDGs, with evidence for a strong relationship between spatial biodiversity patterns and sampling proxies (Figure 2–1, Table 3–1, Table 3–3, Table 3–5, Table 3–7). Other recent studies examining spatial richness patterns in the fossil record have also highlighted strong relationships between diversity and sampling (Song et al. 2020; Dunne et al. 2021; Jones et al. 2021). A lack of fossil localities known from the southern hemisphere in the Early and Middle Triassic, either marine or terrestrial, is a particular source of uncertainty for the LDG shapes described here (Benson & Upchurch 2013; Tabor et al. 2018; also Figure 2–1, Figure 3–1). Introducing more fossils to these datasets, and/or improving the dating resolution of fossils which are known from these palaeolatitudes, could help to resolve this issue in future.

5.2 New insights into LDG drivers

The GLS analyses in Chapter 3 indicate that temperature is likely to be the most influential driver of brachiopod and bivalve LDGs (Table 3–1, Table 3–5, Table 3–7). This is in agreement with many previous analyses of marine LDGs, in

both the fossil record (Naimark & Markov 2011; Kiessling et al. 2012; Mannion et al. 2014; Kröger 2018) and the present day (Tittensor et al. 2010; Belanger et al. 2012; Chaudhary et al. 2016, 2021). Temperatures are also thought to be important in determining the terrestrial Early Triassic LDG, with particularly high temperatures at the lower latitudes thought to be the cause of the equatorial 'tetrapod gap' (Sun et al. 2012; Bernardi et al. 2018, also Chapter 2). However, it remains unclear whether this 'gap' is due to a true biological scarcity or spatial sampling bias.

If temperature was a key driver of both the marine and terrestrial LDGs in the Permian and Triassic, why were they different shapes? The relationship between temperature and diversity is not linear (e.g. Boag et al. 2021), and while there seems to be little evidence of marine invertebrates experiencing sufficiently high temperatures for diversity to be reduced at some latitudes (Figure 3–4), this may not have been the case on land. The severity and rate of warming is likely to have contrasted between the terrestrial and marine realms: although the rate of modern (anthropogenic) climate change varies extensively between local regions, air temperatures are generally rising faster than shallow ocean temperatures, but shifts in the timing of seasonal change appear to be greater in the oceans (Trenberth et al. 2007, Burrows et al. 2011). The environmental conditions on Pangea during the Early Triassic may therefore have been more extreme, with more area above the temperature of peak diversity and a more rapid pace of climate change relative to the oceans (Roscher et al. 2011). However, making direct comparisons between palaeotemperatures is difficult, as estimates generated using both palaeoclimate models and geochemical proxies carry a considerable amount of uncertainty.

The contrasting shapes of marine and terrestrial LDGs in the Permian and Triassic may also be due to the influence of different secondary drivers between these two realms. For example, oceanic oxygenation was highly spatially variable during the PTME (Bond & Wignall 2010). While heavily influenced by temperature (Pörtner 2010; Penn et al. 2018; Boag et al. 2021), other factors are also likely to have influenced the distribution of anoxic waters, such as ocean circulation and nutrient availability (Kiehl & Shields 2005; Schobben et al. 2020). Although proxies such as the degree of bioturbation and the size distribution of pyrite framboids can be used to estimate palaeo-oxygenation within a single section (Wignall & Myers 1988; Wignall & Newton 1998), reliable global reconstructions of Permo-Triassic oceanic oxygen levels are not yet available. Precipitation and water availability have been implicated as important drivers of LDGs on land (Hawkins et al. 2003; Fraser et al. 2014; Saupe et al.

2019a), and the extremely seasonal precipitation regimes reconstructed on Pangea during this time (Parrish 1993; Preto et al. 2010; Roscher et al. 2011; Smith & Botha-Brink 2014; Tabor et al. 2018) are likely to have influenced terrestrial spatial diversity patterns in conjunction with temperatures.

Shallow shelf area has previously been demonstrated to be fundamental to the distribution of marine biodiversity (Valentine & Moores 1970; Tittensor et al. 2010; Chaudhary et al. 2016; Close et al. 2020a), but this is not echoed in the GLS results from Chapter 3. The fit between the palaeogeographies and the fossil localities was relatively poor, which suggests that these reconstructed maps are not yet of sufficient accuracy and resolution to produce reliable estimates of shallow shelf area, which may in turn have influenced this perceived lack of relationship. The degree of continental fragmentation or aggregation may also control the strength of the relationship between shallow shelf area and spatial diversity patterns (Saupe et al. 2020), but this is currently untested.

5.3 The relationship between evolutionary rates and LDGs

Comparison of the latitudinal gradients of origination and extinction (Figure 4–7) and LDGs (Figure 3–2) of Permian and Triassic brachiopods and bivalves reveals no obvious match. Origination and extinction levels were generally latitudinally uniform, but this was not the case for diversity, except perhaps for bivalves during the middle to late Permian. Even the heavy influence of shared sampling bias on both of these analyses (Figure 3–1, Figure 4–3) was not sufficient to produce obviously similar gradients. However, statistical comparison may reveal relationships between the curves, particularly as one might expect a temporal offset between particularly high origination or extinction and a shifting LDG. Migration between latitude bands, which was not directly examined here, may explain some of the discrepancy between origination, extinction and diversity levels within spatio-temporal bins.

The relative consistency of both terrestrial and marine LDGs throughout the middle Permian to Middle Triassic (Figure 2–1, Figure 3–2), and a lack of latitudinal variation in origination and extinction (Figure 4–7), both support the hypothesis that LDG shapes are generally maintained over geological timescales. This fits with previous work which has suggested that LDGs shift during intervals of substantial climate change, after which they are subsequently perpetuated (Hillebrand 2004; Fine 2015; Powell et al. 2015; Svenning et al. 2015). However, there is little evidence that the extreme global warming and

biotic crises of the middle Permian to Early Triassic altered LDGs (Figure 2–1, Figure 3–2), although an LDG shift could have occurred earlier in the icehouse-greenhouse transition, during the early Permian (e.g. Garbelli et al. 2019). An alternative hypothesis, given the results presented here, is that LDGs are largely unaffected by events such as global climate change and mass extinctions, and instead only shift incrementally, even on geological timescales.

5.4 Avenues for further research

Our knowledge of LDGs in deep time remains limited, and there are many clades and time intervals which could be examined to better understand particular facets of spatial diversity patterns and their drivers. For the Permian and Triassic, investigation of the LDGs of conodonts and fishes would provide further insight into whether the spatial distributions of pelagic animals were the same as those of benthic animals, and whether the drivers of those distributions were the same (see Chapter 3). The severity of the PTME for plants has also recently been debated (Fielding et al. 2019; Nowak et al. 2019), and, as the base of the terrestrial food chain, examining their LDG through the PTME and recovery interval and comparing it to that of terrestrial tetrapods could provide insight into the importance of biotic interactions in driving LDGs. Conducting the GLS analyses from Chapter 3 on the terrestrial tetrapod LDGs from Chapter 2 could also provide further insight into the drivers of spatial diversity patterns on land during greenhouse intervals. As with all macroevolutionary studies based on the fossil record, maximising the size of the datasets used, by conducting more fieldwork, cataloguing more collections, and adding more publications to online databases, would improve the reliability of results and facilitate the implementation of more complex statistical approaches.

The approach in Chapter 4 is novel and there are two logical next steps for further development. Firstly, the palaeoenvironmental data and linear regression approach from Chapter 3 could be applied to the latitudinal gradients of origination and extinction produced in Chapter 4. This would facilitate the testing of hypotheses around the relationship between environmental change and macroevolutionary rates. Secondly, alongside origination and extinction, migration is also an important biotic response to environmental change, but it is difficult to quantify, especially when using fossil data. The simulation constructed for Chapter 4 could be adapted to address questions around the best ways to calculate immigration and emigration rates, or range shifts, as well as the extent to which sampling bias masks the true values. Being able to

measure these dynamics would provide considerable insight into how LDGs change shape over time.

Ecological niche modelling is growing in popularity as a tool for addressing questions about the impact of environmental change on macroevolution in deep time (e.g. Saupe et al. 2014, 2019a; Fenton et al. 2016; Chiarenza et al. 2019; Antell et al. 2021). To build on the work conducted here, niche modelling could be used to interrogate whether:

- the PTME extinctions were associated with a loss of the thermal niche space occupied by animals in the late Permian
- the 'disaster taxa' which proliferated in the Early Triassic occupied extreme palaeoenvironments or had unusual thermal niches compared to other animals
- the paucity of fossils from the southern low latitudes during the Early Triassic is more likely to be caused by a lack of suitable habitat or a failure of the animals living there to enter the fossil record

The palaeoclimate data from Chapter 3 could be used for such analyses.

Current methods of estimating diversity from the fossil record are far from perfect, and the development of more accurate metrics would aid investigation of macroevolutionary patterns in deep time. Coverage-based approaches, such as the interpolation applied in Chapters 2 and 3, could be altered or redesigned to better account for variation in spatial sampling (Close et al. 2018, 2020; Alroy 2020; see Chapter 3). Alternative methods for estimating diversity from the fossil record are likely to arise in the near future using approaches such as Bayesian inference (e.g. Silvestro et al. 2014a, b, 2019) and phylogenetics (e.g. Xing et al. 2014; Stadler et al. 2018; Warnock et al. 2020).

Bibliography

Allen, A. P. & Gillooly, J. F. 2006. Assessing latitudinal gradients in speciation rates and biodiversity at the global scale. *Ecol. Lett.* 9:947-954.

Allison, P. A. & Briggs, D. E. G. 1993. Palaeolatitudinal sampling bias, Phanerozoic species diversity, and the end-Permian extinction. *Geology* 21:65-68.

Alroy, J. 1996. Constant extinction, constrained diversification, and uncoordinated stasis in North American mammals. *Palaeo3* 127:285-311.

Alroy, J. 2008. Dynamics of origination and extinction in the marine fossil record. *PNAS* 105:11536-11542.

Alroy, J. 2010. Geographical, environmental and intrinsic biotic controls on Phanerozoic marine diversification. *Palaeontology* 53:1211-1235.

Alroy, J. 2014. Accurate and precise estimates of origination and extinction rates. *Paleobiology* 40:374-397.

Alroy, J. 2015. A more precise speciation and extinction rate estimator. *Paleobiology* 41:633-639.

Alroy, J. 2018. Limits to species richness in terrestrial communities. *Ecol. Lett.* 21:1781-1789.

Alroy, J. 2020. On four measures of taxonomic richness. *Paleobiology* 46:158-175.

Antell, G. S., Kiessling, W., Aberhan, M. & Saupe, E. E. 2020. Marine biodiversity and geographic distributions are independent on large scales. *Curr. Biol.* 30:115-121.

Antell, G. S., Fenton, I. S., Valdes, P. J., Saupe, E. E. 2021. Thermal niches of planktonic foraminifera are static throughout glacial-interglacial climate change. *PNAS* 118:e2017105118.

Barido-Sottani, J., Saupe, E. E., Smiley, T. M., Soul, L. C., Wright, A. M. & Warnock, R. C. M. 2020. Seven rules for simulations in paleobiology. *Paleobiology* 46:435-444.

Barnosky, A. D., Carrasco, M. A. & Davis, E. B. 2005. The impact of the species-area relationship on estimates of paleodiversity. *PLoS Biol.* 3:e266.

Barton, K. 2020. MuMIn: multi-model inference. Version 1.43-17.

Beerling, D. J., Harfoot, M., Lomax, B. & Pyle, J. A. 2007. The stability of the stratospheric ozone layer during the end-Permian eruption of the Siberian Traps. *Phil. Trans. R. Soc. A* 365:1843-1866.

Belanger, C. L., Jablonski, D., Roy, K., Berke, S. K., Krug, A. Z. & Valentine, J. W. 2012. Global environmental predictors of benthic marine biogeographic structure. *PNAS* 109:14046-14051.

Benca, J. P., Duijnstee, I. A. P. & Looy, C. V. 2018. UV-B–induced forest sterility: implications of ozone shield failure in Earth's largest extinction. *Sci. Adv.* 4:e1700618.

Benson, R. B. J. & Butler, R. J. 2011. Uncovering the diversification history of marine tetrapods: ecology influences the effect of geological sampling biases. *Geol. Soc. Lond., Spec. Pub.* 358:191-208.

Benson, R. B. J. & Upchurch, P. 2013. Diversity trends in the establishment of terrestrial vertebrate ecosystems: interactions between spatial and temporal sampling biases. *Geology* 41:43-46.

Benton, M. J., Dunhill, A. M., Lloyd, G. T. & Marx, F. G. 2011. Assessing the quality of the fossil record: insights from vertebrates. *Geol. Soc. Lond., Spec. Pub.* 358:63-94.

Bernardi, M., Petti, F. M. & Benton, M. J. 2018. Tetrapod distribution and temperature rise during the Permian-Triassic mass extinction. *Proc. R. Soc. B* 285:20172331.

Bivand, R. & Lewin-Koh, N. 2020. maptools: tools for handling spatial objects. Version 1.0-2.

Bivand, R. & Rundel, C. 2020. rgeos: interface to geometry engine – open source ('GEOS'). Version 0.5-5.

Bivand, R., Pebesma, E. & Gomez-Rubio, V. 2013. *Applied spatial data analysis with R. Second Edition.* Springer New York.

Bivand, R., Keitt, T. & Rowlingson, B. 2021. rgdal: bindings for the 'geospatial' data abstraction library. Version 1.5-23.

Boag, T. H., Gearty, W. & Stockey, R. G. 2021. Metabolic tradeoffs control biodiversity gradients through geological time. *Curr. Biol.* 31:2906-2913.

Bond, D. P. G. & Wignall, P. B. 2010. Pyrite framboid study of marine Permian-Triassic boundary sections: a complex anoxic event and its relationship to contemporaneous mass extinction. *GSA Bulletin* 122:1265-1279.

Bond, D. P. G., Hilton, J., Wignall, P. B., Ali J. R., Stevens, L. G., Sun, Y. & Lai, X. 2010. The Middle Permian (Capitanian) mass extinction on land and in the oceans. *Earth Sci. Rev.* 102:100-116.

Brayard, A., Bucher, H., Escarguel, G., Fluteau, F., Bourquin, S. & Galfetti, T. 2006. The Early Triassic ammonoid recovery: paleoclimatic significance of diversity gradients. *Palaeo3* 239:374-395.

Brocklehurst, N., Day, M. O., Rubidge, B. S. & Fröbisch, J. 2017. Olson's Extinction and the latitudinal biodiversity gradient of tetrapods in the Permian. *Proc. R. Soc. B* 284:20170231.

Brown, J. H. 1984. On the relationship between abundance and distribution of species. *Am. Nat.* 124:255-279.

Brown, J. H. 2014. Why are there so many species in the tropics? *Jour. Biogeog.* 41:8-22.

Burrows, M. T., Schoeman, D. S., Buckley, L. B., Moore, P., Poloczanska, E. S., Brander, K. M., Brown, C., Bruno, J. F., Duarte, C. M., Halpern, B. S., Holding, J., Kappel, C. V., Kiessling, W., O'Connor, M. I., Pandolfi, J. M., Parmesan, C., Schwing, F. B., Sydeman, W. J., Richardson, A. J. 2011. The pace of shifting climate in marine and terrestrial ecosystems. *Science* 334:652-655.

Button, D. J., Lloyd, G. T., Ezcurra, M. D. & Butler, R. J. 2017. Mass extinctions drove increased global faunal cosmopolitanism on the supercontinent Pangaea. *Nat. Comm.* 8:733.

Chao, A. & Jost, L. 2012. Coverage-based rarefaction and extrapolation: standardizing samples by completeness rather than size. *Ecology* 93:2533-2547.

Chaudhary, C., Saeedi, H. & Costello, M. J. 2016. Bimodality of latitudinal gradients in marine species richness. *Trends Ecol. Evol.* 31:670-676.

Chaudhary, C., Saeedi, H. & Costello, M. J. 2017. Marine species richness is bimodal with latitude: a reply to Fernandez and Marques. *Trends Ecol. Evol.* 32:234-237.

Chaudhary, C., Richardson, A. J., Schoeman, D. S. & Costello, M. J. 2021. Global warming is causing a more pronounced dip in marine species richness around the equator. *PNAS* 118:e2015094118.

Chen, Z.-Q., Kaiho, K. & George, A. D. 2005. Early Triassic recovery of the brachiopod faunas from the end-Permian mass extinction: a global review. *Palaeo3* 224:270-290.

Chiarenza, A. A., Mannion, P. D., Lunt, D. J., Farnsworth, A., Jones, L. A., Kelland, S.-J. & Allison, P. A. 2019. Ecological niche modelling does not support climatically-driven dinosaur diversity decline before the Cretaceous/Paleogene mass extinction. *Nat. Comm.* 10:1091.

Clapham, M. E. 2015. Ecological consequences of the Guadalupian extinction and its role in the brachiopod-mollusk transition. *Paleobiology* 41:266-279.

Clapham, M. E., Shen, S. & Bottjer, D. J. 2009. The double mass extinction revisited: reassessing the severity, selectivity, and causes of the end-Guadalupian biotic crisis (Late Permian). *Paleobiology* 35:32-50.

Clarke, A. 1993. Temperature and extinction in the sea: a physiologist's view. *Paleobiology* 19:499-518.

Clarke, A. & Gaston, K. J. 2006. Climate, energy and diversity. *Proc. R. Soc. B* 273:2257-2266.

Close, R. A., Benson, R. B. J., Upchurch, P. & Butler, R. J. 2017. Controlling for the species-area effect supports constrained long-term Mesozoic terrestrial vertebrate diversification. *Nat. Comm.* 8:15381.

Close, R. A., Evers, S. W., Alroy, J. & Butler, R. J. 2018. How should we estimate diversity in the fossil record? Testing richness estimators using sampling-standardised discovery curves. *Meth. Ecol. Evol.* 9:1386-1400.

Close, R. A., Benson, R. B. J., Saupe, E. E., Clapham, M. E. & Butler, R. J. 2020a. The spatial structure of Phanerozoic marine animal diversity. *Science* 368:420-424.

Close, R. A., Benson, R. B. J., Alroy, J., Carrano, M. T., Cleary, T. J., Dunne, E. M., Mannion, P. D., Uhen, M. D. & Butler, R. J. 2020b. The apparent exponential radiation of Phanerozoic land vertebrates is an artefact of spatial sampling biases. *Proc. R. Soc. B* 287:20200372.

Cohen, K. M., Finney, S. C., Gibbard, P. L. & Fan, J.-X. 2013. The ICS International Chronostratigraphic Chart. *Episodes* 36:199-204.

Colwell, R. K. & Lees, D. C. 2000. The mid-domain effect: geometric constraints on the geography of species richness. *Trends Ecol. Evol.* 15:70-76.

Cooper, R. A., Maxwell, P. A., Crampton, J. S., Beu, A. G., Jones, C. M. & Marshall, B. A. 2006. Completeness of the fossil record: estimating losses due to small body size. *Geology* 34:241-244.

Cornell, H. V. 2013. Is regional species diversity bounded or unbounded? *Biol. Rev.* 88:140-165.

Cox, P. 2001. Description of the "TRIFFID" dynamic global vegetation model. *Hadley Centre Technical Note* 24:1-16.

Crame, J. A. 2001. Taxonomic diversity gradients through geological time. *Divers. Distrib.* 7:175-189.

Crame, J. A. 2020. Early Cenozoic evolution of the latitudinal diversity gradient. *Earth-Science Reviews* 202:103090.

Currie, D. J., Mittelbach, G. G., Cornell, H. V., Field, R., Guegan, J.-F., Hawkins, B. A., Kaufman, D. M., Kerr, J. T., Oberdorff, T., O'Brien, E. & Turner, J. R. G. 2004. Predictions and tests of climate-based hypotheses of broad-scale variation in taxonomic richness. *Ecol. Lett.* 7:1121-1134.

Dai, X. & Song, H. 2020. Toward an understanding of cosmopolitanism in deep time: a case study of ammonoids from the Middle Permian to the Middle Triassic. *Paleobiology* 46:533-549.

Darroch, S. A. & Saupe, E. E. 2018. Reconstructing geographic range-size dynamics from fossil data. *Paleobiology* 44:25-39.

Darroch, S. A. F., Casey, M. M., Antell, G. S., Sweeney, A. & Saupe, E. E. 2020. High preservation potential of paleogeographic range size distributions in deep time. *Am. Nat.* 196:454-471.

Dornelas, M., Gotelli, N. J., McGill, B., Shimadzu, H., Moyes, F., Sievers, C. & Magurran, A. E. 2014. Assemblage time series reveal biodiversity change but not systematic loss. *Science* 344:296-299.

Dunhill, A. M., Hannisdal, B. & Benton, M. J. 2014a. Disentangling rock record bias and common-cause from redundancy in the British fossil record. *Nat. Comm.* 5:4818.

Dunhill, A. M., Benton, M. J., Twitchett, R. J. & Newell, A. J. 2014b. Testing the fossil record: sampling proxies and scaling in the British Triassic-Jurassic. *Palaeo3* 404:1-11.

Dunhill, A. M., Bestwick, J., Narey, H. & Sciberras, J. 2016. Dinosaur biogeographical structure and Mesozoic continental fragmentation: a network-based approach. *Jour. Biogeog.* 43:1691-1704.

Dunhill, A. M., Hannisdal, B., Brocklehurst, N. & Benton, M. J. 2018a. On formation-based sampling proxies and why they should not be used to correct the fossil record. *Palaeontology* 61:119-132.

Dunhill, A. M., Foster, W. J., Azaele, S., Sciberras, J. & Twitchett, R. J. 2018b. Modelling determinants of extinction across two Mesozoic hyperthermal events. *Proc. R. Soc. B* 285:20180404.

Dunne, E. M., Close, R. A., Button, D. J., Brocklehurst, N., Cashmore, D. D., Lloyd, G. T., Butler, R. J. 2018. Diversity change during the rise of tetrapods and the impact of the 'Carboniferous rainforest collapse'. *Proc. R. Soc. B* 285:20172730.

Dunne, E. M., Farnsworth, A., Greene, S. E., Lunt, D. J. & Butler, R. J. 2021. Climatic drivers of latitudinal variation in Late Triassic tetrapod diversity. *Palaeontology* 64:101-117.

Erwin, D. H. 2009. Climate as a driver of evolutionary change. *Curr. Biol.* 19:R575-R583.

Evans, K. L. & Gaston, K. J. 2005. Can the evolutionary-rates hypothesis explain species-energy relationships? *Funct. Ecol.* 19:899-915.

Ezcurra, M. D. 2010. Biogeography of Triassic tetrapods: evidence for provincialism and driven sympatric cladogenesis in the early evolution of modern tetrapod lineages. *Proc. R. Soc. B* 277:2547-2552.

Ezcurra, M. & Butler, R. J. 2018. The rise of the ruling reptiles and ecosystem recovery from the Permo-Triassic mass extinction. *Proc. R. Soc. B* 285:20180361.

Farnsworth, A., Lunt, D. J., Robinson, S. A., Valdes, P. J., Roberts, W. H. G., Clift, P. D., Markwick, P., Su, T., Wrobel, N., Bragg, F., Kelland, S.-J. & Pancost, R. D. 2019a. Past East Asian monsoon evolution controlled by paleogeography, not CO_2. *Sci. Adv.* 5:eaax1697.

Farnsworth, A., Lunt, D. J., O'Brien, C. L., Foster, G. L., Inglis, G. N., Markwick, P., Pancost, R. D. & Robinson, S. A. 2019b. Climate sensitivity on geological timescales controlled by nonlinear feedbacks and ocean circulation. *Geophys. Res. Let.* 46:9880-9889.

Fenton, I. S., Pearson, P. N., Dunkley Jones T., Farnsworth, A., Lunt, D. J., Markwick, P. & Purvis, A. 2016. The impact of Cenozoic cooling on assemblage diversity in planktonic foraminifera. *Phil. Trans. R. Soc. B* 371:20150224.

Field, R., Hawkins, B. A., Cornell, H. V., Currie, D. J., Diniz-Filho, J. A. F., Guégan, J.-F., Kaufman, D. M., Kerr, J. T., Mittelbach, G. G., Oberdorff, T., O'Brien, E. M. & Turner, J. R. G. 2009. Spatial species-richness gradients across scales: a meta-analysis. *Jour. Biogeog.* 36:132-147.

Fielding, C. R., Frank, T. D., McLoughlin, S., Vajda, V., Mays, C., Tevyaw, A. P., Winguth, A., Winguth, C., Nicoll, R. S., Bocking, M. & Crowley, J. L. 2019. Age and pattern of the southern high-latitude continental end-Permian extinction constrained by multiproxy analysis. *Nat. Comm.* 10:385.

Fine, P. V. A. 2015. Ecological and evolutionary drivers of geographic variation in species diversity. *Annu. Rev. Ecol. Evol. Syst.* 46:369-392.

Fine, P. V. A. & Ree, R. H. 2006. Evidence for a time-integrated species-area effect on the latitudinal gradient in tree diversity. *Am. Nat.* 168:796-804.

Foote, M. 1999. Morphological diversity in the evolutionary radiation of Paleozoic and post-Paleozoic crinoids. *Paleobiology* 25:1-115.

Foote, M. 2007. Extinction and quiescence in marine animal genera. *Paleobiology* 33:261-272.

Foote, M. & Sepkoski, J. J. 1999. Absolute measures of the completeness of the fossil record. *Nature* 398:415-417.

Foote, M., Crampton, J. S., Beu, A. G. & Nelson, C. S. 2015. Aragonite bias, and lack of bias, in the fossil record: lithological, environmental, and ecological controls. *Paleobiology* 41:245-265.

Foster, W. J. & Twitchett, R. J. 2014. Functional diversity of marine ecosystems after the Late Permian mass extinction event. *Nat. Geosci.* 7:233-238.

Foster, G. L., Royer, D. L. & Lunt, D. J. 2017. Future climate forcing potentially without precedent in the last 420 million years. *Nat. Comm.* 8:14845.

Fraser, D. 2017. Can latitudinal richness gradients be measured in the terrestrial fossil record? *Paleobiology* 43:479-494.

Fraser, D., Hassall, C., Gorelick, R. & Rybczynski, N. 2014. Mean annual precipitation explains spatiotemporal patterns of Cenozoic mammal beta diversity and latitudinal diversity gradients in North America. *PLoS One* 9:e106499.

Garbelli, C., Shen, S.-Z., Immenhauser, A., Brand, U., Buhl, D., Wang, W.-Q., Zhang, H. & Shi, G.-R. 2019. Timing of Early and Middle Permian deglaciation of the southern hemisphere: brachiopod-based $^{87}Sr/^{86}SR$ calibration. *Earth. Plan. Sci. Lett.* 516:122-135.

Gaston, K. J. 2000. Global patterns in biodiversity. *Nature* 405:220-227.

Gent, P. R. & McWilliams, J. C. 1990. Isopycnal mixing in ocean circulation models. *Jour. Phys. Ocean.* 20:150-155.

Gillooly, J. F., Brown, J. H., West, G. B., Savage, V. M. & Charnov, E. L. 2001. Effects of size and temperature on metabolic rate. *Science* 293:2248-2251.

Gough, D. O. 1981. Solar interior structure and luminosity variations. *Solar Physics* 74:21-34.

Grinnell, J. 1917. The niche-relationships of the California Thrasher. *The Auk* 34:427-433.

Hannisdal, B. & Peters, S. E. 2011. Phanerozoic Earth system evolution and marine biodiversity. *Science* 334:1121-1124.

Harmon, L. J. & Harrison, S. 2015. Species diversity is dynamic and unbounded at local and continental scales. *Am. Nat.* 185:584-593.

Harris, J. M. & Carroll, R. L. 1977. *Kenyasaurus*, a new eosuchian reptile from the Early Triassic of Kenya. *Jour. Paleo.* 51:139-149.

Hawkins, B. A., Field, R., Cornell, H. V., Currie, D. J., Guégan J.-F., Kaufman, D. M., Kerr, J. T., Mittelbach, G. G., Oberdorff, T., O'Brien, E. M., Porter, E. E. & Turner, J. R. G. 2003. Energy, water, and broad-scale geographic patterns of species richness. *Ecology* 84:3105-3117.

Hendricks, J. R., Saupe, E. E., Myers, C. E., Hermsen, E. J. & Allmon, W. D. 2014. The generification of the fossil record. *Paleobiology* 40:511-528.

Hillebrand, H. 2004. On the generality of the latitudinal diversity gradient. *Am. Nat.* 163:192-211.

Hijmans, R. J. 2020. raster: geographic data analysis and modelling. Version 3.4-5.

Hsieh, T. C., Ma, K. H. & Chao, A. 2016. iNEXT: an R package for rarefaction and extrapolation of species diversity (Hill numbers). *Meth. Ecol. Evol.* 7:1451-1456.

Hubbell, S. P. 2001. *The unified neutral theory of biodiversity and biogeography.* Princeton Monographs in Population Biology. Princeton University Press.

Hurvich, C. M. & Tsai, C. L. 1989. Regression and time series model selection in small samples. *Biometrika* 76:297-307.

Hutchinson, G. E. 1957. Concluding remarks. *Cold Spring Harbour Symp. Quant. Biol.* 22:415-427.

Jablonski, D. 2008. Extinction and the spatial dynamics of biodiversity. *PNAS* 105:S11528-S11535.

Jablonski, D., Roy, K. & Valentine, J. W. 2006. Out of the tropics: evolutionary dynamics of the latitudinal diversity gradient. *Science* 314:102-106.

Jablonski, D., Belanger, C. L., Berke, S. K., Huang, S., Krug, A. Z., Roy, K., Tomasovych, A. & Valentine, J. W. 2013. Out of the tropics, but how? Fossils,

bridge species, and thermal ranges in the dynamics of the marine latitudinal diversity gradient. *PNAS* 110:10487-10494.

Jablonski, D., Huang, S., Roy, K. & Valentine, J. W. 2017. Shaping the latitudinal diversity gradient: new perspectives from a synthesis of paleobiology and biogeography. *Am. Nat.* 189:1-12.

Jalil, N.-E. 1999. Continental Permian and Triassic vertebrate localities from Algeria and Morocco and their stratigraphical correlations. *Jour. African Ear. Sci.* 29:219-226.

Jones, L. A., Dean, C. D., Mannion, P. D., Farnsworth, A. & Allison, P. A. 2021. Spatial sampling heterogeneity limits the detectability of deep time latitudinal biodiversity gradients. *Proc. R. Soc. B* 288:20202762.

Kerkhoff, A. J., Moriarty, P. E. & Weiser, M. D. 2014. The latitudinal species richness gradient in New World woody angiosperms is consistent with the tropical conservatism hypothesis. *PNAS* 111:8125-8130.

Kerp, H., Hamad, A. A., Vörding, B. & Bandel, K. 2006. Typical Triassic Gondwanan floral elements in the Upper Permian of the paleotropics. *Geology* 34:265-268.

Kidwell, S. M., & Holland, S. M. 2002. The quality of the fossil record: implications for evolutionary analyses. *Annu. Rev. Ecol. Syst.* 33:561-588.

Kiehl, J. T. & Shields, C. A. 2005. Climate simulation of the latest Permian: implications for mass extinction. *Geology* 33:757-760.

Kiessling, W. & Aberhan, M. 2007. Environmental determinants of marine benthic biodiversity dynamics through Triassic-Jurassic time. *Paleobiology* 33:414-434.

Kiessling, W., Simpson, C. & Foote, M. 2010. Reefs as cradles of evolution and sources of biodiversity in the Phanerozoic. *Science* 327:196-198.

Kiessling, W., Simpson, C., Beck, B., Mewis, H. & Pandolfi, J. M. 2012. Equatorial decline of reef corals during the last Pleistocene interglacial. *PNAS* 109:21378-21383.

Kinlock, N. L., Prowant, L., Herstoff, E. M., Foley, C. M., Akin-Fajiye, M., Bender, N., Umarani, M., Yeong Ryu, H., Şen, B. & Gurevitch, J. 2018. Explaining global variation in the latitudinal diversity gradient: meta-analysis confirms known patterns and uncovers new ones. *Global. Ecol. Biogeog.* 27:125-141.

Kocsis, Á. T., Reddin, C. J. & Kiessling, W. 2018. The biogeographical imprint of mass extinctions. *Proc. R. Soc. B* 285:20180232.

Kraft, N. J. B., Comita, L. S., Chase, J. M., Sanders, N. J., Swenson, N. G., Crist, T. O., Stegen, J. C., Vellend, M., Boyle, B., Anderson, M. J., Cornell, H. V., Davies, K. F., Freestone, A. L., Inouye, B. D., Harrison, S. P. & Myers, J. A. 2011. Disentangling the drivers of beta diversity along latitudinal and elevational gradients. *Science* 333:1755-1758.

Kröger, B. 2018. Changes in the latitudinal diversity gradient during the Great Ordovidian Biodiversification Event. *Geology* 127-130.

Krystyn, L., Richoz, S., Baud, A. & Twitchett, R. J. 2003. A unique Permian-Triassic boundary section from the Neotethyan Hawasina Basin, Central Oman Mountains. *Palaeo3* 191:329-344.

Liao, W., Wang, Y., Kershaw, S., Weng, Z. & Yang, H. 2010. Shallow-marine dysoxia across the Permian-Triassic boundary: evidence from pyrite framboids in the microbialite in South China. *Sed. Geol.* 232:77-83.

Lomolino, M. V. 2000. Ecology's most general, yet protean pattern: the species-area relationship. *Jour. Biogeog.* 27:17-26.

Looy, C. V., Ranks, S. L., Chaney, D. S., Sanchez, S., Steyer, J.-S., Smith, R. M. H., Sidor, C. A., Myers, T. S., Ide, O. & Tabor, N. J. 2016. Biological and physical evidence for extreme seasonality in central Permian Pangea. *Palaeo3* 451:210-226.

Lunt, D. J., Farnsworth, A., Loptson, C., Foster, G. L., Markwick, P., O'Brien, C. L., Pancost, R. D., Robinson, S. A. & Wrobel, N. 2016. Palaeogeographic controls on climate and proxy interpretation. *Climate of the Past* 12:1181-1198.

Mannion, P. D., Upchurch, P., Carrano, M. T. & Barrett, P. M. 2011. Testing the effect of the rock record on diversity: a multidisciplinary approach to elucidating the generic richness of sauropodomorph dinosaurs through time. *Biol. Rev.* 86:157-181.

Mannion, P. D., Benson, R. B. J., Upchurch, P., Butler, R. J., Carrano, M. T. & Barrett, P. M. 2012. A temperate palaeodiversity peak in Mesozoic dinosaurs and evidence for Late Cretaceous geographical partitioning. *Global Ecol. Biogeog.* 21:898-908.

Mannion, P. D., Upchurch, P., Benson, R. B. J. & Goswami, A. 2014. The latitudinal biodiversity gradient through deep time. *Trends Ecol. Evol.* 29:42-50.

Marcot, J. D., Fox, D. L. & Niebuhr, S. R. 2016. Late Cenozoic onset of the latitudinal diversity gradient of North American mammals. *PNAS* 113:7189-7194.

Marshall, C. R. & Quental, T. B. 2016. The uncertain role of diversity dependence in species diversification and the need to incorporate time-varying carrying capacities. *Phil. Trans. R. Soc. B* 371:20150217.

Marshall, C. R., Finnegan, S., Clites, E. C., Holroyd, P. A., Bonuso, N., Cortez, C., Davis, E., Dietl, G. P., Druckenmiller, P. S., Eng, R. C., Garcia, C., Estes-Smargiassi, K., Hendy, A., Hollis, K. A., Little, H., Nesbitt, E. A., Roopnarine, P., Skibinski, L., Vendetti, J. & White, L. D. 2018. Quantifying the dark data in museum fossil collections as palaeontology undergoes a second digital revolution. *Biol. Lett.* 14:20180431.

Martin, P. R. & McKay, J. K. 2004. Latitudinal variation in genetic divergence of populations and the potential for future speciation. *Evolution* 58:938-945.

Martindale, R. C., Foster, W. J. & Velledits, F. 2019. The survival, recovery and diversification of metazoan reef ecosystems following the end-Permian mass extinction event. *Palaeo3* 513:100-115.

McGhee, G. R., Clapham, M. E., Sheehan, P. M., Bottjer, D. J. & Droser, M. L. 2013. A new ecological-severity ranking of major Phanerozoic biodiversity crises. *Palaeo3* 370:260-270.

Meseguer, A. S. & Condamine, F. L. 2020. Ancient tropical extinctions at high latitudes contributed to the latitudinal diversity gradient. *Evolution* 74:1966-1987.

Mittelbach, G. G., Schemske, D. W., Cornell, H. V., Allen, A. P., Brown, J. M., Bush, M. B., Harrison, S. P., Hurlbert, A. H., Knowlton, N., Lessios, H. A., McCain, C. M., McCine, A. R., McDade, L. A., McPeek, M. A., Near, T. J., Price, T. D., Ricklefs, R. E., Roy, K., Sax, D. F., Schluter, D., Sobel, J. M. & Turrelli, M. 2007. Evolution and the latitudinal diversity gradient: speciation, extinction and biogeography. *Ecol. Lett.* 10:315-331.

Müller, R. D., Cannon, J., Qin, X., Watson, R. J., Gurnis, M., Williams, S., Pfaffelmoser, T., Seton, M., Russell, S. H. J. & Zahirovic, S. 2018. GPlates: Building a virtual Earth through deep time. *Geochem. Geophys. Geosyst.* 19:2243-2261.

Naimark, E. B. & Markov, A. V. 2011. Northward shift in faunal diversity: a general pattern of evolution of Phanerozoic marine biota. *Biol. Bull. Rev.* 1:71-81.

Nowak, H., Schneebeli-Hermann, E. & Kustatscher, E. 2019. No mass extinction for land plants at the Permian-Triassic transition. *Nat. Comm.* 10:384.

Parrish, J. T. 1993. Climate of the supercontinent Pangea. *J. Geol.* 101:215-233.

Paul, C. R. C. 1982. The adequacy of the fossil record. In Joysey, K. A. & Friday, A. E. (eds.) *Problems of Phylogenetic Reconstruction.* New York: Academic, p75-117.

Payne, J. L. & Clapham, M. E. 2012. End-Permian mass extinction in the oceans: an ancient analog for the twenty-first century? *Annu. Rev. Earth Plan. Sci.* 40:89-111.

Penn, J. L., Deutsch, C., Payne, J. L. & Sperling, E. A. 2018. Temperature-dependent hypoxia explains biogeography and severity of end-Permian marine mass extinction. *Science* 362:eaat1327.

Peters, S. E. 2005. Geologic constraints on the macroevolutionary history of marine animals. *PNAS* 102:12326-12331.

Peters, S. E. & Heim, N. A. 2011. Macrostratigraphy and macroevolution in marine environments: testing the common-cause hypothesis. *Geol Soc. Lond., Spec. Pub.* 358:95-104.

Petsios, E., Thompson, J. R., Pietsch, C. & Bottjer, D. J. 2019. Biotic impacts of temperature before, during and after the end-Permian extinction: a multi-metric and multi-scale approach to modelling extinction and recovery dynamics. *Palaeo3* 513:86-99.

Pinheiro, J., Bates, D., DebRoy, S., Sarkar, D. & R Core Team. 2021. nlme: linear and nonlinear mixed effects models. Version 3.1-152.

Pörtner, H. O. 2002. Climate variation and the physiological basis of temperature dependent biogeography: systemic to molecular hierarchy of thermal tolerance in animals. *Comp. Biochem. Physiol. A* 132:739-761.

Pörtner, H. O. 2010. Oxygen- and capacity-limitation of thermal tolerance: a matrix for integrating climate-related stressor effects in marine ecosystems. *Jour. Exp. Biol.* 213:881-893.

Powell, M. G. 2007. Geographic range and the genus longevity of late Paleozoic brachiopods. *Paleobiology* 33:530-546.

Powell, M. G. 2009. The latitudinal diversity gradient of brachiopods over the past 530 million years. *J. Geol.* 117:585-594.

Powell, M. G. & Glazier, D. S. 2017. Asymmetric geographic range expansion explains the latitudinal diversity gradient of four major taxa of marine plankton. *Paleobiology* 43:196-208.

Powell, M. G., Beresford, V. P. & Colaianne, B. A. 2012. The latitudinal position of peak marine diversity in living and fossil biotias. *Jour. Biogeog.* 39:1687-1694.

Powell, M. G., Moore, B. R. & Smith, T. J. 2015. Origination, extinction, invasion, and extirpation components of the brachiopod latitudinal biodiversity gradient through the Phanerozoic Eon. *Paleobiology* 41:330-341.

Preto, N., Kustatscher, E. & Wignall, P. B. 2010. Triassic climates – state of the art and perspectives. *Palaeo3* 290:1-10.

Qian, H. & Ricklefs, R. E. 2007. A latitudinal gradient in large-scale beta diversity for vascular plants in North America. *Ecol. Lett.* 10:737-744.

Qian, H., Badgley, C. & Fox, D. L. 2009. The latitudinal gradient of beta diversity in relation to climate and topography for mammals in North America. *Global Ecol. Biogeog.* 18:111-122.

Rabosky, D. L. & Hurlbert, A. H. 2015. Species richness at continental scales is dominated by ecological limits. *Am. Nat.* 185:572-583.

Raja, N. B. & Kiessling, W. 2021. Out of the extratropics: the evolution of the latitudinal diversity gradient of Cenozoic marine plankton. *Proc. R. Soc. B* 288:20210545.

Rampino, M. R. & Shen, S.-Z. 2019. The end-Guadalupian (259.8Ma) biodiversity crisis: the sixth major mass extinction? *Hist. Biol.* 33:716-722.

Raup, D. M. 1978. Cohort analysis of generic survivorship. *Paleobiology* 4:1-15.

R Core Team. 2018 - 2021. R: a language and environment for statistical computing. R Foundation for Statistical Computing.

Reddin, C. J., Kocsis, Á. & Kiessling, W. 2018. Marine invertebrate migrations trace climate change over 450 million years. *Global Ecol. Biogeog.* 27:704-713.

Reddin, C. J., Kocsis, Á. & Kiessling, W. 2019. Climate change and the latitudinal selectivity of ancient marine extinctions. *Paleobiology* 45:70-84.

Rodríguez, P. & Arita, H. 2004. Beta diversity and latitude in North American mammals: testing the hypothesis of covariation. *Ecography* 27:547-556.

Rohde, K. 1992. Latitudinal gradients in species diversity: the search for the primary cause. *Oikos* 65:514-527.

Rolland, J., Condamine, F. L., Jiguet, F. & Morlon, H. 2014. Faster speciation and reduced extinction in the tropics contribute to the mammalian latitudinal diversity gradient. *PLoS Biol.* 12:pe1001775.

Root, T. 1988. Energy constraints on avian distributions and abundances. *Ecology* 69:330-339.

Roscher, M., Stordal, F. & Svensen, H. 2011. The effect of global warming and global cooling on the distribution of the latest Permian climate zones. *Palaeo3* 309:186-200.

Ros-Franch, S., Márquez-Aliaga, A. & Damborenea, S. E. 2014. Comprehensive database on Induan (Lower Triassic) to Sinemurian (Lower Jurassic) marine bivalve genera and their paleobiogeographic record. *Paleontological Contributions* 8:1-219.

Rosenzweig, M. L. 1995. *Species Diversity in Space and Time.* Cambridge University Press.

Rosindell, J., Hubbell, S. P. & Etienne, R. S. 2011. The Unified Neutral Theory of Biodiversity and Biogeography at age ten. *Trends Ecol. Evol.* 26:340-348.

Roy, K., Jablonski, D. & Valentine, J. W. 1995. Thermally anomalous assemblages revisited: patterns in the extraprovincial latitudinal range shifts of Pleistocene marine mollusks. *Geology* 23:1071-1074.

Roy, K., Jablonski, D. & Valentine, J. W. 2000. Dissecting latitudinal diversity gradients: functional groups and clades of marine bivalves. *Proc. R. Soc. B* 267:293-299.

Saupe, E. E., Hendricks, J. R., Portell, R. W., Dowsett, H. J., Haywood, A., Hunter, S. J. & Lieberman, B. S. 2014. Macroevolutionary consequences of profound climate change on niche evolution in marine molluscs over the past three million years. *Proc. R. Soc. B* 281:20141995.

Saupe, E. E., Myers, C. E., Peterson, A. T., Soberón, J., Singarayer, J. Valdes, P. & Qiao, H. 2019a. Spatio-temporal climate change contributes to latitudinal diversity gradients. *Nat. Ecol. Evol.* 3:1419-1429.

Saupe, E. E., Farnsworth, A., Lunt, D. J., Sagoo, N., Pham, K. V. & Field, D. J. 2019b. Climatic shifts drove major contractions in avian latitudinal distributions throughout the Cenozoic. *PNAS* 116:12895-12900.

Saupe, E. E., Qiao, H., Donnadieu, Y., Farnsworth, A., Kennedy-Asser, A. T., Ladant, J.-B., Lunt, D. J., Pohl, A., Valdes, P. & Finnegan, S. 2020. Extinction intensity during Ordovician and Cenozoic glaciations explained by cooling and palaeogeography. *Nat. Geosci.* 13:65-70.

Savicky, P. 2014. pspearman: Spearman's Rank correlation test. Version 0.3-0.

Sax, D. F. 2001. Latitudinal gradients and geographic ranges of exotic species: implications for biogeography. *Jour. Biogeog.* 28:139-150.

Schemske, D. W., Mittelbach, G. G., Cornell, H. V., Sobel, J. M. & Roy, K. 2009. Is there a latitudinal gradient in the importance of biotic interactions? *Annu. Rev. Ecol. Evol. Syst.* 40:245-269.

Schluter, D. 2016. Speciation, ecological opportunity, and latitude. *Am. Nat.* 187:1-18.

Schobben, M., Foster, W. J., Sleveland, A. R. N., Zuchuat, V., Svensen, H. H., Planke, S., Bond, D. P. G., Marcelis, F., Newton, R. J., Wignall, P. B. & Poulton, S. W. 2020. A nutrient control on marine anoxia during the end-Permian mass extinction. *Nat. Geosci.* 13:640-646.

Schoener, T. W. 1976. The species-area relations within archipelagoes: models and evidence from island land birds. *Proc. XVI Inter. Ornith. Cong.* p629-642.

Scotese, C. R. 2016. PALEOMAP PaleoAtlas for GPlates and the PaleoData Plotter Program. Version 2.

Scotese, C. R. 2018. PALEOMAP PaleoAtlas for GPlates and the PaleoData Plotter Program. Version 3.

Scotese, C. R. & Wright, N. 2018. PALEOMAP Paleodigital Elevation Models (PaleoDEMs) for the Phanerozoic.

Sepkoski, J. J. 1984. A kinetic model of Phanerozoic taxonomic diversity. III. Post-Paleozoic families and mass extinctions. *Paleobiology* 10:246-267.

Shaw, J. O., Briggs, D. E. G. & Hull, P. M. 2021. Fossilization potential of marine assemblages and environments. *Geology* 49:258-262.

Shen, S-Z. & Shi, G-R. 1996. Diversity and extinction patterns of Permian Brachiopoda of South China. *Hist. Biol.* 12:93-110.

Shen, S.-Z. & Shi, G.-R. 2004. Capitanian (Late Guadalupian, Permian) global brachiopod palaeobiogeography and latitudinal diversity pattern. *Palaeo3* 208:235-262.

Shishkin, M. A. & Novikov, I. V. 2017. Early stages of recovery of the East European tetrapod fauna after the end-Permian crisis. *Paleo. Jour.* 51:612-622.

Sidor, C. A., Vilhena, D. A., Angielczyk, K. D., Huttenlocker, A. K., Nesbitt, S. J., Peecook, B. R., Steyer, J.-S., Smith, R. M. H. & Tsuji, L. A. 2013. Provincialization of terrestrial faunas following the end-Permian mass extinction. *PNAS* 110:8129-8133.

Silvestro, D., Schnitzler, J., Hsiang Liow, L., Antonelli, A. & Salamin, N. 2014a. Bayesian estimation of speciation and extinction from incomplete fossil occurrence data. *Syst. Biol.* 63:349-367.

Silvestro, D., Salamin, N. & Schnitzler, J. 2014b. PyRate: a new program to estimate speciation and extinction rates from incomplete fossil data. *Methods Ecol. Evol.* 5:1126-1131.

Silvestro, D., Salamin, N., Antonelli, A. & Meyer, X. 2019. Improved estimation of macroevolutionary rates from fossil data using a Bayesian framework. *Palaeobiology* 45:546-570.

Smith, A. B. 2007. Marine diversity through the Phanerozoic: problems and prospects. *Jour. Geol. Soc. Lond.* 164:731-745.

Smith, A. B. & McGowan, A. J. 2007. The shape of the Phanerozoic marine palaeodiversity curve: how much can be predicted from the sedimentary rock record of Western Europe? *Palaeontology* 50:765-774.

Smith, R. M. H. & Botha-Brink, J. 2014. Anatomy of a mass extinction: sedimentological and taphonomic evidence for drought-induced die-offs at the Permo-Triassic boundary in the main Karoo Basin, South Africa. *Palaeo3* 396:99-118.

Soininen, J., Heino, J. & Wang, J. 2018. A meta-analysis of nestedness and turnover components of beta diversity across organisms and ecosystems. *Global Ecol. Biogeog.* 27:96-109.

Song, H., Wignall, P. B., Chen, Z.-Q., Tong, J., Bond, D. P. G., Lai, X., Zhao, X., Jiang, H., Yan, C., Niu, Z., Chen, J., Yang, H. & Wang, Y. 2011. Recovery tempo and pattern of marine ecosystems after the end-Permian mass extinction. *Geology* 39:739-742.

Song, H., Wignall, P. B., Tong, J.-N. & Yin, H.F. 2013. Two pulses of extinction during the Permian-Triassic crisis. *Nat. Geosci.* 6:52-56.

Song, H., Wignall, P. B. & Dunhill, A. M. 2018. Decoupled taxonomic and ecological recoveries from the Permo-Triassic extinction. *Sci. Adv.* 4:eaat5091.

Song, H., Huang, S., Jia, E., Dai, X., Wignall, P. B. & Dunhill, A. M. 2020. Flat latitudinal diversity gradient caused by the Permian-Triassic mass extinction. *PNAS* 117:17578-17583.

Sørensen, J. G., Kristensen, T. N. & Loeschcke, V. 2003. The evolutionary and ecological role of heat shock proteins. *Ecol. Lett.* 6:1025-1037.

Stadler, T., Gavryushkina, A., Warnock, R. C. M., Drummond, A. J. & Heath, T. A. 2018. The fossilized birth-death model for the analysis of stratigraphic range data under different speciation modes. *Jour. Theor. Biol.* 447:41-55.

Stampfli, G. M., Hochard, C., Vérard, C., Wilhelm, C. & von Raumer, J. 2013. The formation of Pangea. *Tectonophysics* 593:1-19.

Stanley, G. D. 1988. The history of early Mesozoic reef communities: a three-step process. *Palaios* 3:170.183.

Stegen, J. C., Ferriere R. & Enquist, B. J. 2012. Evolving ecological networks and the emergence of biodiversity patterns across temperature gradients. *Proc. R. Soc. B* 279:1051-1060.

Sun, Y., Joachimski, M. M., Wignall, P. B., Yan, C., Chen, Y., Jiang, H., Wang, L. & Lai, X. 2012. Lethally hot temperatures during the Early Triassic greenhouse. *Science* 338:366-370.

Svenning, J.-C., Eiserhardt, W. L., Normand, S., Ordonez, A. & Sandel, B. 2015. The influence of paleoclimate on present-day patterns in biodiversity and ecosystems. *Annu. Rev. Ecol. Evol. Syst.* 46:551-572.

Tabor, N. J., Sidor, C. A., Smith, R. M. H., Nesbitt, S. J. & Angielczyk, K. D. 2018. Paleosols of the Permian-Triassic: proxies for rainfall, climate change, and major changes in terrestrial tetrapod diversity. *J. Vert. Paleo.* 37:S240-S253.

Tittensor, D. P., Mora, C., Jetz, W., Lotze, H. K., Ricard, D., Berghe, E. V. & Worm, B. 2010. Global patterns and predictors of marine biodiversity across taxa. *Nature* 466:1098-1101.

Tomašových, A., Kennedy, J. D., Betzner, T. J., Kuehnle, N. B., Edie, S., Kim, S., Supriya, K., White, A. E., Rahbek, C., Huang, S., Price, T. D. & Jablonski, D. 2016. Unifying latitudinal gradients in range size and richness across marine and terrestrial systems. *Proc. R. Soc. B* 283:20153027.

Trenberth, K. E., Jones, P. D., Ambenje, P., Bojariu, R., Easterling, D., Klein Tank, A., Parker, D., Rahimzadeh, F., Renwick, J. A., Rusticucci, M., Soden, B. & Zhai, 2007. Observations: surface and atmospheric climate change. In Solomon, S., Qin, D., Manning, M., Chen, Z., Marquis, M., Averyt, K. B., Tignor, M. & Miller, H. L. (eds.). *Climate Change 2007: The Physical Science Basis. Contribution of Working Group I to the Fourth Assessment Report of the Intergovernmental Panel on Climate Change*. Cambridge University Press, p235-336.

Trotter, J. A., Williams, I. S., Nicora, A., Mazza, M. & Rigo, M. 2015. Long-term cycles of Triassic climate change: a new $\delta^{18}O$ record from conodont apatite. *Earth Plan. Sci. Lett.* 415:165-174.

Valdes, P. J., Armstrong, E., Badger, M. P. S., Bradshaw, C. D., Bragg, F., Crucifix, M., Davies-Barnard, T., Day, J. J., Farnsworth, A., Gordon, C., Hopcroft, P. O., Kennedy, A. T., Lord, N. S., Lunt, D. J., Marzocchi, A., Parry, L. M., Pope, V., Roberts, W. H. G., Stone, E. J., Tourte, G. J. L. & Williams, J. H.

T. 2017. The BRIDGE HadCM3 family of climate models: HadCM3@Bristol v1.0. *Geosci. Model Dev.* 10:3715-3743.

Valentine, J. W. & Moores, E. M. 1970. Plate-tectonic regulation of faunal diversity and sea level: a model. *Nature* 228:657-659.

Valentine, J. W., Jablonski, D., Krug, A. Z. & Roy, K. 2008. Incumbency, diversity, and latitudinal gradients. *Paleobiology* 34:169-178.

Vavrek, M. J. 2016. The fragmentation of Pangaea and Mesozoic terrestrial vertebrate biodiversity. *Biol. Lett.* 12:20160528.

Vilhena, D. A. & Smith, A. B. 2013. Spatial bias in the marine fossil record. *PLoS One* 8:e74470.

Villier, L. & Korn, D. 2004. Morphological disparity of ammonoids and the mark of Permian mass extinctions. *Science* 306:264-266.

von Humboldt, A. & Bonpland, A. 1807. Essay on the geography of plants. In Jackson, S. T. (ed.). Romanowski, S. (trans.). 2009. *Essay on the Geography of Plants*. University of Chicago Press, p49-144.

Wall, P. D., Ivany, L. C. & Wilkinson, B. H. 2009. Revisiting Raup: exploring the influence of outcrop area on diversity in light of modern sample-standardization techniques. *Paleobiology* 35:146-167.

Wall, P. D., Ivany, L. C. & Wilkinson, B. H. 2011. Impact of outcrop area on estimates of Phanerozoic terrestrial biodiversity trends. *Geol. Soc. Lond., Spec. Pub.* 358:53-62.

Warnock, R. C. M., Heath, T. A. & Stadler, T. 2020. Assessing the impact of incomplete species sampling on estimates of speciation and extinction rates. *Paleobiology* 46:137-157.

Weir, J. T. & Schluter, D. 2007. The latitudinal gradient in recent speciation and extinction rates of birds and mammals. *Science* 315:1574-1576.

Whiteside, J. H., Grogan, D. S., Olsen, P. E. & Kent, D. V. 2011. Climatically driven biogeographic provinces of Late Triassic tropical Pangea. *PNAS* 108:8972-8977.

Wickham, H., Averick, M., Bryan, J., Chang, W., D'Agostino McGowan, L., François, R., Grolemund, G., Hayes, A., Henry. L., Hester, J., Kuhn, M., Lin Pedersen, T., Miller, E., Milton Bache, S., Müller, K., Ooms, J., Robinson, D., Seidel, D. P., Spinu, V., Takahashi, K., Vaughan, D., Wilke, C., Woo, K. & Yutani, H. 2019. Welcome to the Tidyverse. *Jour. Open Source Soft.* 4:1686. Version 1.3.0.

Willig, M. R., Kaufmann, D. M. & Stevens, R. D. 2003. Latitudinal gradients of biodiversity: pattern, process, scale, and synthesis. *Annu. Rev. Ecol. Evol. Syst.* 34:273-309.

Wignall, P. B. 2015. *The Worst of Times: How Life on Earth Survived Eighty Million Years of Extinctions*. Princeton University Press.

Wignall, P. B. & Myers, K. J. 1988. Interpreting benthic oxygen levels in mudrocks: a new approach. *Geology* 16:452-455.

Wignall, P. B. & Newton, R. 1998. Pyrite framboid diameter as a measure of oxygen deficiency in ancient mudrocks. *Am. Jour. Sci.* 298:537-552.

Wignall, P. B. & Newton, R. 2003. Contrasting deep-water records from the Upper Permian and Lower Triassic of South Tibet and British Columbia: evidence for a diachronous mass extinction. *Palaios* 18:153-167.

Wignall, P. B., Sun, Y., Bond, D. P. G., Izon, G., Newton, R. J., Védrine, S., Widdowson, M., Ali, J. R., Lai, X., Jiang, H., Cope, H. & Bottrell, S. H. 2009. Volcanism, mass extinction, and carbon isotope fluctuations in the Middle Permian of China. *Science* 324:1179-1182.

Willmer, P., Stone, G. & Johnston, I. 2005. *Environmental Physiology of Animals.* Blackwell Publishing.

Wright, D. H. 1983. Species-energy theory: an extension of species-area theory. *Oikos* 41:496-506.

Wu, Y., Chu, D., Tong, J., Song, H., Dal Corso, J., Wignall, P. B., Song, H., Du, Y. & Cui, Y. 2021. Six-fold increase of atmospheric pCO$_2$ during the Permian-Triassic mass extinction. *Nat. Comm.* 12:2137.

Xing, Y., Onstein, R. E., Carter, R. J., Stadler, T. & Linder, H. P. 2014. Fossils and a large molecular phylogeny show that the evolution of species richness, generic diversity, and turnover rates are disconnected. *Evolution* 68:2821-2832.

Zacaï, A., Monnet, C., Pohl, A., Beaugrand, G., Mullins, G., Kroeck, D. M. & Servais, T. 2021. Truncated bimodal latitudinal diversity gradient in early Paleozoic phytoplankton. *Sci. Adv.* 7:eabd6709.

Zaffos, A., Finnegan, S. & Peters, S. E. 2017. Plate tectonic regulation of global marine animal diversity. *PNAS* 114:5653-5658.